Understanding the Resurgence of an Eliminated Disease:
Spatial, Attitudinal, and Regulatory Factors Underlying Measles Outbreaks in the Post-Elimination Era

by

Nina Brooks Masters

A dissertation submitted in partial fulfillment
of the requirements for the degree of
Doctor of Philosophy
(Epidemiological Science)
in the University of Michigan
2021

Doctoral Committee:

Professor Matthew L. Boulton, Chair
Assistant Professor Paul L. Delamater, University of North Carolina
Associate Professor Marisa C. Eisenberg
Associate Professor David Hutton
Assistant Professor Jon Zelner

Nina B. Masters

mastersn@umich.edu

ORCID iD: 0000-0002-3155-6058

Dedication

To my parents: thank you for teaching me to pursue my dreams, humoring my childhood love of infectious diseases, and, most importantly, vaccinating me.

Acknowledgements

There are many individuals without whom I could not have completed this dissertation and to whom I am so very grateful. First, I would like to thank my committee chair, Dr. Matthew Boulton. You helped me become a better scientific writer and communicator during the MPH and PhD, told me to pursue the research questions that interested me most, and gave me the academic and intellectual freedom to do so. I also want to thank Dr. Jon Zelner, who nurtured and encouraged my passion for infectious disease modeling, pushed me to become fluent in R and Github, and believed in my coding skills long before I did. Without your mentorship, guidance, and hours of reading code, Jon, this dissertation wouldn't have been possible.

I am also grateful to my other committee members, Dr. Marisa Eisenberg, Dr. Paul Delamater, and Dr. David Hutton. Marisa, without your courses on infectious disease modeling, I never would have ended up as a modeler, and I so appreciate your mentorship, humor, and technical expertise. Paul, I am so glad I cold-emailed you after reading some of your papers on vaccine exemptions, and grateful to now know all about the field of medical geography! David, I deeply appreciate you helping me understand the policy implications of my research. I also want to thank Dr. Matthew Kay for your mentorship in the world of data visualization and information storytelling that has really helped me to communicate my research effectively.

Thank you also to the members of the EpiBayes Research Group, who made me feel like I was part of a team, and who gave me a research community, especially during the strange, lonely months of the COVID-19 pandemic. A special shout out to Ryan Malosh for your immeasurable advice and friendship, and to Rob Trangucci, for hours of zoom calls explaining advanced Bayesian statistical concepts. And to the rest of my SPH colleagues, past and present, you helped me get through this process in one piece!

I am so grateful to my friends at Michigan who have supported me throughout this journey. To my GEO co-stewards in the School of Public Health, especially Ben, Zak, and Kat, thank you for being such a powerful support system throughout my time at Michigan. To the student organizers who co-led our efforts to get asynchronous classes on Election Day – thank you for helping to do our part to turn Michigan Blue! Megan – thank you for countless dinners, discussions, and adventures – you made our weird little corner of Ann Arbor feel like home.

Finally, thank you to my family. Thank you for championing my successes, for celebrating (and reading!) my publications, and for helping me through the rejections and setbacks along the way. I would not have achieved my PhD without your steadfast support. To my sister Julia, I am especially grateful for the year and a half we shared in Ann Arbor during your MSW, and your support during the dark days of Comps preparation. Matt, thank you for standing by my side these three years – despite the distance (and the pandemic). I don't know where I'd be without your commitment to cheering me on, making me smile, and always supporting me when times are tough.

Table of Contents

List of Tables

List of Figures

List of Equations

List of Appendices

List of Abbreviations

ACIP	Advisory Committee on Immunization Practices
CDC	Centers for Disease Control and Prevention
V_c	Critical Vaccination Fraction
DHS	Demographic and Health Surveys
HIC	High Income Country
LMIC	Low and Middle Income Country
MCV	Measles-Containing Vaccine
MDHHS	Michigan Department of Health and Human Services
MMR	Measles-Mumps-Rubella
NME	Non-Medical Exemption
PBE	Personal Belief Exemption
PACV	Parental Attitudes on Childhood Vaccination
R_o	Basic Reproduction Number
SAGE	Strategic Advisory Board of Experts
USAID	United States Agency for International Development
VAE	Vaccine Adverse Event
VPD	Vaccine-Preventable Disease
WHO	World Health Organization

Abstract

Since the introduction of the highly effective measles-mumps-rubella (MMR) vaccine in 1971, measles incidence has decreased by over 95% globally. In 2012, the Measles and Rubella Initiative set to eliminate measles in five WHO regions by 2020. However, a recent global resurgence of measles amid rising levels of vaccine hesitancy threatens elimination. This dissertation explored three factors that may have contributed to this measles resurgence: spatial clustering of non-vaccination, rising vaccine hesitancy, and policies allowing non-medical exemptions (NMEs).

Aim 1 evaluated the consequences of spatial clustering of non-vaccination and the risks posed by using aggregate surveillance estimates to predict outbreaks. This analysis used a spatial dynamic compartmental model, fixing overall vaccination coverage at 95% (the WHO elimination vaccination threshold for measles) and simulating outbreaks across a landscape of non-vaccination clustering motifs. Simulation output revealed that measles outbreaks occurred even at 99% overall vaccination coverage when clustering of non-vaccination was present, calling into question the appropriateness of large-scale herd immunity measures. Aggregation of vaccination data obscured fine-scale clustering and significantly downwardly biased predicted outbreak probability and size, thus underestimating risk.

Aim 2 applied the theoretical findings from Aim 1 using school-level kindergarten vaccination data from the Michigan Department of Health and Human Services from 2008-2018. While Aim 1 showed the importance of clustering in driving outbreaks, there is no standard, best practice metric or scale to assess non-vaccination clustering. Across four metrics and four spatial scales, estimates of clustering varied significantly. Measures of exposure performed better than measures of spatial autocorrelation and segregation, both in terms of sensitivity to changing vaccination rates and outbreak-relevant interpretations. All metrics were better able to capture clustering when finer-scaled data were used. Aggregating vaccination data negatively biased estimates of how many students were at-risk of disease, using herd immunity thresholds for measles, mumps, and rubella. Since most public reporting of vaccination rates occurs at the county or state level, these results indicate that such aggregation underestimates the population of at-risk children in Michigan.

Aim 3 assessed the impact of regulatory changes on vaccine exemptions; namely Michigan's 2015 Administrative Rules change requiring parents to attend a vaccine education session at their local health department prior to receiving an NME. This policy had mixed results. While initially the state experienced a 32% decline in the number of exemptions, NMEs returned nearly to pre-policy levels after four years. School type was a significant predictor of NME receipt: compared to public schools, private schools had approximately twice and virtual schools about five times the rate of exemptions. Additionally, philosophical, religious, and medical exemption clusters manifested in distinct geographies. This suggests that if future policy changes affect access to certain types of exemptions in Michigan, they may have a spatially heterogeneous impact.

Together, this dissertation illustrates that regulatory policies which permit vaccine-hesitant parents to obtain NMEs for their children result in geographically heterogeneous landscapes of non-vaccination, clustered by sociodemographic and social characteristics. This heterogeneity leads to violations in the assumptions underlying vaccination thresholds set for disease elimination initiatives. Acknowledging such heterogeneity in vaccination patterns, using finer-scale data to identify communities with low vaccination rates, measuring clustering with appropriate and interpretable statistics, and constructing vaccination policies that effectively reduce rates of exemptions are necessary to combat the resurgence of measles and achieve global elimination goals.

Chapter 1 Introduction

This dissertation explores three factors that may have contributed to the resurgence of vaccine-preventable diseases (VPDs), such as measles, despite access to effective vaccination and health care services in the United States. Together, spatial clustering of vaccine attitudes and exemptions, the growth of vaccine hesitancy, and regulatory policies allowing non-medical vaccine exemptions (NMEs) can impact transmission dynamics, permitting measles' resurgence across the globe despite an effective vaccine and relatively high national coverage rates. Chapter 2 examines the consequences of spatial clustering of non-vaccination and the risks posed by aggregate surveillance estimates in containing and predicting outbreak size and probability. Chapter 3 uses four spatial clustering metrics and geographic scales to assess the landscape of clustering of NMEs in Michigan from 2008-2018, applying the theoretical proof-of-concept from Chapter 2 to real vaccination data. Chapter 4 evaluates Michigan's 2015 Administrative Rules change requiring parents to attend an in-person waiver education session at their local health department prior to receiving a non-medical vaccine exemption waiver, and the impacts of this policy on vaccine hesitancy and spatial clustering of susceptibility.

1.1 Specific aims and hypotheses

Aim 1*:* Given a theoretical, spatial measles model on a 16x16 grid schematically representing contiguous neighborhoods and fixing average vaccination at ~95% (the herd immunity threshold for measles assuming homogeneous mixing), how do different clustering motifs impact disease risk? At what scale is clustering important for changing transmission dynamics? At what scale-resolution should vaccination levels be examined?

Hypothesis 1: As clustering increases, the risk of disease acquisition both for individuals in the population and the R_o of a given 'introduced case' will increase, accompanied by more sporadic outbreaks with higher caseloads. Outbreaks occurring under more clustered scenarios may also have the potential to cause more cases, thus creating greater morbidity and mortality. Additionally, high-risk areas might be obscured if the vaccination coverage in this gridded environment is aggregated to too high a scale (i.e. at the neighborhood or quadrant level). This has implications for disease surveillance in practice: the results of this aim could ensure increased awareness of the limitations associated with the current scope and scaling of surveillance regarding clustered non-vaccination.

Aim 2: What is the vaccination landscape among children enrolled in kindergarten in the state of Michigan from 2008-2018? How does the interpretation of clustering of non-vaccination change as different clustering metrics are used (Moran's I, Isolation Index, Modified Aggregation Index, Theil Index)? As the scale of aggregation grows (from school to Census block to Census tract to

school district to county), what is the incremental impact on identification of unvaccinated students and high-risk schools vulnerable to outbreaks?

Hypothesis 2: The landscape of vaccination exemptions will not be homogeneous across the state, with vaccination outcomes clustered both at the school (micro-level) and regional (higher-aggregation) levels. However, different metrics will be differentially able to identify and quantify such clustering. It is important to balance the surveillance/aggregation level with the capacity to evaluate data on a sufficiently fine scale to identify those at risk. Aggregating from school to school district may still permit identification of the most at-risk schools (e.g. those with >10% NME rate), however at higher levels of aggregation the most high-risk schools may not be identifiable, missing important local clustering which generates pockets of susceptibility and promotes outbreak risk.

Aim 3: Did Michigan's 2015 Administrative Rules change to mandate immunization information sessions for parents at the local health department prior to obtaining an NME reduce NME rates across the state? Was the reduction in rates uniform across school districts or geographically clustered? What were socio-demographic predictors of NMEs before and after the policy change, and did any predictors change over time?

Hypothesis 3: This change in administrative policy did reduce the overall number of NMEs, but those reductions occurred predominantly where the majority of NMEs obtained prior to the 2015 rule change were convenience exemptions because children weren't vaccinated in time for school, not exemptions driven by conviction. We also hypothesize that increasing distance to the

health department will lead to decreased exemption rates after the policy was implemented due to the additional difficulty in obtaining an exemption if the health department is further away, with only parents who have the strongest convictions continuing to exempt their children.

1.2 Background and significance

1.2.1 Global measles resurgence

Measles natural history and transmission

Measles is a highly contagious paramyxovirus and despite decades of successful vaccination campaigns, it remains one of the leading causes of infectious mortality in children in low- and middle- income countries (LMICs). In 2018, there were more than 140,000 deaths from measles, mostly occurring among children under the age of five.[1] Measles is spread through direct or airborne contact between individuals.[2] The measles virus is highly communicable, capable of infecting up to 90% of susceptible persons who come into contact with an infected case, and is able to live for up to two hours in the air after an infected individual has coughed or sneezed.[2] This contributes to the extremely high transmission rate of measles, with one of the largest basic reproductive numbers (R_o, the number of individuals an infected person could infect in an entirely susceptible population) of any infectious disease (R_o = 12-18).[1,3]

Clinically, measles results in a distinct febrile rash illness, with affected individuals infectious from four days before to four days after rash onset.[2] Measles can also cause significant morbidity, with between 20% and 25% of cases leading to hospitalization, and serious complications including encephalitis (about 1 in 1,000 cases), pneumonia (about 1 in 20 cases), and rarely, subacute sclerosing panencephalitis (SSPE), a fatal central nervous system disease

which develops about 7-10 years after acute measles illness.[1,2] Measles can be fatal, especially in young children, with ~ 2-3 per 1,000 cases resulting in death.[2] Measles' well-defined period of communicability, anchored around a highly visible and pathognomonic rash, along with an easily obtained and interpreted IgM antibody test, have made measles the paradigm of a rapidly-diagnosed disease. Additionally, measles is extremely well-reported in the United States, as one case constitutes an outbreak for reporting purposes. The intense surveillance of measles, along with the distinctive signs and symptoms of illness, have helped public health officials institute effective control measures against its spread in the United States.

The measles vaccine, a live vaccine, was first licensed in 1963 and combined with mumps and rubella vaccines as the measles-mumps-rubella vaccine (MMR) in 1971.[1] The Centers for Disease Control and Prevention (CDC) in the United States currently recommends two doses of the MMR vaccine for optimal protection: the first between the age of 12 and 15 months, and the second between 4 and 6 years of age.[4] The vaccine is highly effective and generally induces lifelong immunity, with 2 doses conferring 97% protection against measles.[2] Since the introduction of this MMR vaccine in 1971, measles incidence has decreased by over 95% globally, and measles-related mortality has decreased by over 92%. Currently, the majority of deaths occur in children under the age of five in LMICs.[1]

Due to the success of the vaccine, the lack of non-human reservoirs, and ease of clinical diagnosis, the Measles and Rubella Initiative along with the Global Vaccine Action Plan targeted measles for global elimination, seeking to reduce incidence to fewer than five cases per million across the world and eliminate measles in five WHO regions by the end of 2020.[5,6] However, despite significant improvements in vaccination coverage, which reduced the death toll of measles from >500,000 in 2000 to 110,000 in 2017, more recent progress with elimination

efforts has slowed,[7] as cases are re-emerging and vaccine coverage is declining.[8] Though measles' easily clinically identifiable rash was one of the key features that initially made it a feasible target for elimination, the rarity of measles cases now in high-income countries (HICs) has created a conundrum in which many doctors have never actually seen a case of measles. This leads to missed cases, misdiagnosis, and reduced awareness.[9] Measles' high transmission rate further complicates elimination goals: to halt ongoing transmission, an extremely high critical vaccination fraction (V_c, the proportion of the population which must be vaccinated to reach herd immunity) is needed, in the range of 95%.[1,3]

Recent resurgence in the U.S. and other developed countries

Although the CDC certified measles as eliminated from the WHO Region of the Americas in 2000,[10] declining vaccination coverage has threatened this elimination status, which is conditional on no circulating, epidemiologically-linked disease for more than 12 continuous months.[10,11] A large measles outbreak in Disneyland, California was the first major measles outbreak in the U.S. since the declaration of elimination, with 147 cases from 2014-2015.[12,13] This outbreak was particularly significant as it showed the vulnerability to disease that accompanies decreases in *local* vaccination coverage in certain geographic areas.[12] This outbreak contributed to the national spike in measles cases seen in the U.S. in 2014, as shown in Figure 1.1.[14] Despite the notable increase in measles cases in 2014, there were no significant changes in overall vaccination coverage in U.S. children aged 19-35 months over this time period which could explain the increased case burden based on data from the CDC's National Immunization Survey (NIS). This further highlights that changes in local vaccination rates were driving increased susceptibility to measles – but those local differences were obscured by national

averages – with vaccination coverage varying up to 38.1 percentage points among the 50 states.[15] The Disneyland outbreak proved to be a harbinger of future measles outbreaks, as 2019 witnessed 1,282[16] cases of measles across 31 states,[14] the highest number of cases since 1992. Additionally, the 2019 outbreaks in the United States were just one week shy of reaching 12 continuous months of measles transmission, only days away from losing measles elimination status granted 19 years prior. However, 2019 was a bad year for measles not just in the United States – globally, 2019 had the most measles cases and deaths in 26 years, with the WHO warning the global community that increased vigilance is urgently needed to avoid further steps backwards.[17]

Outbreak response

One of the largest outbreaks of 2019 occurred in New York City among the Orthodox Jewish community in Brooklyn.[18] The New York State school immunization survey showed that overall measles vaccination coverage for children in Pre-K through 12th grade was 98%,[1] well above the threshold thought to be sufficient to confer herd immunity. An analysis at a finer-scale revealed that the schools affected by the outbreak had a measles vaccination coverage rate of only 77%, not high enough to interrupt disease transmission.[19] Struggling to control the outbreak and prevent spread throughout the broader metropolitan area that is home to over eight million people, the New York City Department of Health and Mental Hygiene declared the measles outbreak a public health emergency.[10] New York City required all unvaccinated individuals aged 6 months or older in four Brooklyn zip codes experiencing the outbreak to receive an MMR vaccine, with a penalty of $1,000 for refusal.[20,21] It is important to note that measles vaccination can also be used for post-exposure prophylaxis within 72 hours of exposure with high levels of

success in averting disease. Therefore, vaccination for those in high-risk areas could impart immunity both in terms of pre- and post-exposure prophylaxis.[1]

While the goal of this vaccination order was to protect the community from the virus, the mandate was deemed by many to be overly prescriptive, causing controversy and raising ethical questions about infringement of personal liberty in the name of public health.[10,19] Rockland County, also in New York State, employed a different well-known and frequently used public health strategy, preventing those who were unvaccinated from going to school in the county and only allowing students to return to school when school-level vaccination rates reached 95%.[21] This practice of school exclusion, a form of social distancing, is a well-accepted and proven method of communicable disease control that has been used in this country for over a century. Despite these practices being intended to prioritize community safety and reduce viral spread, the public can (and often does) respond to these outbreak control measures with anger, frustration, and pushback, especially among those who fear vaccination or intentionally resist vaccination for personal, philosophical, or religious reasons. These reactions show how important it is to understand the historical precedent for such vaccination mandates and highlight the ways in which legislation can effectively prevent outbreaks and reduce the need for such controversial, stringent methods to control an ongoing outbreak.

The following introductory discussion will detail three factors that have contributed to the measles resurgence in high-income countries (HICs) despite access to effective, nearly universally available vaccination: (1) spatial factors, including clustering of non-vaccinated individuals, (2) attitudinal factors such as vaccine hesitancy, and (3) regulatory factors, such as legislative and administrative policies regarding vaccine exemptions, which can either permit or restrict access to vaccine exemptions, impacting vaccination rates dramatically.

1.2.2 Spatial factors: clustering of non-vaccinators

The impact of spatial clustering on disease

One important contributor to the re-emergence of measles in high-income countries (HICs) is spatial clustering of non-vaccinated individuals, which promotes the spread of disease and can be obscured by aggregate vaccination coverage statistics. Herd immunity thresholds calculated for disease elimination initiatives inherently assume homogeneity of vaccination, contact, and disease transmission at the level at which vaccination coverage is measured . However, these assumptions do not hold when individuals are geographically or socially clustered by vaccination status, increasing the effective R_o and, correspondingly, the V_c. Clustering of susceptibility can allow diseases to spread considerably despite national vaccination coverage thresholds theoretically capable of interrupting transmission (under the assumptions of homogeneity) being met, or even exceeded.[22]

A 2018 landmark paper by Olive et al. predicted high-risk areas for measles outbreaks in the United States based on the presence of geographic clusters of NMEs creating pockets of susceptibility, which the authors referred to as coldspots.[23] Additionally, Truelove et al. explored the impact of spatial clustering of immunity on measles elimination and found that using data from the Tanzania Demographic and Health Survey (DHS), spatial clustering of non-vaccination increases the V_c by 3% for measles, by 6% for mumps, by 8% for rubella, and by 19% for cholera.[22] Spatial heterogeneities in coverage are particularly pertinent for diseases like measles, which is near elimination, as the impact of clustering on the probability of an outbreak becomes exponentially greater as regions approach elimination vaccination thresholds (~94-95% for measles).[22] In the United States, clustering of non-vaccination is likely driven by some combination of attitudinal, access-related, and sociodemographic factors.[24] While there is strong

evidence that vaccine exemptions (specifically religious and philosophical exemptions) are clustered geographically, further research is needed to understand how and if vaccine hesitancy is also geographically clustered, or if regulatory and sociodemographic factors drive this clustering to manifest in spatial *exemption* patterns rather than any notable patterning of underlying hesitancy *beliefs*.[24–27]

Identifying a meaningful scale of spatial clustering

When defining spatial scales to measure clustering of vaccination outcomes, the potential intervention, the level of surveillance, and the reality of obtaining data at a certain level of granularity must all be taken into consideration. In addition to these factors, it is important to note the spatial scale at which vaccination coverage estimates are meaningful and actionable. Many studies of vaccination explore aggregate measures at the national level. However, such national estimates obscure transmission dynamics that exist at a finer scale and challenge the interpretation of concepts such as herd immunity, because coverage estimates of large regions cannot safely assume herd immunity is maintained at the level at which diseases circulate.

Cliff et al. conducted one of the first spatial analyses of measles transmission in 1992, tackling this question directly by exploring the correlation of monthly measles cases among Northeastern states, finding that sub-national variability in vaccination and disease risk was significant.[28] Measles incidence was dominated by local transmission: two-thirds of the states studied experienced measles outbreaks due to spread from affected neighboring states.[28] Beyond motivating spatial analysis of measles transmission, Cliff et al. called for "a finer geographic grid than the system of states", highlighting the need for additional study to determine the levels of meaningful spatial heterogeneity and clustering.[28] However, the optimal level of granularity that

should be analyzed to permit the identification of clusters and actionable interventions for VPDs has yet to be clearly identified and incorporated into vaccination reporting in the United States. It is also important that any chosen level of granularity is considered acceptable by the public, legislators, and public health authorities. The following discussion highlights analyses that have been used to examine heterogeneities in measles vaccination coverage and outbreak risk on variable spatial scales, starting with the most aggregated, low-resolution, and progressing to the most granular.

At the largest, most zoomed-out spatial scale, measles transmission occurs in a global context. The African continent has particularly rampant measles transmission, necessitating vaccination coverage levels above the V_c to meet elimination targets and reduce disease burden. However, there appears to be notable spatial heterogeneity at the sub-continental level, as country-specific differences provide insight into vaccination programs and coverage between contiguous countries.[29,30] Brownwright et al. identified that the average measles-containing vaccine (MCV) coverage across 10 contiguous sub-Saharan African countries from 2008-2013 was 83.6% using data from the Demographic and Health Surveys (DHS), nationally representative household surveys established by the United States Agency for International Development (USAID) in 1984 and administered in over 90 countries around the world.[29] However, this aggregate number obscured significant country-to-country differences with serious implications for disease control in each country: vaccination coverage ranged from a low of 69.6% in Madagascar, to a high of 95% in Rwanda.[29]

Sub-national analyses have identified distinct patterns of spatial clustering using the geographic scale of the cluster variable from the DHS and at larger, regional scales.[30] Such studies have shown that while many reports simply evaluate national averages of vaccination

coverage, predicted outbreak risk within these spatial clusters was highly variable, with clusters often occurring along national borders.[29] Even sub-national aggregate data can pose problems for distribution of resources and/or interventions, as in Namibia, where Ntirampeba et al.[31] found regional data created a "spatial misalignment problem if the purpose is to make decisions at the constituency level," highlighting the need for the scale of analysis to *match* the scale of a potential intervention.

An alternative is to use multiple spatial scales: Wesolowski et al. sought to incorporate spatial patterns of individual movement by using travel data from mobile phones to approximate individual connectivity for measles outbreak risk in Pakistan.[32] This project incorporated three scales of data: regional measles incidence, national-level vaccination coverage, and human travel data at a much finer scale, but overall yielded poor predictive ability.[32] Lo et al. used higher-level variables, such as statewide NME laws, and mandated vaccination regulations within schools, to evaluate cost-effectiveness and public health burden of declining MMR vaccination rates.[33] Utilizing county- and state-level data, they found a 5% decline in MMR coverage could increase annual measles cases threefold, which would cost the United States $2.1 million.[33]

In some cases, different scales of analysis can have different yields in terms of understanding the epidemiology of a given disease, as in Malawi, where the cause of a resurgence in measles cases after declining annual disease burden was unknown. Using health facility catchment areas as the unit of analysis, Kundrick et al. found significant variation in vaccination coverage (from 61% to 99%) and found that previous district-level analyses had obscured important variability and clusters of susceptibility at the health facility-level.[34] In this case, finer-resolution data in Malawi yielded *very different findings* and helped identify the root cause of why there had been infectious disease spreading in communities: the authors were able

to identify and target interventions to specific health facilities catchment areas with low vaccination rates and high rates of disease spread. This shows that choosing the right scale of analysis can provide actionable public health solutions that would not be possible if data at coarser spatial scales were used instead.

Beyond health-facility catchment areas, it is unclear what costs and benefits are associated with finer-resolution data. Approximating individual movement with mobile phone records has limitations, with the potential to introduce more error and noise[35], and such high-resolution mapping of vaccination coverage may not afford significantly more information than DHS cluster-level data.[36] Two papers have attempted to tackle individual-level spatial heterogeneity, which may not be appropriate nor feasible for interpreting the impact of clusters of non-vaccination on community risk within populations, though they provide a good construct for understanding the relative risk of individuals within a broader community. [37,38]

These examples illustrate that violations of the assumption of homogeneity of measles vaccination and population mixing, both required to calculate the V_c to maintain herd immunity, may result in a dangerously inaccurate picture of susceptibility. This motivates the use of an appropriate geographic scale to avoid a spatial misalignment problem when analyzing measles non-vaccination. The literature discussed above exemplifies the feasibility of examining spatial measles vaccine heterogeneity at many different scales. Significant heterogeneity was identified consistently at a sub-district level, be it local constituency[31], DHS cluster[29] or school-district[33], though the use of finer scales of analysis such as cellular mobility data[32] and individual person-to-person data[38] may be less appropriate for understanding community dynamics and predicting high-risk areas in near-elimination frameworks. As such, an analysis that examines vaccination coverage and/or refusal rates at these different levels, and how aggregation to these levels

changes predictive power to assess outbreak risk, is important. Additionally, clarifying the scale at which clustering of reduced vaccination occurs and is significant for impacting disease risk is necessary to inform vaccination policy and target effective interventions.

Spatial clustering implications for COVID-19 management and vaccine distribution

It is imperative to better understand and control the spread of preventable diseases such as measles while the COVID-19 pandemic is ongoing, especially before a vaccine is widely available. Elucidating the impact of spatial clustering of differential immunity and clarifying the most effective scale of surveillance will be useful to produce concrete solutions to reduce case burden and health service utilization. Recent research has highlighted that non-pharmaceutical interventions (such as social distancing and mask wearing) may have downstream implications for seasonal cycles of respiratory viruses typically occurring in the winter, such as respiratory syncytial virus (RSV) and influenza. While mask wearing and social distancing may result in less circulating illness in the 2020-2021 flu season, the 2021-2022 flu season may be significantly worse as a buildup of susceptibility occurs in concert with reductions in non-pharmaceutical interventions.[39] This research indicates that nontraditional seasonal patterns of illness may occur in the years following the COVID-19 pandemic, and that attention to spatial clustering of immunity will be highly relevant to targeting interventions and reducing morbidity in the wake of COVID-19.

Additionally, spatial clustering analyses have direct implications for managing COVID-19 therapeutic and vaccine distribution, as the clustering of susceptibility and immunity is likely to occur in the communities both least and most hard-hit in the first waves of transmission.[40] Truelove et al. showed that fine-scale spatial clustering of non-vaccination resulted in the largest

increases in the critical vaccination fraction for diseases with lower values of R_o. Because the R_o of COVID-19 is about four fold lower than that of measles, analyses exploring the impact of spatial clustering of COVID-19 susceptibility may be as or more acute than analogous explorations into spatial clustering of measles non-vaccination.[22]

1.2.3 Attitudinal factors: vaccine hesitancy

History of vaccine hesitancy

The modern anti-vaccine movement gained significant momentum in 1998 after Andrew Wakefield's publication of his now-infamous article in *The Lancet* linking measles-mumps-rubella (MMR) vaccination with neurodevelopmental issues, such as autism.[41] By the late 1990s, many vaccine-preventable diseases (VPDs) were no longer commonplace in the U.S., and thus parents making vaccination decisions for their children were no longer witnessing these diseases regularly in their daily life. As a result, the timing of Wakefield's article, published as VPD rates were waning, gave rise to growing parental distrust of vaccines and influenced their risk calculation about whether to vaccinate their children. Parents worried that the risks of vaccine complications were potentially greater than the risks of contracting the disease itself, since fear of VPDs had decreased as preventable diseases faded from the collective global memory. While Wakefield was found guilty of falsification of data and lost his medical license (in addition to all other authors retracting the conclusions of the paper besides Wakefield himself),[42] it took *The Lancet* until 2010 – 12 years – to retract his paper. Unfortunately, his so-called findings produced an enduring conviction in many parents across the globe that vaccines cause autism, a conviction that remains common to this day. Wakefield's article also had a significant impact on vaccination rates in the United Kingdom, where MMR coverage dropped from ~90% in 1996 to

<80% in 2001.[43] The sticky myth that vaccines cause autism is not supported by scientific research. Instead, the social and geographical patterning of autism diagnoses likely reflects social diffusion, with researchers finding that parents discussing autism diagnoses among their children was most consistent with the increased diagnosis and spatial patterning of autism in California.[44]

Despite the fact that Wakefield's article was published in 1998, vaccine hesitancy was not formally defined by the World Health Organization's (WHO) Strategic Advisory Group of Experts on Immunization (SAGE) Vaccine Hesitancy Working Group until 2011.[45] The WHO defined the continuum of vaccine hesitancy as: "delay in acceptance or refusal of vaccines despite availability of vaccination services. Vaccine hesitancy is complex and context specific, varying across time, place and vaccines. It is influenced by factors such as complacency, convenience and confidence."[45] Since the WHO's definition, the SAGE Working Group on Vaccine Hesitancy developed a globally relevant survey tool to assess vaccine hesitancy in 2015. Though this has a broader reach than the first survey created to assess vaccine hesitancy, the Parental Attitudes on Childhood Vaccines (PACV) survey, developed in 2011,[46,47] there are very few quantitative scales which are broadly validated ways to measure vaccine hesitancy in epidemiologic research. Additional research and validated scales to assess different components of vaccine hesitancy are much needed.

Recent research on vaccine hesitancy

Vaccine hesitancy was defined recently, and the body of literature assessing vaccine hesitancy, its predictors, and its effects on community susceptibility to VPDs is therefore still fairly small. Though Wakefield's study has been widely discredited, studies have found that parents of children with autism are still less likely to vaccinate younger siblings.[48,49] According

to the affect heuristic,[50] individuals who perceive more benefit to something (i.e. a vaccination), are also more likely to believe that it is safer, while those who have more negative feelings towards vaccination are more likely to perceive the risks as higher. Vaccine hesitancy has been shown to hinge upon such heuristics[51] – heavily involving emotions and intuitive thinking, and contributing to the reason why conspiracy theories and anecdotal case reports can so effectively fuel fear about vaccine adverse events (VAEs) outweighing the benefits of vaccination. Unfortunately, the role of these heuristics and cognitive biases in the development of vaccine hesitancy can also help explain why the damage done by Wakefield's 1998 paper has proved so difficult to undo.[52]

Vaccine hesitancy defies convenient explanation in terms of socioeconomic and demographic factors. In HICs, vaccine hesitancy is more common in more affluent and highly educated (college education and beyond) groups. However, vaccine *hesitancy* may not exactly track with vaccine *uptake*, which also includes access-related factors, with children living below the federal poverty level found to have lower vaccination coverage than those above it.[15,53] The relationship between sociodemographic predictors, vaccine hesitancy, and uptake is somewhat unclear and may differ in LMICs. An additional consideration when reflecting on potential differences in both vaccine hesitancy and uptake between HICs and LMICs is the inverse equity hypothesis, which postulates that new interventions are first adopted by the wealthy, thus increasing and perpetuating inequalities with the poorest falling behind all other groups.[54] For this reason, combined with the affect heuristic described above, it is plausible that there would be a meaningful distinction observed between HICs and LMICs whereby hesitancy (fueled by lower perception of individual risk from VPDs, among other factors), is higher in HICs, yet vaccination uptake is higher in those regions as well, while access factors in LMICs cause vaccination

outcomes to lag behind even though vaccine hesitancy may not be as pronounced of a phenomenon. Further research is needed to identify the predictors of vaccine hesitancy in different global and societal contexts, which may influence how parents develop and act on vaccine hesitancy.[55–57]

It is important to note that vaccine hesitancy is not a static phenomenon – but can and likely does change over time based on experiences with vaccinating one's children, discussing vaccinations with others, or events in the popular news media. Thus, studies assessing parental attitudes around vaccines at different times (pregnancy, during the first year of a child's life, after the child has been vaccinated) will likely have different conclusions.[58] Few studies have explored vaccine hesitancy, attitudes, knowledge, and beliefs of parents with young children, [59,60] and fewer still have explored how vaccine hesitancy changes over time from pregnancy through the child's early years when children receive most of their vaccinations.[61,62] Vaccine attitudes during pregnancy are not necessarily predictive of later vaccination behavior, so depending on experiences with vaccination, a hesitant pregnant woman may have a fully-vaccinated child.[63] More research is needed to understand how hesitancy develops and changes over time.

The few studies on vaccine hesitancy among mothers of young children have shown that mothers are most unsure about vaccination during pregnancy.[61] A cohort study of young mothers in Washington state found that vaccine hesitancy significantly decreased between the child's birth and second birthday.[58] The decrease in vaccine hesitancy seems to have been driven by improving confidence that vaccines are safe and effective.[58] On the other hand, parents may become more hesitant toward vaccines if their child has a perceived contraindication to vaccination.[62] In a study conducted in Germany, where there are no vaccine mandates (only recommendations), vaccine hesitancy was assessed by asking about perceived risk and concern

about VPDs, perceived risk and concern about VAEs, and general attitudes and experiences with vaccination.[63] The authors found that the first experience a mother has with vaccinating her child is crucial to changing risk perceptions and vaccination concerns.[63] Taken together, these studies show the significance of early vaccination events on mothers' beliefs about vaccination.

Even mothers intending to vaccinate their children prefer to have physicians who are flexible regarding vaccination schedules. A study of first time expectant mothers showed that the majority of mothers wanted their children to receive all the vaccines recommended by the CDC/Advisory Committee on Immunization Practices (ACIP) (75%) with a smaller proportion wanting all the vaccines but spaced out further than the recommended schedule (10.5%).[64] Despite this sentiment, these mothers felt it was important (23%) or very important (36.5%) that their pediatrician be flexible regarding the childhood vaccines and schedules.[64] Additionally, 94.5% of mothers believed they should ask questions about vaccine safety and importance to their pediatricians, which highlights the important role that conversations with health care providers may play in vaccination decision-making: primary care provider recommendation continues to be one of the strongest influencers of parents' decision to vaccinate.[64]

Opel et al. identified that there are two broadly different communication strategies used by providers, participatory and presumptive, that influence parental decision making about vaccines and speak to this desire for provider flexibility.[65] The more flexible participatory format, such as "what do you want to do about shots" opens a different conversation with parents than the presumptive format, such as "we have to do some shots".[65] Significantly fewer parents ultimately accepted all vaccines at the end of the visit if providers used participatory conversations, but were more likely to highly rate their physician experience if the provider initiated with a participatory conversation, speaking to the survey results above that mothers

desire flexibility from their pediatricians.[65] This presents a challenge for clinicians, as the participatory approach has generally become increasingly favored, but such an approach needs to be balanced against the value of increasing vaccine uptake.

The concept of a 'flexible' vaccination schedule was popularized by Dr. Robert Sears' 2007 bestseller, "*The Vaccine Book: Making the Right Decision for Your Child".*[66] The book contains 'Dr. Bob's Alternative Vaccine Schedule', a formula he provides parents to withhold or space out vaccines, claiming that the CDC's and American Academy of Pediatrics' schedule has children receive too many vaccines at once, overwhelming their immune systems.[67] Part of what is so dangerous about this alternative schedule is that it seems to provide a middle ground for parents – not just accepting or rejecting all pediatric vaccinations, but allowing parents to make a so-called 'informed' decision, though most of Dr. Sears' patients avoid vaccinations.[67] Unfortunately, Dr. Sears' narrative has produced an enduring sentiment among many parents that children's immune systems are incapable of handling the routine vaccination schedule. Additionally, Dr. Sears is under investigation by the Medical Board of California for medical vaccine exemptions he wrote in 2016, in addition to facing a 35-month probation charge for gross negligence.[68] Despite his legal troubles, he has many followers who delay or skip vaccinations for their children, unnecessarily extending the period during which children are susceptible to *preventable* diseases due to untimely vaccination.

Overall, more research is needed to understand the factors that drive vaccine hesitancy, as well as where these factors are likely to cluster: in schools, in neighborhoods, or centered around providers with certain conversational styles around pediatric vaccinations. Increased legislation to tighten loopholes for NMEs is important to improve overall vaccination uptake, however a monolithic regulatory approach is unlikely to be wholly successful in reducing vaccine

hesitancy. More buy-in is needed from vaccination providers who can understand the power of experiences (personal, friend, or media-mediated) on vaccine acceptance and from policymakers, who together can help to identify ways to communicate with patients and develop policy to improve vaccination uptake.[69] An important component of this future research is to understand the ways in which uncertainty around disease risk and vaccine risk, as well as the role of communication of this uncertainty, fuels vaccine hesitancy.

Vaccine hesitancy and the COVID-19 pandemic

Since the COVID-19 pandemic emerged onto the global scene in December, 2019, infectious disease dynamics, public health policy, therapeutics, and vaccinations have been in the public eye considerably more than in the recent past. By April 2020, most of the U.S. population was under a shelter-in-place order of some kind, with highly criticized lockdowns seeming the only way to ensure population safety until the advent of a COVID-19 vaccine.[70] Despite COVID-19 being an infectious disease pandemic responsible for massive economic, public health, hospital capacity overflow, and daily life disruption, surveys have found that a sizeable proportion of the population is resistant to trusting a COVID-19 vaccine: surveys in France found that 26% of respondents would not take a COVID-19 vaccine,[71,72] and studies in the U.S.[73] and Italy[74] found that only 58% and 59% of respondents, respectively, intended to be vaccinated. It is also important to consider how vaccine hesitancy may reinforce observed disparities in COVID-19 morbidity and mortality,[75] a topic that the COVID Collaborative (a bipartisan group comprising former FDA Commissioners, CDC Directors, U.S. Surgeons General, leading public health experts, and members of front-line health worker advocacy groups, among others) has been exploring. In a November 2020 survey, the COVID Collaborative found that only 14% of

Black Americans and 34% of Latinx Americans believe that the COVID-19 vaccine would be safe, and only 18% of Black Americans and 40% of Latinx Americans trust that a COVID-19 vaccine would be effective.[76] These are highly troubling statistics that could threaten to increase observed disparities in COVID-19 infection among racial minorities in the United States.

With increasing politicization of a vaccination effort surrounding the November 2020 Election by President Trump, including rejecting the Food and Drug Administration (FDA)'s guidance about vaccine safety protocols,[77] trust in the government assuring vaccine safety and efficacy is eroding, contributing to increased vaccine hesitancy.[78] The COVID Collaborative survey found that this particular element was a significant driver of lacking trust, and such diminished trust followed racial lines, with only 4% of surveyed Black Americans and 18% of surveyed Latinx Americans having trust in the Trump Administration's COVID-19 response.[76] Additionally, 75% fewer Blacks and Latinx Americans would be willing to take a COVID-19 vaccine if it were granted only Emergency Use Authorization from the FDA.[76]

While the findings from the COVID Collaborative pertain directly to a COVID-19 vaccine, such findings indicate that public confidence in vaccines could be diminishing confidence in other vaccines as well.[79] This change in attitude towards vaccination is particularly dangerous in the context of COVID-19, where pediatric vaccination rates are plunging across the United States as individuals avoid non-essential medical visits and many preventive services have been suspended during the pandemic, potentially leaving many children under-immunized upon returning to the classroom.[80,81] It is critical now, more than ever, to understand the drivers of vaccine hesitancy and learn how to combat vaccine refusal effectively to reduce resurgent outbreaks of many VPDs concurrent with the COVID-19 pandemic.

1.2.4 Regulatory factors: vaccine mandates and exemptions

Historical precedent of vaccine mandates

The last element contributing to the resurgence of measles is the regulatory (legislative and administrative) system that permits vaccine exemptions for non-medical (i.e. philosophical and/or religious) reasons. The history of both compulsory vaccination and permissible reasons for exemptions harkens back to the late 1800s, when infectious diseases had high levels of endemic transmission across the US, and individual states began passing laws making vaccines compulsory for schoolchildren.[82] After a landmark case in 1905, *Jacobson v. Massachusetts*, the Supreme Court determined that public health vaccination mandates were constitutional, confirming that states do have the police power to protect public health and safety, even if doing so subordinates individual liberties to the common good.[83,84] This derives from the concept of *parens patriae,* Latin for "parent of his/her country," which grants the state the legal power to act as parent to those who cannot or will not take care of themselves as a constitutional doctrine.[85]

This case was raised by Pastor Henning Jacobson, who had been vaccinated against smallpox as a child and claimed both he and one of his sons endured adverse vaccine effects. He thus refused to vaccinate his other children after moving to Massachusetts, despite such vaccinations being mandatory for school entry, and refused to pay the fine incurred by not vaccinating his children.[83] The Court's interpretation of *parens patriae* was strengthened in *Zucht v. King* in 1922, where a young Rosalyn Zucht was excluded from entering both public and private schools in San Antonio, Texas after refusing her smallpox vaccination.[86] The Supreme Court ruled that schools could refuse to admit students who failed to meet the vaccination requirements from *Jacobson v. Massachusetts*.[86] Despite appeals to violations of

personal liberty, the court's affirmation of the constitutionality of these mandates would set the stage for compulsory vaccination laws moving forward.[86,87]

These landmark Supreme Court decisions affirmed the constitutionality of *parens patriae* for compulsory vaccination, but only 17 states had measles vaccination requirements for school entry in 1969.[87] Of these, only 12 states required vaccination against all 6 diseases for which routine vaccinations were available at the time.[87] Subsequent trouble controlling the spread of measles in the 1960s and 1970s prompted rapid change in state laws across the US, laying the groundwork for the mandatory vaccination laws in place today.[87] By the early 1980s, all 50 states had some requirements for children's school entry conditional on immunization status, a dramatic change from the legal landscape just a decade prior.[87] However, with new laws around mandatory vaccination came new loopholes and exemptions. Differences in state exemption policies created a mixed landscape of vaccination exemptions in the U.S., with some states permitting NMEs for religious, and/or philosophical reasons and others not.[82] Exemption rates have increased in recent years, coinciding with the resurgence of measles in the U.S.[23,88]

The resurgence of measles has drawn attention to the notion of these loopholes in exemption policies in the U.S. and contrasted the situation in the U.S. with that of other countries. However, it is important to note that mandatory vaccination is not a common practice worldwide: a recent study found that of 193 countries surveyed, only 105 (54%) had evidence of a national mandatory vaccination policy requiring at least one vaccine.[89] Of those, a slight majority, 62 countries (59%), enforce penalties on individuals who do not comply with vaccination requirements.[89] However, those penalties were highly variable – ranging in severity from one-time fines to jail time.[89] Some countries opt for different types of systems, like

Australia, which have no compulsory vaccinations, but use negative financial incentives to promote vaccination instead.[90]

Landscape of NMEs across the United States

In addition to the varied global landscape of mandatory vaccination policies mentioned above, within the United States (which has no national vaccination mandate), individual states have highly variable vaccination requirements. The ease of obtaining an NME range from very restrictive to very permissive (Figure 1.2) based upon the state. At one extreme, Ohio parents can simply sign a note indicating their child has immunity or disease history, exempting them from vaccination. By contrast, Mississippi, which has not allowed NMEs since 1999, has the best pediatric vaccination rates in the US, with no reported cases of measles since 1992.[91,92]

These state-by-state differences are becoming increasingly significant as rising parental concern around vaccine safety and effectiveness has led to more parents refusing vaccinations for their children, increasing the number of children with NMEs in the United States.[87] One of the great paradoxes of measles, and VPDs in general, in that as greater success is achieved in controlling them, there are fewer cases, and the perceived risk becomes low compared to negative press about vaccines, thus fueling the disproportionate fears about vaccine adverse reactions. It is for this reason that vaccines are often considered to be a victim of their own success, viewed less favorably as they effectively conquer infectious disease.

Beyond state-level differences, NME rates also vary by sociodemographic factors and by school type.[93] A study in California found that private schools had 2.2-fold higher NME rates than public schools for the 2009-2010 school year, while Waldorf schools had personal belief exemption (PBE) rates of an astonishing 45.1%, 19 times higher than public schools.[93] However,

understanding these statistics is complex. Under-vaccination (individuals who receive some, but not all, of their recommended vaccinations) and non-vaccination (individuals who receive no vaccines) broadly comprise two distinct groups: those who are under-vaccinated are often minorities of lower socioeconomic status with less education, while non-vaccinated children are often white, wealthy, highly-educated, and have private insurance.[92] The non-linear association of socio-demographics and overlapping networks of school, work, and household connections, complicated by variable state laws, make teasing apart issues related to vaccine hesitancy and exemptions quite challenging.

From 1991 to 2004, the average state-level NME rate in the U.S. increased from 0.98% to 1.48%, primarily driven by personal beliefs or philosophical exemptions (PBEs).[87,94] From 2011-2016, the rate of NMEs further increased from 1.75% to 2.25%.[95] These historical trends were summarized by Olive et al., who found that PBEs have risen in 12 of the 18 states that allow them (AR, AZ, ID, ME, MN, ND, OH, OK, OR, PA, TX, UT) since 2009.[23] Within these states, some standout metropolitan areas with very high numbers of NMEs might represent potential 'hotspots' for disease: notably Seattle, Spokane, and Portland in the Northwest; Salt Lake City, Provo, Houston, Fort Worth, Plano, and Austin in the Southwest; Troy, Warren, Detroit, and Kansas City in the Midwest; and Pittsburgh in the Northeast.[23] Olive et al. predicted that high numbers of NMEs in these densely populated urban areas would hasten outbreaks. This prediction was surprisingly accurate, with 5 of these cities in the top-10-risk category later experiencing a measles outbreak in 2019.

Legislation regarding vaccination rules and exemptions have occurred in parallel to these rising NME rates, with 10 major legislative changes occurring from 2011-2016 across the US.[95] Nine of these 10 policies made NMEs *harder* to obtain. Even more striking is how many pieces

of legislation related to vaccine mandates and exemptions have been introduced in recent years, with 26 states introducing 70 bills from 2014-2018, though only 11 of these 70 bills passed.[93] In the wake of the highly publicized Disneyland outbreak in California in 2014, most of these introduced bills (56/70) sought to make exemptions harder to obtain, and none of the bills proposing laxer requirements for vaccination exemptions (14/70) passed.[93] Michigan, after having the fourth highest NME rate in the country in 2014, modified its state Administrative Rules, effective January 1st, 2015, to make parents attend an in-person educational waiver education session at their local health department prior to a health department official signing their requested non-medical exemption waiver. Interestingly, this did not require a legal or legislative change and was instead implemented through the Michigan Department of Health and Human Services (MDHHS) Administrative Rules to avoid political conflict.[93] This bypass of the Republican legislature was strategic on MDHHS's part since the Republican-held legislature would not have been sympathetic to the proposal, and represents yet another pathway by which vaccines and exemptions can be regulated, with less fanfare than the legislative route.

In addition to reducing NME rates, such regulatory changes can impact the clustering of non-vaccinations, which is another important driver of outbreaks. In California, NME rates among kindergarteners increased from 0.73% in 2000 to 3.09% in 2013, though this increase was accompanied by a concerning increase in geographic clustering, making outbreaks even more likely.[24] Delamater et al. found evidence that regions with high levels of NMEs in 2000, which tended to have higher median household income and higher proportion of white race,[96] acted as seed locations, stimulating NMEs in nearby areas and showing evidence of social contagion.[24] California's responded to this increase in NMEs with two separate legislative changes to the ease with which exemptions could be obtained. In 2014, California passed Assembly Bill 2109 (AB

2109), which required parents to submit proof of discussing the risks of non-vaccination with a health care practitioner before obtaining an NME, a similar idea to Michigan's vaccine waiver education program, yet involving a trusted health care practitioner rather than a team of vaccine educators at the local health department.[25] California's AB 2109 led to a 0.3% decrease per year in NMEs, but ultimately had no lasting impact on geographic clustering of exemptions, rendering those communities in high exemption clusters at continued high risk of VPD outbreaks.[93]

A more stringent legislative effort in California went into effect just two years later, on July 1st, 2016. SB 277 eliminated philosophical vaccine exemptions entirely, accompanying an increase in childhood vaccination coverage by 3% in the following year.[93] However, as philosophical exemption rates plummeted, the rate of *medical* exemptions after SB 277 increased by 300%, indicating that vaccine hesitant parents in California may have been acquiring medical exemptions from doctors willing to provide them (including Dr. Robert Sears).[93] Additionally, SB 277's fine print states that students with an NME obtained before the 2016 school year need not receive mandatory vaccinations until the 7th grade school checkpoint, reducing the short-term effectiveness of this legislation.[26,27] However, despite these caveats, it does appear that SB 277 both reduced the number of under-vaccinated children and the number of schools inside geographic clusters of NMEs, thus likely reducing the risk of VPD outbreaks across the state.[25] Nonetheless, the implementation of SB 277 so soon after AB 2109 made it impossible to evaluate the longer-term outcomes of an education-based hurdle to non-medical exemptions in California, leaving room for further evaluation of the efficacy of such a policy.

Recent changes in legislation

As of December 2020, all but five states (California, Maine, Mississippi, New York and West Virginia) offer NMEs for either religious, personal or philosophical reasons.[97] Due to significant concern about the spread of measles across the U.S. in light of highly publicized and widespread measles outbreaks in 2019, three states changed their exemption laws over the course of 2019 to make non-medical vaccine exemptions harder to obtain at the state level.[97] New York State eliminated religious exemptions for vaccinations in response to the spread of measles in Orthodox Jewish communities,[98] Maine signed a law repealing religious and philosophical vaccine exemptions, and Washington signed a bill to limit personal belief exemptions to measles vaccinations.[97]

NMEs and disease risk

Olive et al.'s 2018 study[23] was surprisingly accurate at predicting hotspots for future measles outbreaks based on rates and geographic clustering of NMEs across the US, which illustrated an important, prospective proof-of-concept that clusters of NMEs can predispose regions to outbreaks. Additionally, Sarkar et al.[99] used a quantitative model to identify which U.S. counties were at the highest risk of a measles outbreak in 2019, using four factors to develop a risk profile at the county-level: international air travel volume, NME rates, population, and the incidence rate of measles at the origin location. Since its publication, 30 of the 45 counties that have reported a measles outbreak in the U.S. have been in either what Sarkar et al. deemed a "high-risk" county or were adjacent to a high-risk county.

Thus there is evidence that state laws allowing NMEs do have a direct effect on the rate of NMEs, and subsequently, the rate of preventable disease outbreaks within those states. In

addition, the restrictiveness of these NME requirements has been found to have an effect on the number of NMEs that are issued to parents, with states with more restrictive laws that impose greater hurdles and burdens on parents having fewer NMEs.[24] States with comparatively easy exemption policies have a higher average rate of NMEs (2.97%) compared to those with medium (1.77%) and hard (1.84%) exemption policies, though these differences were not significant.[95] The fact that the restrictiveness of the state policy affects NME rates has direct implications for how legislation regulating NMEs may influence vaccination coverage and illustrates that pursuing stricter regulations for obtaining NMEs is a useful and important avenue for reducing community susceptibility to VPDs.[84]

Finally, children with an NME have a higher risk of both acquiring and transmitting VPDs. Children with vaccine exemptions are as much as 35 times more likely to contract measles as nonexempt children, and 6 times more likely to contract pertussis.[87] In fact, studies have found evidence consistent with the hypothesis that geographic clusters of NMEs and waning immunity to the pertussis vaccine might be responsible for the resurgence of pertussis in the US.[100] In a study looking at pertussis in Michigan, Omer et al. found that Census tracts in an exemption cluster were three times as likely to also be a cluster for pertussis than tracts outside of an exemption cluster.[101] Similarly, in Oregon, geographic clusters of non-immunized children were found to drive a measles outbreak across the community.[102] Thus NMEs increase the risk of both acquiring and transmitting infectious diseases, further solidifying the importance of pursuing more stringent NME regulation as an actionable public health measure.

1.2.5 Goals of this dissertation

This introduction has discussed three factors that may have contributed to the global resurgence of VPDs, such as measles, despite access to effective vaccination and health care services. First, spatial clustering of non-vaccination creates small pockets of susceptibility, or coldspots, which can impact transmission dynamics and be missed by aggregate surveillance estimates, allowing outbreaks to occur in regions thought to be safe from VPDs due to high aggregate vaccine coverage. Second, vaccine hesitancy encompasses a spectrum of behaviors and attitudes towards vaccination, culminating in vaccine refusal. The origins of vaccine hesitancy are not fully understood, and its association with sociodemographic factors are also complex. More research needs to be done to understand how vaccine hesitancy changes over time and clusters geographically. Finally, regulatory factors such as variable state policies allowing religious and philosophical NMEs contribute to increased numbers of exempted children, and permit geographically clustered regions of non-vaccination and underlying anti-vaccine sentiment to proliferate, increasing community-wide susceptibility to VPDs. This dissertation will delve into these three factors in more detail to better understand their individual and collective contributions to the resurgence of measles in the United States as well as more local evaluations of the risk of outbreaks and vaccine policy effectiveness in Michigan.

Figure 1.1 Measles cases in the U.S. by year, 2010 – 2019. Adapted from CDC [103]

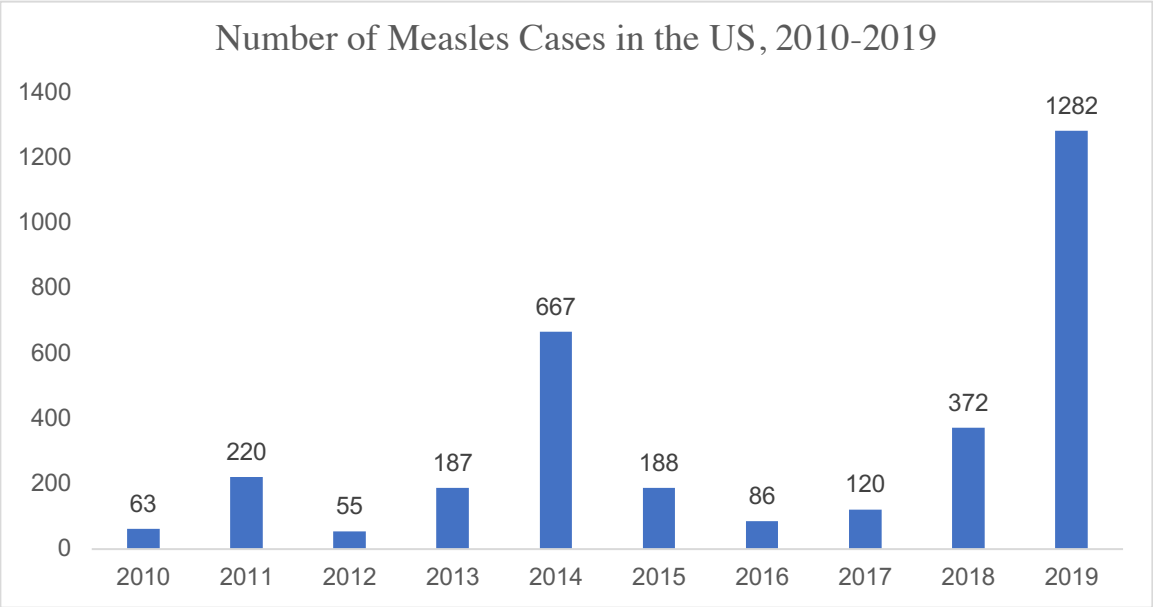

Figure 1.2 Landscape of U.S. vaccine exemptions permitted by state [104]

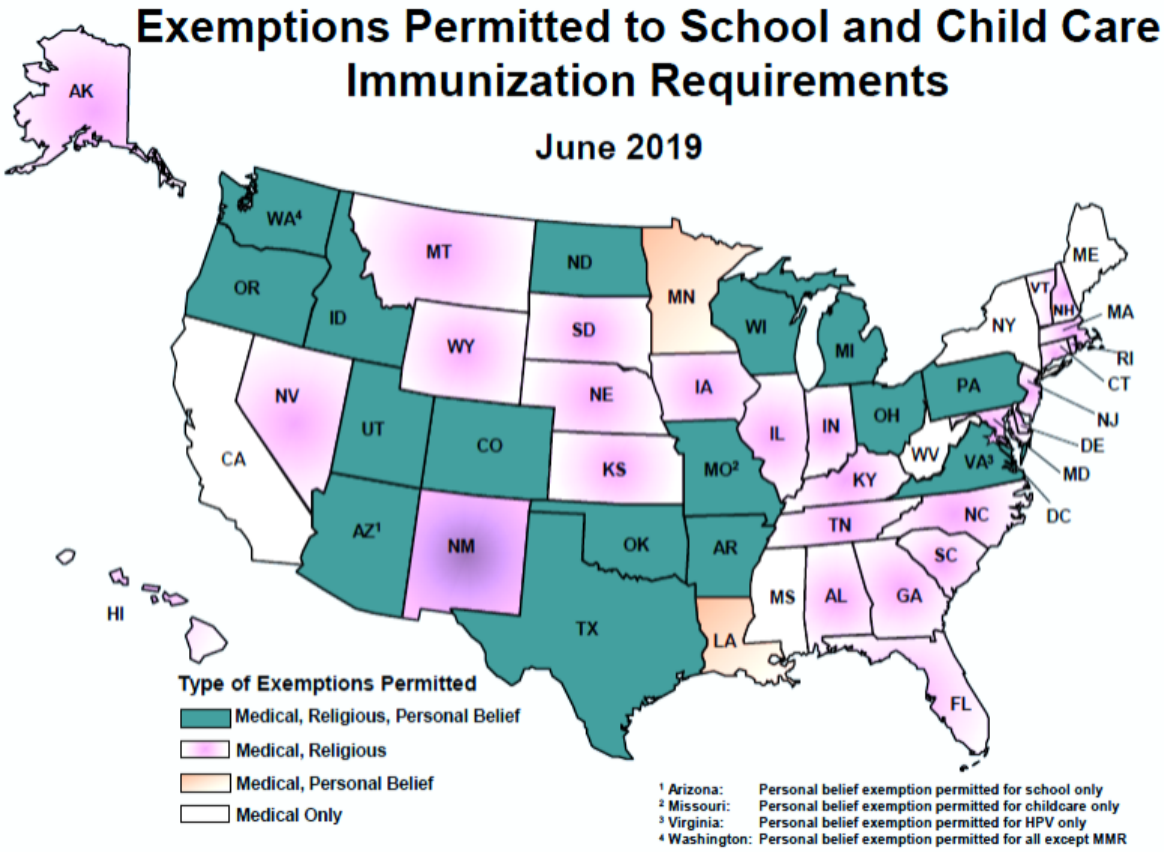

Chapter 2 Does Fine-Scale Spatial Clustering of Measles Non-Vaccination Increase Outbreak Potential? A Simulation-Based Study of the Impacts of Heterogeneous Non-Vaccination and Aggregated Reporting Data[1]

2.1 Significance statement

The U.S. witnessed large, persistent measles outbreaks in 2019, nearly losing its elimination status, despite achieving national measles vaccination coverage above the WHO recommendation of 95%. Previous research has shown that measles outbreaks in high-coverage contexts are driven by spatially clustered non-vaccination, locally depressing immunity levels. We perform a series of computational experiments to assess the impact of non-vaccination clustering on outbreak potential and how predictions of disease risk might be biased by measuring vaccination rates at coarse spatial scales. When non-vaccination is locally clustered, reporting aggregated data can substantially underestimate outbreak risk. This research illustrates that finer-scale vaccination data is needed to prevent a return to endemic measles transmission.

---

[1] This chapter has been published as: Masters NB, Eisenberg M, Delamater PL, Kay M, Boulton ML, Zelner J. Fine-scale spatial clustering of measles non-vaccination that increases outbreak potential is obscured by aggregated reporting data, *PNAS* 2020;117(45): 28506-28514.

2.2 Abstract

The U.S. experienced historically high numbers of measles cases in 2019, despite achieving national measles vaccination rates above the WHO recommendation of 95% coverage with two doses. Since the COVID-19 pandemic began, resulting in suspension of many clinical preventive services, pediatric vaccination rates in the U.S. have fallen precipitously, dramatically increasing the risk of measles resurgence. Previous research has shown that measles outbreaks in high-coverage contexts are driven by spatial clustering of non-vaccination, which decreases local immunity below the herd immunity threshold. However, little is known about how to best conduct surveillance and target interventions to detect and address these high-risk areas, and most vaccination data is reported at the state-level – a resolution too coarse to detect community-level clustering of non-vaccination characteristic of recent outbreaks. In this paper, we perform a series of computational experiments to assess the impact of clustered non-vaccination on outbreak potential and the magnitude of bias in predicting disease risk posed by measuring vaccination rates at coarse spatial scales. We find that when non-vaccination is locally clustered, reporting aggregate data at the state- or county-level can result in substantial underestimates of outbreak risk. The COVID-19 pandemic has shone a bright light on the weaknesses in U.S. infectious disease surveillance, as well as a broader gap in our understanding of how to best use detailed spatial data to interrupt and control infectious disease transmission. Our research clearly outlines that finer-scale vaccination data should be collected to prevent a return to endemic measles transmission in the US.

2.3 Introduction

The Global Vaccine Action Plan set a goal of measles elimination in five WHO regions by 2020. However, re-emergence of measles in ostensibly post-elimination settings and slow progress in endemic settings have thwarted these international control efforts, with 187/194 (96%) of WHO member states reporting measles cases in 2019.[105] Globally, the first half of 2019 witnessed the most reported measles cases since 2006, with 791,143 suspected cases in 2019, compared to 484,077 in 2018, a 63% increase.*(2,3)* Recent drops in vaccination coverage have threatened the WHO American Region's measles elimination status, attained in 2000.[10]

In the United States, a 2014 measles outbreak originating at Disneyland was the largest, most-publicized outbreak event since the declaration of elimination.[12] Majumder et al. estimated that the vaccination rate among those infected in this outbreak was between 50%-86%, much lower than California's state average of 92.8% (± 3.9%), [3,15] and the national average of 91.9%.[15] Local variability in measles vaccine coverage likely contributed to the size of the outbreak, with Pingali et al. finding 93 regions, or 'coldspots', encompassing 31% of California's primary schools, where many kindergarteners were not up-to-date for recommended vaccinations.[108] This demonstrates how fine-scale clustering of non-vaccination can increase the likelihood of outbreaks while 'flying below the radar' of statewide statistics. Such exemption clusters have also been responsible for outbreaks of pertussis in Michigan[109] and Florida[110], and measles in Oregon.[102] Vaccination heterogeneity is a key threat to measles elimination and control: in the U.S. alone, 2019 saw 1,282 cases of measles in 31 states, the most since 1992, making a return to endemic measles likely if these trends are not rapidly reversed. [16]

2.3.1 Redefining vaccination coverage targets

To meet global elimination goals, the WHO has set vaccination coverage targets of 95% for the first and second doses of the pediatric measles-containing vaccine (MCV).[5,6] High coverage of MCV is necessary because measles is highly contagious with a basic reproduction number (R_0), of 12-18, among the highest known values, though estimates of the R_o are quite variable.[111,112] Although the MMR vaccine is highly immunogenic, with two doses conferring 97% protection, [2] the proportion of the population that needs to be vaccinated or have natural immunity from prior disease to prevent outbreaks, known as the critical vaccination fraction (V_c),[2] is nonetheless very high, around 94-95% [1,3]. A key assumption underlying most estimates of V_c is that the population is evenly mixed and that all susceptible, infectious, and immune individuals contact each other with equal probability. However, when non-vaccinated individuals are geographically clustered, this formula can underestimate V_c by as much as 3%, so that outbreaks remain possible despite statewide vaccination coverage targets being met or exceeded.[22]

---

[2] This can be calculated as $R = R_0 * ((1 - (V_c * V_E))$, where $1 - (V_c * V_E)$ is the proportion of the population that remains susceptible after vaccination. The V_c can be expressed in terms of infectiousness and vaccine efficacy:

$$V_c = \frac{1 - \frac{1}{R_0}}{V_E}$$

where V_E is the proportion of vaccinated individuals protected from disease, or the vaccine efficacy.[22]

2.3.2 What is the right scale of surveillance?

While the role of heterogeneous mixing and infectiousness in populations in increasing outbreak risk for vaccine-preventable diseases (VPDs) has been demonstrated in prior studies [23,24,26,108,109,113–116], public health surveillance systems typically report vaccination coverage at the county and state level – obscuring this risk. For example, in Michigan, 4.54% of kindergarteners statewide had vaccination waivers for the 2018-2019 school year – meeting the WHO threshold of 95% overall vaccination. That same year, a large measles outbreak occurred in Oakland County, where the waiver rate was 7.14%, but school-district waiver rates ranged from 0 – 23.4%, and two schools reported > 50% waivers (Figure 2.1A).

Additionally, many clinical preventive services have been suspended in the wake of the COVID-19 pandemic, with many individuals fearful of doctors and non-emergent visits delayed, which has led to plummeting pediatric vaccination rates nationally; an estimated 400,000 *fewer* measles-containing vaccine (MCV) doses were ordered January 6 - April 18, 2020 than were ordered over the same period last year.[80] In Michigan, vaccination rates have dropped to dangerously low levels for measles in particular – with only 70.9% of 16-month-old children currently up to date for MCV – down from 76.1% last year.[81] As such, understanding the role that clustering of non-vaccination for measles plays in outbreak risk is especially important – as existing clusters are likely to be magnified by plummeting pediatric vaccination rates. Furthermore, elucidating at what scale aggregate surveillance data is too unreliable to capture such fine-scale heterogeneity will be necessary to successfully implement control strategies for *both* emergent measles outbreaks and ongoing COVID-19 infections. Because granular vaccination data is not readily available to researchers, this paper uses a simplified, schematic

model to provide proof-of-concept and understand the mechanisms by which clustering of non-vaccination, and aggregation of such data, impact population health and outbreak risk.

2.4 Methods

2.4.1 Simulated environment

To understand how aggregation of surveillance data may impact outbreak risk assessment, we constructed a spatial measles transmission model in a simulated city of 256,000 people laid out on a 16x16 grid. Our model includes four nested levels analogous to those found in real vaccination data, 1000-person *blocks* (1 cell), 4000-person *tracts* (4 cells), 16,000 person *neighborhoods* (16 cells), and 64,000 person *quadrants* (64 cells). This configuration allows us to fix the population average vaccination coverage while varying the spatial distribution of coverage at multiple scales to isolate the specific impact of clustering at different levels. Our model encoded contact between individuals within each block and with contiguous blocks, as school-aged children have primarily local contacts. Contact between blocks used queen's contiguity, in which all surrounding cells are considered neighbors (cells which share an edge or a corner with the index cell, such that cells in the center of the grid would have eight neighbors). The spatially dependent force of infection was split such that 50% of transmission occurred *within* cells and 50% of transmission was *split between all neighboring cells equally*. We fixed population-wide measles vaccine coverage at the WHO threshold for measles (95%) while varying the spatial distribution and intensity of local clustering of vaccination (Figure 2.1B-C). In all simulations, R_0 was fixed at 16, and the average community vaccination coverage was 95%, which represents a scenario in which a completely homogeneous model would predict that an outbreak is not possible.

2.4.2 Clustering motifs of non-vaccination

Clustering motifs were generated using stratified random sampling at the quadrant, neighborhood, tract, and block level to produce different landscapes and spatial distributions of non-vaccinators within this population. The motifs were created by sampling 12,800 (5% of the total population) unvaccinated individuals into individual cells with probability proportional to the intensity of clustering at each of the four nested spatial levels, allowing us to explore the difference in outcomes between motifs with equivalent vaccination coverage but with large- vs. fine-scale clustering, and vice-versa. A depiction of this process is shown in Figure 2.6. In all simulations, we assigned the top-left quadrant to be the most highly-clustered quadrant, and explored scenarios in which 85% of the non-vaccinators were in that quadrant, and the remaining 15% evenly distributed among the remaining quadrants, to the least clustered case in which a quarter of non-vaccinators were deposited in each quadrant. Three additional sets of probabilities generated the full set of clustering motifs: 70%, 58%, and 40% of non-vaccinators in the top left quadrant, distributing the remaining 30%, 42%, and 60% of non-vaccinators evenly among remaining quadrants, respectively. Of the 625 potential clustering motifs representing every combination of probabilities, 336 were consistent with a scenario of 95% vaccination coverage at the population level, i.e. where the proportion of non-vaccinators in each cell was ≤ 1.

2.4.3 Model structure

We modeled transmission using a deterministic, compartmental, Susceptible-Infected-Recovered (SIR) model (Equation 2.1) where the clustering motifs representing different landscapes of non-vaccination were used as initial conditions for the compartmental transmission

model (Figure 2.7) [22,23]. For simplicity, no vital dynamics were included due to a simulation time of one year.

2.4.4 Measuring clustering

Clustering of non-vaccination in each motif was measured using Moran's I, a measure of global spatial autocorrelation[117] and the isolation index, a measure of the proportion of within-group contacts in a population with two main sub-groups (i.e. vaccinated and unvaccinated)[118]. Moran's I (Equation 2.2) ranges from -1 to 1, where a value of -1 corresponds to perfect clustering of dissimilar values (e.g. high-low clustering), 0 indicates no autocorrelation, and 1 indicates perfect clustering of similar values (e.g. high-high)[117]. By contrast, the Isolation Index (Equation 2.3) measures exposure, specifically the extent to which non-vaccinated individuals contact each other: if there is little systematic separation of the groups, the value of isolation will approach the global percent of non-vaccinators, and will approach 1 when non-vaccinators are highly concentrated in one geographic location.[118]

2.4.5 Measuring aggregation effects

To examine the how the resolution of vaccination data impacts model-based risk predictions, we created counterfactual simulations to see how much error was incurred by coarsening the spatial vaccination data. This is analogous to quantifying 'Type M' errors of magnitude described by Gelman et al.[119] The clustering motifs described above were regarded as the 'true' vaccination data, with resolution at the block level. The grid was coarsened by moving up the levels of aggregation shown in Figure 2.1: block-level data was aggregated up to the tract level, where the four cells that belong to each tract were averaged and non-vaccinators were

redistributed to the contributing cells. This process was then repeated at the neighborhood and quadrant level. Once these aggregated motifs were generated, we ran the SIR model on the coarsened grids to see how the predicted case burden differed from that of the block-level, 'true' data, using the difference in these predictions to characterize the bias from aggregating this data.

2.4.6 Statistical analysis and simulation protocol

Simulations were conducted in R version 3.6.0 using the *deSolve* package. The SIR model was simulated across the clustering motifs and the outbreak potential and cumulative incidence were calculated for four scenarios: an initial seed case dropped in the center of each quadrant to capture spatially heterogeneous outcomes based upon the location of the introduced case. The attack rate (AR) after one year of simulation time was calculated, with AR = 1 year cumulative incidence / initial susceptibles. For each motif, ten simulations were run for a seed case dropped in *each* quadrant to capture stochastic variation due to the multinomial probability distribution used to generate the motifs themselves, generating 40 simulated runs for each motif. The Moran's I and Isolation Index of the starting motifs were calculated by generating the motifs 30 times each and taking the average value to account for sampling differences. The Isolation Index was normalized using the formula: normalized Isolation = (Isolation Index - minimum Isolation) / (maximum Isolation – minimum Isolation)) for easier interpretation. For assessing outbreak potential, we defined an outbreak as a simulation with 5 or more secondary cases. Code used to generate all simulations, motifs, and datasets can be found at: https://github.com/epibayes/Measles-Spatial-Clustering-and-Aggregation-Effects/

2.4.7 Sensitivity analysis

Numerous sensitivity analyses were conducted to evaluate the robustness of our findings to different assumptions. Our baseline model uses density-dependent transmission where the force of infection for neighbor-driven transmission dependent on the number of neighbors, and we assessed the model instead with a frequency-dependent force of infection. Additionally, the baseline model assumed that 50% of transmission occurred within cell, and 50% was divided between neighboring cells. We varied this percentage of between-cell transmission from 10% to 75% to examine the impact of changing neighbor-driven transmission. Finally, the overall percentage of vaccination was modified from the baseline scenario of 95%, with sensitivity analyses using 94%, 98%, and 99% overall vaccination (yielding a total number of possible motifs that did not exceed cell-level populations over 1,000 of 296, 543, and 620, respectively). We also assessed combinations of different vaccination percentages and between-cell transmission rates to explore the impact of varying both parameters at once.

2.5 Results

2.5.1 Impact of clustering on outbreak probability and size

The intensity of clustering of vaccination and contact between non-vaccinators was assessed using Moran's I [117] and the Isolation Index [118]. In both univariate and multivariate models, for 95% overall vaccination, a change from the minimum to maximum values of normalized Isolation was associated with an 80% increase in AR (~7,325 cases), while no association was observed for Moran's I (Table 2.1). This suggests that isolation better captures the central role of clustering of susceptible individuals than Moran's I, which is agnostic about the nature of clustering measured (i.e. of non-vaccination *or* vaccination).

2.5.2 Impact of clustering on outbreak risk and magnitude

Simulations from this model at 95% coverage across all possible clustering motifs (n = 336) yielded an average cumulative AR of 30% (Table 2.2). Sensitivity analyses evaluating the cumulative incidence and AR at 94%, 98%, and 99% coverage showed that large outbreaks were possible at all coverage rates when non-vaccination was spatially clustered. By contrast, a full environment-level simulation (with spatially randomly distributed non-vaccinators, i.e. no encoded clustering), revealed that at 95% vaccination coverage and above, there was fewer than 1 secondary case, and only 1.24 secondary cases observed for 94% overall vaccination, indicating that herd immunity is upheld when there is no spatial clustering of non-vaccination (Table 2.3). In all simulations, when the initial case was seeded in the quadrant inhabited by the majority of non-vaccinators, a larger outbreak was predicted as compared to seeding cases in the other quadrants, with introductions to quadrant furthest in cartesian distance from the low-vaccination area resulting in fewest overall cases and longest time-to-peak of cases. Most cases occurred in cells with low vaccination rates, though there was spillover to adjacent cells due to high levels of infection pressure from their low-coverage neighbors (Figure 2.2). Sensitivity analyses of frequency-dependent transmission yielded similar cumulative incidence counts to the density-dependent baseline model (Table 2.4).

Our simulations consistently showed that increasing clustering at each level of aggregation (blocks, tracts, neighborhoods, and quadrants) corresponded to higher cumulative incidence of cases (see Appendix A Figure A.5- Figure A.8). In addition to exploring the outbreak size as an outcome, we evaluated outbreak probability, defining three thresholds for an outbreak: 5, 10, and 20 cases over the course of one year. For 94% overall vaccination, 93.5% of simulation runs yielded outbreaks (defined as 5 or more cases), and there was a 92.3%

probability of an outbreak with a threshold of 20 cases (see Appendix A Table A.3, Figure A.13, Figure A.14). For 95% overall vaccination, 89.0% of simulation runs generated a 5+ case outbreak, and 87.4% of simulation runs generated a 20+ case outbreak. For 99% vaccination coverage, the outbreak probability was much lower: 19.3% of simulation runs generated 5 or more cases, and 18.1% of runs generated 20 or more cases. These results show that outbreak probability decreases as coverage increases, yet in this clustered landscape of non-vaccination, even for 99% overall vaccination rates, there was a sizeable proportion of simulation runs that were able to generate outbreaks.

2.5.3 Impact of measurement scale on outbreak size prediction errors

Our design analysis consisted of taking the block-level 'ground truth' results of each simulation and aggregating these data up to each of the levels in Figure 2.1. This resulted in large downward biases in both the simulated probability of observing outbreaks and their predicted size. The expected outbreak size for simulations at 95% overall vaccination was predicted to be 3886 (AR=30.4%) cases using unaggregated data, 2122 (AR=16.6%) using tract-level aggregation (45.4% reduction), 911 (AR=7.1%) using neighborhood-level aggregation (76.5% reduction), and 227.3 cases when aggregated to the quadrant level (94.2% reduction) (Figure 2.3). Figure 2.4 illustrates how this aggregation process obscures fine-scale spatial heterogeneity for three selected motifs, where three very different underlying patterns of non-vaccination and resultant outbreak potential converge to an identical motif with an expected AR of 51% when aggregated to the quadrant level. Across all motifs, the downward bias in the estimated isolation index increased with the intensity of aggregation (Appendix A Figure A.9).

Aggregating vaccination data resulted in consistent underestimates of outbreak potential, with this bias growing as a function of the intensity of clustering in the input motif and the level of aggregation (Figure 2.5). This trend was observed across all motifs, with models using data aggregated to the tract-level predicting 41% - 65% fewer cases than simulations using non-aggregated data, and neighborhood-level aggregation resulting in 72-99% fewer cases detected (at 94% and 99% overall vaccination, respectively) (Appendix A Table A.4). Quadrant-level aggregation resulted in greater than 90% reduction in detected cases at *all* tested vaccination levels. The proportion of expected cases plotted by isolation index of the initial motif can be seen in Figure 2.5A, however it is important to recall that increasing isolation index corresponds to increased simulated cumulative incidence, thus higher levels of aggregation yield reduced accuracy in predicting outbreak potential, with greater numbers of cases *missed*, as vaccination landscapes become more clustered (Figure 2.5B). This phenomenon was observed for all simulated vaccination levels (see Appendix A Figure A.10, Figure A.11, Figure A.12).

2.6 Discussion

Our results illustrate how failure to account for fine-scale heterogeneity in susceptibility can result in overly optimistic estimates of outbreak potential. This mismatch between assumptions of homogeneous mixing which underlie the classical calculation of the V_c and the reality of local clustering of non-vaccination can lead to missed opportunities for preventing outbreaks. This is underscored by the finding that even at 99% overall vaccination coverage, theoretically far exceeding the V_c for measles, deviations from homogeneity permitted outbreaks to occur. We found increasing isolation of non-vaccination predicted increased cumulative

incidence at all vaccination levels, suggesting that the isolation index can be used to assess area-level outbreak vulnerability.

Additionally, our models show that aggregation-based estimates of outbreak risk relying on assumptions of homogeneity have the potential to mischaracterize the population at risk. As fine-scale vaccination data was aggregated, or 'coarsened', a large downward bias resulted in the projected number of cases, which grew with successive levels of aggregation. This has immediate implications for vaccine-coverage surveillance in the US, highlighting that finer-scale data are needed to fully understand community susceptibility to outbreaks of measles and other VPDs. This accords with Truelove et al. and Brownright et al.'s suggestions, [22,120] that setting the classical V_c as a national or state-wide vaccination target may ultimately permit endemic transmission, necessitating a greater focus on assessments of finer-scale vaccination levels. Similarly, Tatem [121] argues that fine-scale analysis can better highlight communities at risk, though public health surveillance would to need to be strengthened and enhanced, requiring a greater structural investment for this to be carried out effectively. Additionally, as shown in Figure 1A, regions without available vaccination data are often aggregated up into areal estimates of vaccination coverage, propagating errors associated with this missingness upward, which only further highlights the need for collection and dissemination of finer-scale vaccination data in order to make informed decisions about populations at risk.

An important caveat is that while vaccination data is collected at the school-level for entry requirements, publicly released data instead are typically aggregated to the county- or state-level despite the existence of finer-scaled data, representing a lost opportunity for improving surveillance. Leslie et al. found that only 20 U.S. states report school-level data, 4 report school-district level data, 19 report county-level data, and 2 report health department level data, but only

a subset (n = 26) provide such data online, with 14 states providing data only after onerous Freedom of Information Act Requests.[122] Additionally, the CDC receives state-level vaccination data, which is far from the granular scale needed to set national policies that are sensitive to local vulnerability to measles.[123]

Identifying the scale at which vaccination data is reported and available for analysis is not straightforward and comes with important trade-offs between privacy, feasibility, and cost. Many policy benchmarks are set at the national level, which may fail to account for transmission dynamics playing out on a smaller scale, as coverage estimates of large regions cannot assume herd immunity is maintained at the scale of transmission. When defining such a spatial scale, relevant considerations comprise the potential intervention, the scale of surveillance, the reality of obtaining high-quality, granular data, and the level at which vaccination coverage estimates are meaningful and actionable.

A number of different spatial scales have been explored in the literature, with notable heterogeneity in vaccination coverage identified at the sub-continental level, subnational [120], and regional levels.[30] If the geographic level of data is mismatched to the scale of an intervention,[31] reliance on aggregated data may result in diminished effectiveness of aid and interventions, leading to erroneous conclusions about what works for preventing VPD outbreaks [34]. To address varied findings at different levels of analysis, some authors have also attempted to use multiple spatial scales, though such studies have yielded poor predictive ability.[32,33,] At the finest spatial scales, such as human individual movement[37,38] or mobility data using cell phone records,[35] there is significant potential for the introduction of too much noise, yielding less informative results.[36] As such, it is important to acknowledge that more research must be done to elucidate a feasible and actionable spatial scale to evaluate vaccination coverage, especially in countries nearing

measles elimination where significant heterogeneity is may undermine elimination efforts if unidentified.

2.6.1 Strengths and limitations

This study has many strengths. Much of the literature surrounding spatial clustering of non-vaccination utilizes complex methods of identifying 'hotspots' of infection in an environment with many complicating factors surrounding the reliability and accuracy of geographic and immunization coverage data, such as data that is spatially 'jittered' to preserve anonymity. [22,120] Our work provides a much needed proof-of-concept, illustrating that fixing vaccination coverage and adjusting only the degree of clustering has large impacts on the risk and magnitude of outbreaks. Additionally, the literature on spatial heterogeneity in vaccination coverage is typically focused on patterns observed in vaccination coverage or serology data. Our use of simulation in an idealized environment allows for a better understanding of the implications of the types of clustering identified in these earlier analyses for outbreak risk.

This study has some limitations as well. We used an SIR model, which does not use an incubation period (which could be encoded using an SEIR model with a compartment for latent infection) because the time dynamics of transmission were not a key focus of this paper, and both models will result in the same predictions of epidemic size. We also did not consider vaccine failure (i.e. assumed 100% vaccine effectiveness), and thus our results likely *underestimate* the number of cases that could occur in a worst-case-scenario. Additionally, we used a deterministic transmission model to highlight the impact of clustering of non-vaccination and aggregation, yet the occurrence and size of outbreaks is in reality a function of both stochasticity in the population distribution of susceptibility – which we model explicitly – and

demographic stochasticity in transmission dynamics, which our model omits. The use of a deterministic model allowed us to focus specifically on the stochastic variation of the spatial distribution of non-vaccination, but our results should be interpreted in light of this choice. Finally, a square grid with fixed population size of 256,000 individuals is a stylized, simplified representation of a city, and is not meant to directly represent the complexity of real-world contact networks, but instead seeks to capture a mix of local and non-local transmission. Making optimal use of these findings necessitates understanding how this heterogeneity impacts dynamics in the context of more heterogeneous and multi-layered contact networks. Finally, the model's dynamics are dependent upon our choice to analyze a population smaller than the critical population size of ~400-500,000, above which endemic circulation becomes possible. This allowed us to focus on the types of outbreak scenarios that are currently of the most pressing concern, but limits applications of this research to endemic transmission.

2.7 Conclusions

We show that the assumptions of spatially homogeneous vaccination coverage and contact result in an underestimation of the true number of individuals who need to be vaccinated to prevent outbreaks. Fine-scale clustering, as measured by high values of the Isolation Index, produced scenarios with the greatest outbreak potential. Since such fine-scale vaccination data is not broadly available in the United States, it is difficult to allocate resources, plan vaccination strategies, and respond to imported measles cases in a way that is responsive this type of localized clustering. Especially given the ongoing pandemic, it is imperative to better understand and control the spread of preventable diseases such as measles – focusing on concrete ways to reduce case burden and health service utilization - as the coming school year is likely to see

unprecedented challenges as COVID-19 cases grow and the fall influenza season approaches. The approach here is also likely to have important implications for managing COVID-19 therapeutic/vaccine distribution, as clustering of susceptibility and immunity are likely to occur in the communities both least and most hard-hit in the first waves of transmission. As noted by Truelove et al., fine-scale clustering of the sort described here resulted in the largest increases in the critical vaccination fraction for diseases with lower values of R_0. This suggests that issues around spatial clustering of susceptibility to COVID-19, which has an R_o roughly four times lower than measles, may be as or more acute as in the scenarios described here.[22] This research thus motivates the need not only for increased vaccination coverage, but also for the collection of finer-scale vaccination data to create 'susceptibility maps' that can guide policy-makers and health practitioners to preferentially direct resources to those areas at highest risk of outbreaks.

Figure 2.1 Impact of spatial aggregation of vaccination data on coverage estimates

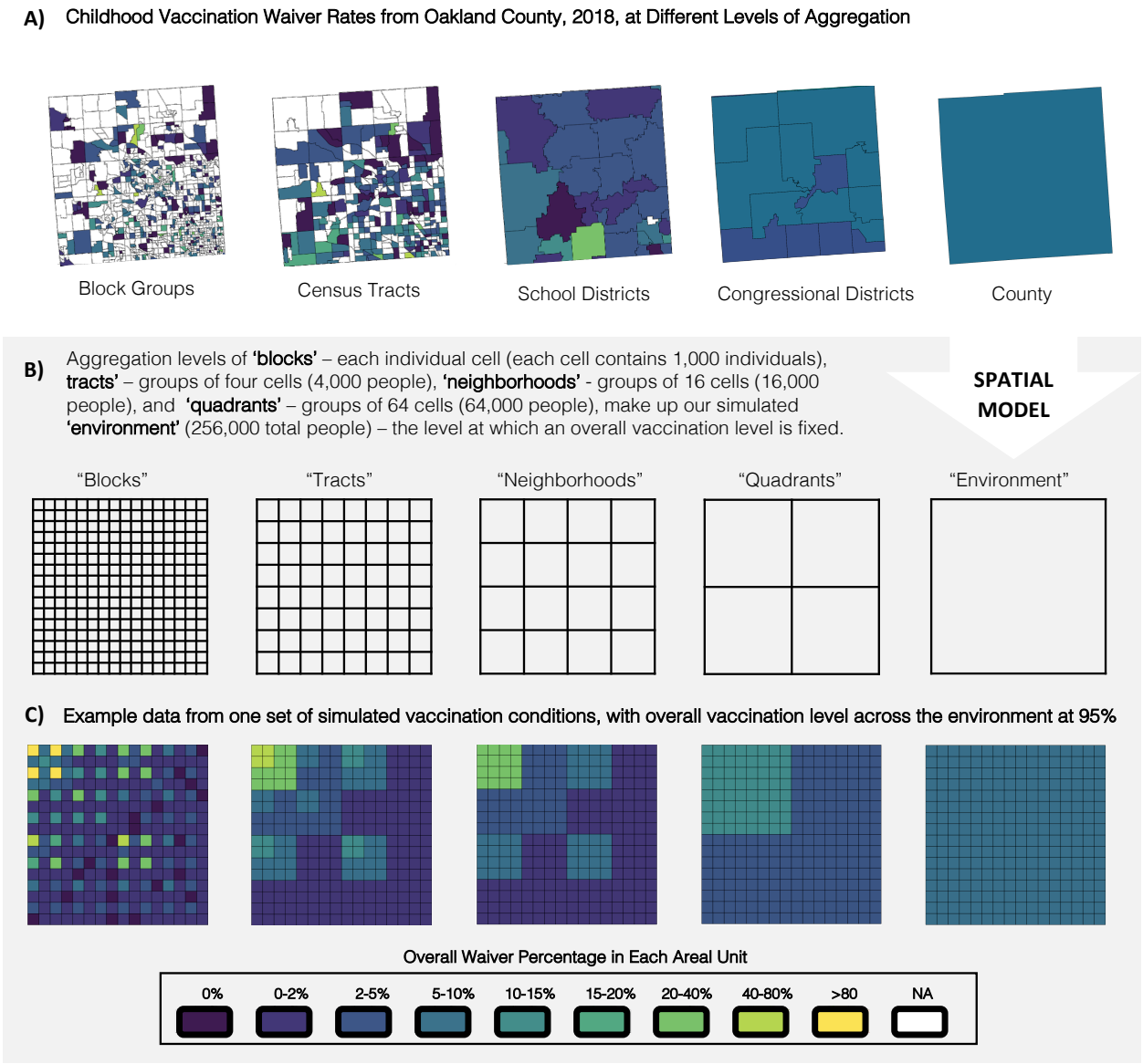

A) Vaccination coverage data from Oakland County, Michigan at five different levels of spatial scale: block groups, Census tracts, school districts, congressional districts, and the county-level. B) Schematic illustrating the spatial model used in this study, with a 256-grid cell environment, each which contains 1,000 individual people, divided into spatial scales of 'blocks' (all grid cells), 'tracts' (groups of four cells), 'neighborhoods' (groups of 16 cells), 'quadrants' (groups of 64 cells), and finally the entire vaccination 'environment' (all 256 cells aggregated to one unit), the level at which overall vaccination percentages are fixed for analysis (i.e. at 95%, 98%). C) Example data from one simulated set of vaccination conditions, fixed at 95% overall vaccination, showing impact of aggregation to these different scales on loss of granularity of block-level data.

Figure 2.2 Distribution of non-vaccination at baseline (left) and case burden after 1 year (right) for four selected clustering motifs with 95% overall vaccination coverage

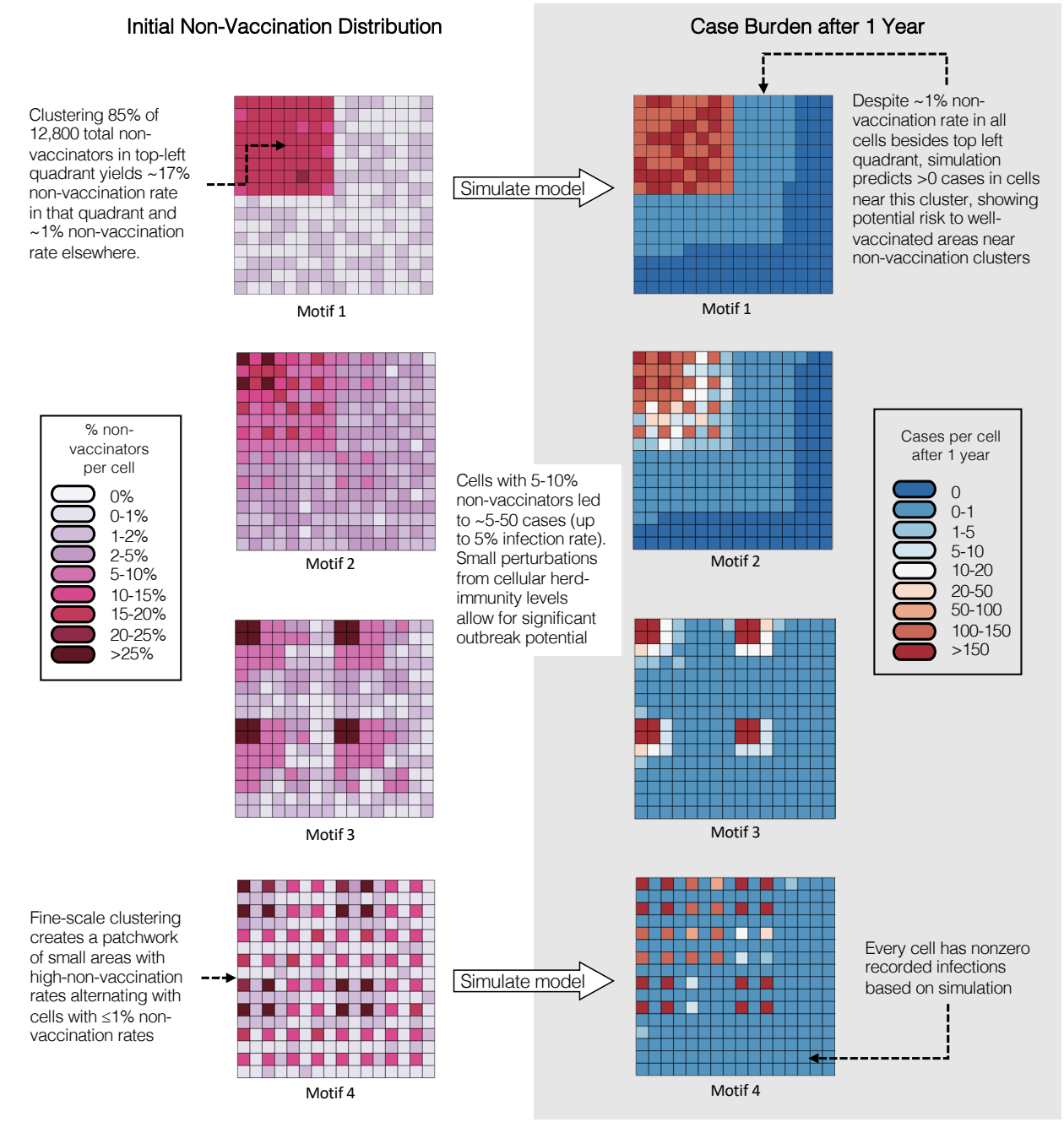

In each case, a seed infection was introduced into the top left quadrant and cases spread throughout and beyond the demarcated boundaries of high-risk unvaccinated regions, as can be seen for motifs 1 and 2. For motif 3, the four foci of non-vaccination with >25% unvaccinated proportions are the hardest hit in terms of attack rate after 1 year, with > 150 cases per cell (>15% attack rate), but the surrounding cells, with 5-10% non-vaccination, see 10-50 cases after 1 year, representing a 1-5% attack rate. Finally, for motif 4, a fine-scale clustering pattern creates local cells with high attack rates, but all cells have a nonzero attack rate.

Figure 2.3 Impact of scale of aggregation on estimated outbreak size (cumulative incidence) at 94%, 95%, 98%, and 99% overall vaccination coverage

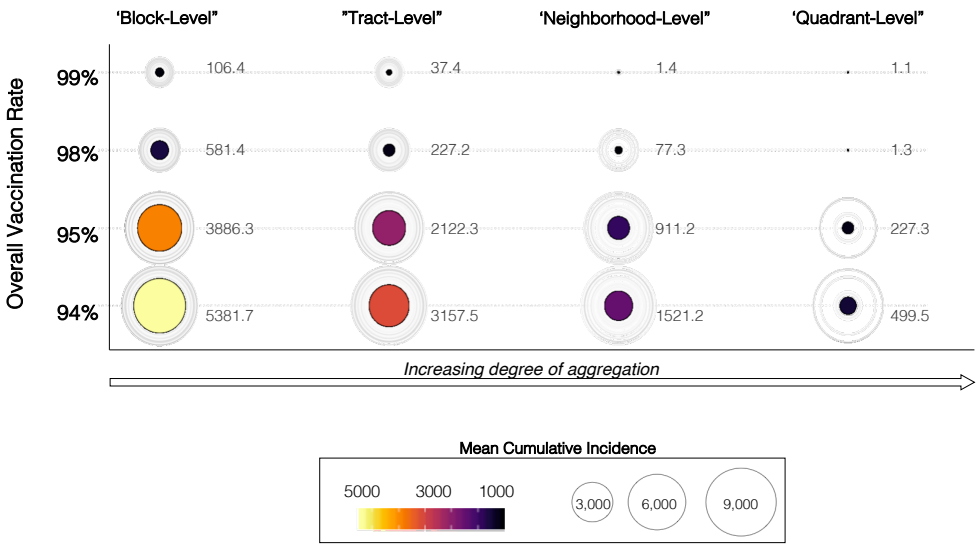

The mean cumulative incidence (outbreak potential) across all clustering motifs, varying levels of overall vaccination (94%, 95%, 98%, 99%), shows notable **reduced predicted outbreak size** as data is aggregated up from the block level, or ' ground truth' in the simulation results, meaning that evaluating data at high levels of aggregation might not only **miss potential local clusters of heterogeneity that can prompt a large-scale outbreak, but poorly predict outbreak risk.**

Cumulative incidence at four different levels of vaccination coverage: 94%, 95%, 98%, 99%, including non-aggregated vaccination data (block-level) resolution to tract level (4-cell) resolution, to neighborhood (16 cell), and finally quadrant-level (64-cell) shows the reduction in estimated case burden as aggregation increases, a pattern that holds true across all levels of vaccination.

Figure 2.4 Aggregated vaccine coverage systematically downplays outbreak risk, an example using three distinct motifs which are aggregated to become an identical motif at the quadrant level

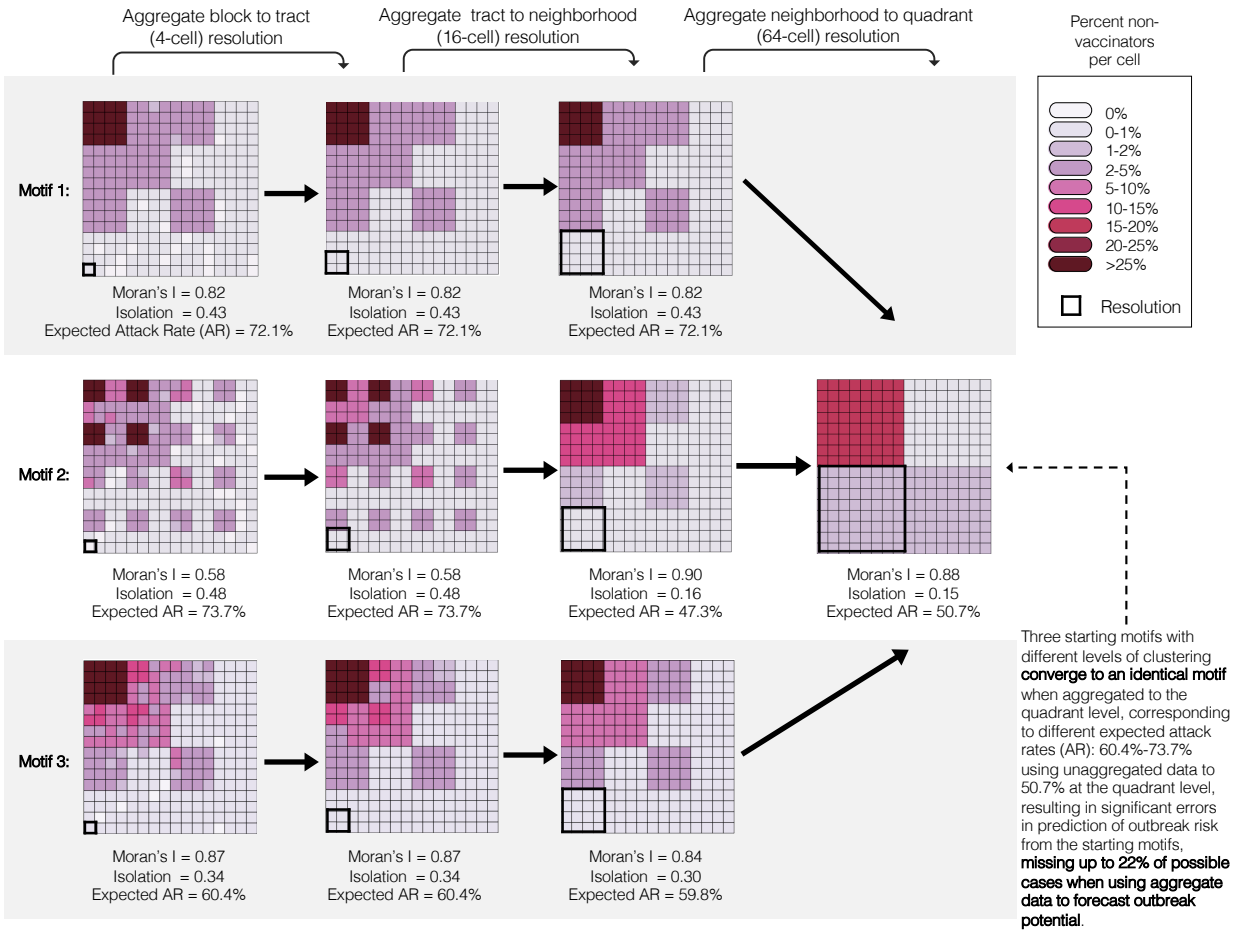

Aggregation from 'true' 256-cell (block-level) resolution to tract level (4-cell) resolution, to neighborhood (16-cell), and finally quadrant-level (64-cell) resolution using a starting vaccination motif with overall vaccination at 95%. Three different motifs with different clustering patterns were subsequently aggregated up these three levels and yielded the same aggregate motif at the quadrant level, illustrating that large-scale vaccination data can mask significant heterogeneity at finer scales.

Figure 2.5 Underestimates of outbreak risk grow with increasing Isolation Index of non-vaccinators in initial clustering motifs

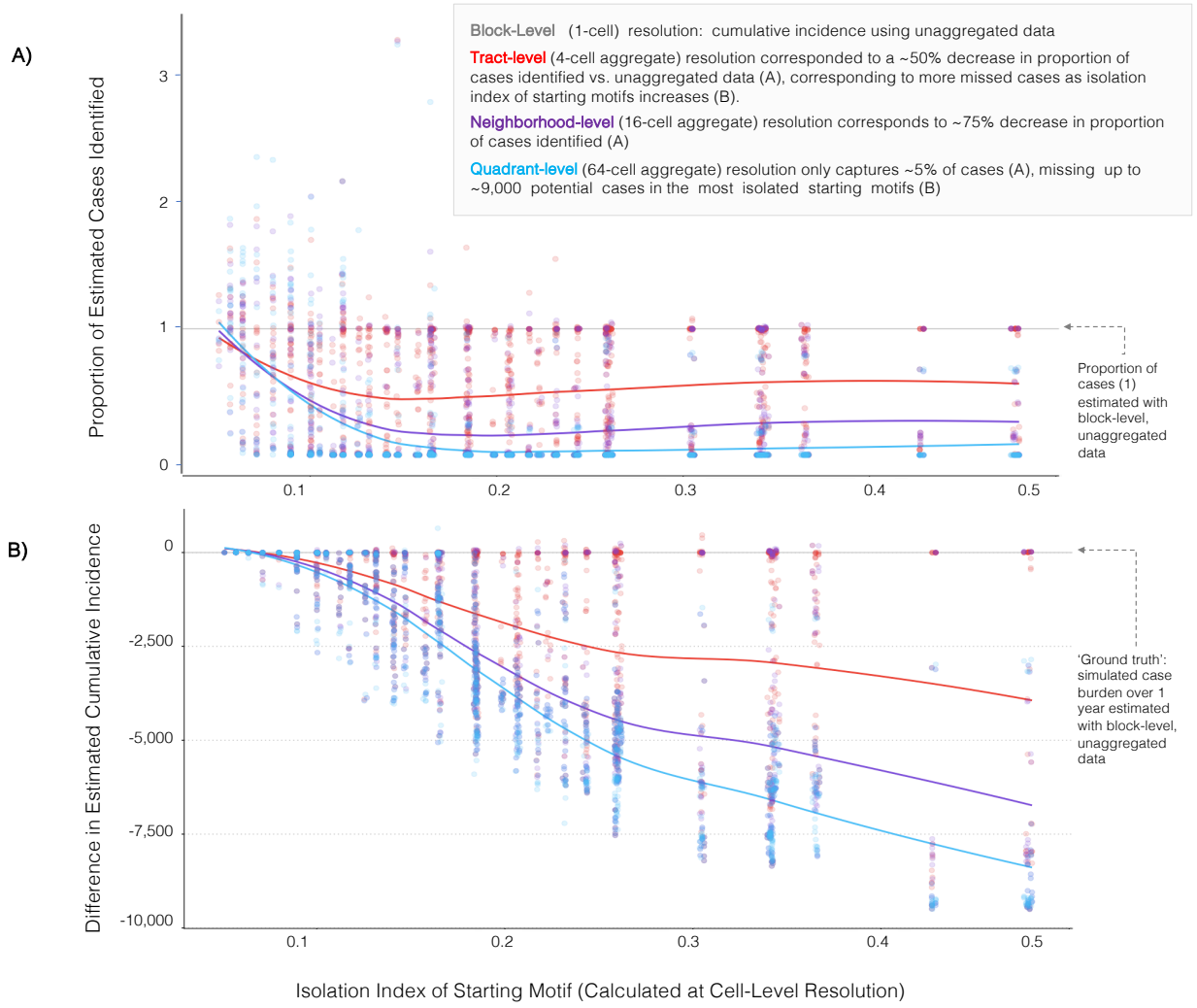

A) Proportion of estimated cases identified, treating the block-level, or individual-cell level simulation results as 'truth', in grey, when motifs are aggregated to the tract, neighborhood, and quadrant levels, sorted by Isolation Index of starting motif. B) Difference in number of estimated cases, or cumulative incidence, by aggregation level and Isolation Index of initial motif, illustrating greater loss in predicted number of cases as both aggregation level and Isolation Index increase.

Figure 2.6 Simplified representation of generation of clustering motifs using stratified sampling at four levels of aggregation

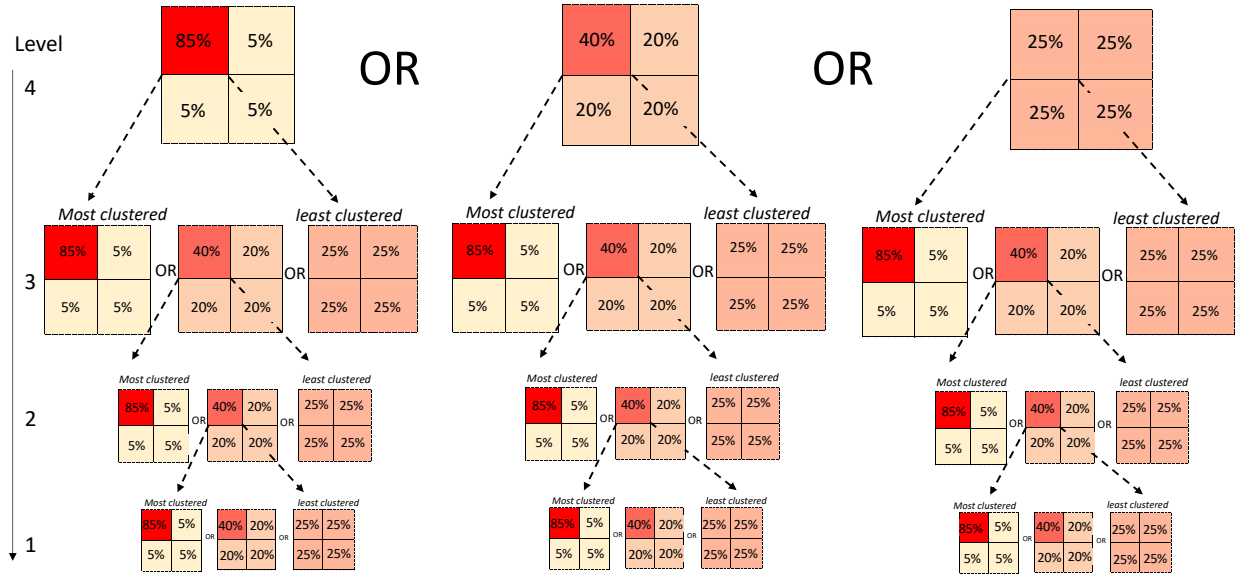

Motifs were generated by toggling the 'degree' of clustering in the upper left quadrant at each spatial scale to create 625 different possible vaccination motifs for each fixed overall vaccination level (i.e. 94%, 95%, 98%, 99%). Overall, a set of cumulative probabilities were used to generate these motifs, as described in the methods, with a maximum 'clustering' degree of 85% of non-vaccinators at a given level clustered into the top left quadrant (and 15% in the remaining three quadrants), to 70% of non-vaccinators being clustered into the top left quadrant (with 30% split between the remaining three quadrants), to 58% clustering in the top left, 40%, and finally the homogeneous case with 25% in all quadrants at each spatial scale. These cumulative probabilities were applied at these four nested levels (level 4 = quadrant, level 3 = neighborhood, level 2 = tract, and level 1 = block) to generate the motifs used in the simulations.

Figure 2.7 Susceptible-Infected-Recovered (SIR) compartmental model schematic diagram

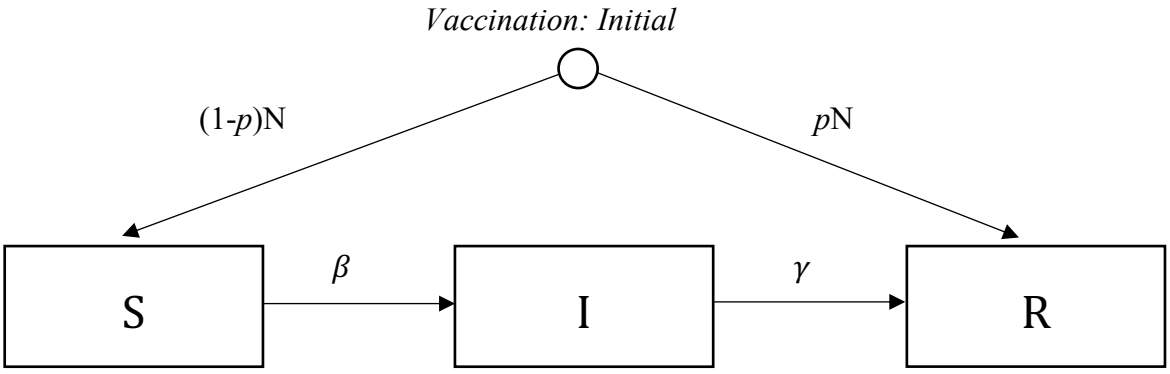

Compartments represent Susceptible (S), Infected (I), and Recovered individuals (R), with state transitions characterized by **β**, the probability of becoming infected and **γ**, the recovery from infection. Finally, p, the probability of vaccination, renders an individual recovered, not susceptible. For the purposes of this model, we are assuming vaccination occurs prior to individuals entering the landscape/simulation.

Table 2.1 Linear multivariate model fit of attack rate by clustering at each level

	Univariate Analysis			Multivariate Analysis		
Predictor	**Attack Rate Estimate (CI Estimate)**	**p-value**	**R^2**	**Attack Rate Estimate (CI Estimate)**	**p-value**	**R^2**
Moran's I	0.011 (140.9)	0.069	0.000	--		
Isolation index*	0.832 (10,660)	<0.001	0.801	0.572 (7,325.5)	<0.001	
Level 1 clustering**	0.059 (752.3)	<0.001	0.132	0.048 (620.1)	<0.001	
Level 2 clustering**	0.048 (619.8)	<0.001	0.090	0.040 (509.7)	<0.001	
Level 3 clustering**	0.041 (522.9)	<0.001	0.064	0.033 (428.1)	<0.001	
Level 4 clustering**	0.036 (463.8)	<0.001	0.050	0.029 (377.5)	<0.001	
						0.826

**Isolation index was normalized so that a one-unit increase in Isolation Index represented the spread from the minimum value to maximum value of the Isolation Index for a given level of overall vaccination*
***The clustering levels were operationalized as ordinal variables with steps increasing from 25% (homogeneous) in one quadrant, 40%, 58%, 70%,and 85%.*

95% Overall Vaccination: Linear multivariate model fit to attack rate over 1 year of simulation time, with estimates from models with cumulative incidence as the outcome in parentheticals, shows that clustering at each level (level 1 – level 4) all correspond to higher cumulative incidence

Table 2.2 Mean simulated cumulative incidence and attack rate by vaccination coverage

	Vaccination Level			
Seed Quadrant	94% Coverage (15,360 non-vaccinators)	95% Coverage (12,800 non-vaccinators)	98% Coverage (5,120 non-vaccinators)	99% Coverage (2,560 non-vaccinators)
1	6576 (42%)	4758 (37%)	1054 (21%)	296 (12%)
2	5265 (34%)	3779 (29%)	475 (9%)	56 (2%)
3	5267 (34%)	3778 (29%)	473 (9%)	54 (2%)
4	4748 (31%)	3249 (25%)	325 (6%)	19 (0.7%)
Overall	**5489 (36%)**	**3891 (30%)**	**582 (11%)**	**106 (4%)**

Here we see that the estimated mean number of cases at each vaccination level, across all clustering motifs, decreases significantly from 94% to 99%, yet clustering indicates that even at 99% vaccination coverage, there is still a mean attack rate of 4%.

Table 2.3 Simulation results of null model containing no spatial clustering

Overall vaccination level	Quadrant of seed case	Cumulative incidence after 1 year	Average CI (across four quadrants)	Average AR (across four quadrants)
94%	1 2 3 4	1.0466 1.2724 1.4038 1.2378	1.240	0.008%
95%	1 2 3 4	0.7459 0.7749 0.8043 0.8561	0.795	0.006%
98%	1 2 3 4	0.1647 0.1764 0.1912 0.2639	0.199	0.004%
99%	1 2 3 4	0.0533 0.0633 0.0893 0.1095	0.079	0.003%

Simulation results of 'null model' containing no spatial clustering of non-vaccination, but just random sampling of 94, 95, 98, and 99% vaccination coverage, respectively, across the 256-cell grid. Seeding a case into each quadrant yielded just over 1 secondary case, on average, for 94% overall vaccination, corresponding to a one-year attack rate (AR) of 0.008%, with the average CI decreasing to 0.795 cases for 95% vaccination, 0.199 for 98% vaccination, and 0.079 cases for 99% vaccination, indicating that herd immunity is upheld at 95% vaccination and above.

Table 2.4 Sensitivity analysis of frequency-dependent transmission

	Vaccination Level			
Seed Quadrant	94% Coverage (15,360 non-vaccinators)	95% Coverage (12,800 non-vaccinators)	98% Coverage (5,120 non-vaccinators)	99% Coverage (2,560 non-vaccinators)
1	6161.1 (40%)	4694.1 (37%)	1030.3 (20.1%)	281.3 (11%)
2	5102.0 (33%)	3612.7 (28%)	423.8 (8.3%)	46.9 (1.8%)
3	5097.8 (33%)	3618.5 (28%)	431.2 (8.4%)	49.7 (1.9%)
4	4631.5 (30%)	3142.5 (25%)	291.2 (5.7%)	22.5 (0.8%)
Overall	**5248 (34%)**	**3766 (29%)**	**544.2 (10.6%)**	**100 (4%)**

Sensitivity analysis of frequency-dependent transmission: mean simulated cumulative incidence results and attack rate (in parentheticals) by overall vaccination level and location of seed quadrant for selected vaccination coverage rates: 94%, 95%, 98%, and 99%. Here we see very small differences from the density-dependent transmission baseline model.

Equation 2.1 Deterministic differential equations of the SIR model [124]

$$\frac{dS}{dt} = -\beta SI$$

$$\frac{dI}{dt} = \beta SI - \gamma I$$

$$\frac{dR}{dt} = \gamma I$$

Equation 2.2 Global Moran's I [117]

$$I = \frac{N}{W}\frac{\sum_i \sum_j w_{ij}(x_i - \bar{x})(x_j - \bar{x})}{\sum_i (x_i - \bar{x})^2}$$

Where N is the number of spatial units that are indexed by i and j, and x is the variable of interest, and $\bar{x}$ is the mean of x; w_{ij} is a matrix of spatial weights with zeroes on the diagonal and W is the sum of all weights w_{ij}.

Equation 2.3 The Isolation Index [118]

$$\sum_{i=1}^{n}\left[\left(\frac{x_i}{X}\right)\left(\frac{x_i}{t_i}\right)\right]$$

Where x_i is the number of non-vaccinators per cell, X is the total number of non-vaccinators in the environment, and t_i is the total population in each cell.

Chapter 3 Measuring Multiple Dimensions of Non-Vaccination Clustering in Michigan from 2008-2018[3]

3.1 Significance statement

Recent research has illustrated the importance of clustered non-vaccination for outbreak potential, however there is no best practice for how to measure this clustering of non-vaccination, or at what spatial scale. Numerous clustering metrics are available in the statistical, geographic, and epidemiologic literature, but these were not all conceptualized with transmission risk in mind, and their values and interpretation may also vary with the scale of aggregation used and population-level non-vaccination rates. In this chapter, school-level kindergarten vaccine exemption data are used to characterize the spatiotemporal landscape of vaccine exemptions in Michigan from 2008-2018 using four different metrics at four geographic aggregation levels. This analysis reveals that these different clustering metrics tell very different stories about the landscape of non-vaccination clustering in Michigan, and we recommend measuring fine-scale vaccination data whenever possible with the Isolation Index to best predict outbreak risk.

---

[3] This work has been published as: Masters NB, Delamater PL, Boulton ML, Zelner J. Measuring multiple dimensions and indices of non-vaccination clustering in Michigan: 2008-2018, *American Journal of Epidemiology*. 2020. *Epub ahead of print.* DOI: 10.1093/aje/kwaa264

3.2 Abstract

Michigan experienced a significant measles outbreak in 2019 amidst rising rates of non-medical vaccine exemptions (NMEs) and low vaccination coverage compared with the rest of the United States. There is a critical need to better understand the landscape of non-vaccination in Michigan to assess the risk of vaccine-preventable outbreaks in the state, yet there is no agreed-upon best practice for characterizing spatial clustering of non-vaccination, and numerous clustering metrics are available in the statistical, geographic, and epidemiologic literature. We used school-level NME data to characterize the spatiotemporal landscape of vaccine exemptions in Michigan from 2008-2018 using Moran's I, the Isolation Index, Modified Aggregation Index, and the Theil Index at four spatial scales. We also used thresholds of 5%, 10%, and 20% non-vaccination to assess the bias incurred when aggregating vaccination data. We found that aggregating school-level data to levels commonly used for public reporting can lead to large biases in identifying the number and location of at-risk students, and that different clustering metrics yielded variable interpretations of the non-vaccination landscape in Michigan. This paper shows the importance of choosing clustering metrics with their mechanistic interpretations in mind: be it large- or fine-scale heterogeneity, or between-and-within group contributions to spatial variation.

3.3 Introduction

Childhood vaccination is highly effective in reducing the burden of disease, preventing an estimated 20 million cases of infectious illness and more than 40,000 deaths per year in the United States.[125] However, increasing parental concerns about vaccine safety and religious and

civil liberties worldwide have led to growing rates of vaccine hesitancy, defined by the WHO as the "delay in acceptance or refusal of vaccines despite availability of vaccination services"[45]. The global upsurge in vaccine hesitancy has been accompanied by rising rates of nonmedical exemptions (NMEs) from required childhood vaccinations.[87]

In the United States, the NME rate for children entering kindergarten increased from 1.2% in 2009 to 2.5% in 2018.[126,127] This trend of increasing NME rates is further complicated by variability in vaccination mandates across U.S. states, which determine the ease with which an NME can be obtained.[91,92,128] As of May 2020, 45 states (all except for California, Maine, Mississippi, New York and West Virginia) offer NMEs for religious or philosophical reasons.[97] In Michigan, both philosophical and religious exemptions are permitted. In Michigan, a state administrative rule change in 2015 required that parents attend an in-person education session at their local health department prior to obtaining an exemption.[126,129] Beyond this requirement, Michigan imposes no additional NME restrictions.

A number of studies have examined the relationship between NMEs and the occurrence of outbreaks of vaccine-preventable diseases (VPDs), finding that vaccine-exempted children have a substantially higher risk of acquiring and transmitting VPDs than those without; exempt children are up to 35 times more likely to contract measles, and 6 times more likely to acquire pertussis.[87,100] Michigan and many other states experienced large measles outbreaks in 2019, which prompted a number of states to amend their vaccination policies: New York eliminated religious exemptions,[98] Maine removed both religious and philosophical vaccine exemptions, and Washington state eliminated philosophical exemptions for the measles, mumps, and rubella (MMR) vaccine.[97] However, Michigan did not alter its policies beyond the 2015 administrative rule change.

It is important to explore community-level patterns of vaccination, e.g., identifying geographic clusters of vaccine exemptions can help target pockets of population-level susceptibility to reduce outbreak potential.[22,24,26,29,108] Vaccination and exemption rates are typically reported at coarse geographic scales such as states or counties,[123,127] with finer-scale data not widely used for evaluation and policymaking purposes.[122,123] However, vaccination behavior has been shown to vary locally, resulting in localized clusters of unvaccinated, susceptible individuals with high rates of within-group contact.[26,87,100,108,130,131] These exemption clusters have been related to outbreaks of pertussis in Michigan[101] and Florida[110], and measles in Oregon.[102] Additionally, during the 2019 measles outbreaks in the US, 89% of cases occurred in under- or non-vaccinated individuals.[103,132]

The manner in which school-level vaccination data is collected, distributed, and shared is salient when evaluating patterns of NMEs in the context of drawing conclusions about local and population-scale susceptibility to VPDs. In most states, vaccination histories are collected at kindergarten entry (age 5-6 years) and again in sixth or seventh grade. If communities have persistently high waiver rates, over time a sizeable portion of the student body will be unvaccinated and therefore susceptible to VPDs.[24,26,96] As such, the spatiotemporal landscape of vaccine exemption is important to understand the link between persistent kindergarten exemptions and subsequent outbreak risk.

While there is a critical need to better understand the landscape of non-vaccination in Michigan and other states, there is no agreed-upon best practice for characterizing the relationship between spatial clustering of non-vaccination and VPD outbreak risk. Numerous clustering metrics are available in the statistical, geographic, and epidemiologic literature, but these were not all conceptualized with transmission risk in mind. Additionally, their values and

qualitative interpretation may vary with the scale of aggregation and the population-level rate of non-vaccination. The most commonly utilized metric for assessment of clustering at the population level is Moran's I[29,30,38,131,133], though researchers have also used the Modified Aggregation index[108], Isolation Index[134], and Theil index[134] to evaluate clustering of non-vaccination. In this paper, we use school-level NME data to characterize the spatiotemporal landscape of vaccine exemptions in Michigan from 2008-2018 using each of these metrics and we varied the level of geographic aggregation used for data inputs to these measures. The study period from 2008-2018 was used because it captures Michigan's immunization waiver trends over the past decade and both predates and follows the Michigan Department of Health and Human Services' 2015 modification of State administrative rules requiring parents to undergo an education session at their local health department prior to obtaining a non-medical vaccine exemption (NME). The objectives of this analysis are to better understand how spatial clustering of non-vaccination in Michigan has varied in recent years, and the extent to which each metric captures the important dimensions of this variation, including sensitivity to the 2015 administrative rules change.

3.4 Methods

3.4.1 Data preparation

Annual school-level vaccination and exemption data were obtained from the Michigan Department of Health and Human Services (MDHHS) containing school-level vaccination records from 2008-2018 including school name, calendar year, grade (kindergarten, 7th grade, or other), number of children enrolled, number of students up-to-date for required vaccinations, and number of vaccine exemption waivers issued per year by waiver type (personal belief, medical,

or religious exemption). Of the 84,175 total records (representing each school with potential entries for each grade from 2008-2018) from 5,252 unique schools, 76,922 (91.5%) records were matched to an address by comparing the data to Michigan school vaccination data from before 2013, when the data included school addresses. An additional 5,871 records were matched using the district and building codes for schools, and 775 schools were matched by searching Michigan's Educational Entity Master Data.[135] This resulted in 5,086 (96.8%) matched and 166 unmatched schools. Names for these 166 schools were edited to address potential syntax inconsistencies: periods, dashes, and contractions were removed, resulting in an additional 97 matches. Of the 69 schools which were searched manually, 37 were matched to an address, leaving 32 unmatched schools and 5,220 matched schools (though only 4 of the 32 unmatched schools had nonzero enrollment from 2008-2018, Appendix B, Table B.1).

The 5,220 schools with identified street addresses were geocoded using ESRI ArcMap (Redlands, CA) version 10.7.1 in ArcGIS and re-projected to the NAD1983 Michigan Georef Projection. Schools were subset to those with matching street addresses (excluding matches by zip code, county, or post office) only, yielding 5,053 schools. 2,978 schools over the study period contained vaccination data on kindergarten students. We only used data on kindergarten students because the kindergarten entry point has many more required vaccinations, and we believe that exploring vaccine waivers for kindergarten students is thus more informative. When spatially linking data with the final set of geocoded schools, the analytic sample comprised a total of 2,896 schools. These data were spatially joined to the 2010 Census block groups, tracts, school districts, and counties.

3.4.2 Vaccine exemption rate calculations

Yearly kindergarten-entry data was summed for schools falling in each block group, tract, school district, and county. For each level of data aggregation and year, the percent of kindergarteners with combined vaccine exemption waivers was calculated by dividing the number of students with a waiver by the total number of students enrolled.[24] In this data source, the number of students with exemptions is not broken down by what vaccines were exempted, and thus a student with an exemption for one antigen would be indistinguishable from a completely unvaccinated student.

3.4.3 Assessing aggregation bias in identifying high-risk schools

At each level of aggregation, we assessed the number of students with waivers in a given geographic unit. We imposed waiver rate thresholds as criteria for defining schools as 'high-risk' based on estimates of the critical vaccination fraction (V_c) of common vaccine preventable diseases, where $V_c = 1 - 1/R_o$ (R_o is the reproductive number of the pathogen).[136] As such, we chose approximate waiver thresholds of 5%, 10%, and 20% at which the V_c would be exceeded for common preventable diseases: measles (R_o = 12-18, V_c ~95%),[22] mumps (R_o = 7 – 8.5, V_c ~89%)[137], and rubella, (R_o ~ 6, V_c ~83%).[138] For each threshold, we classified the number of schools that met or exceeded that threshold for a given year and used the kindergarten enrollment figures to determine the total number of children at-risk: the enrollment for all schools at or above these thresholds. For each level of aggregation, we repeated this procedure to identify how many block groups, tracts, school districts, and counties exceeded each threshold, and multiplied by the population of students within that spatial unit to determine the at-risk population. We then

determined the bias associated with aggregating to different spatial scales, using the school-level data as the 'gold standard'.

3.4.4 Clustering metrics

We used four statistics to explore spatial clustering of non-vaccination and the impact of aggregation on each: Moran's I[117], Isolation Index[139], Modified Aggregation Index[108], and Theil Index[140]. Moran's I is a measure of global spatial autocorrelation, which describes similarity between observations located near each other:[117]

Equation 3.1 Moran's I

$$Eq.\,3.1 \qquad I = \frac{N}{W}\frac{\sum_i \sum_j w_{ij}(x_i - \bar{x})(x_j - \bar{x})}{\sum_i (x_i - \bar{x})^2}$$

where N is the number of spatial units indexed by i and j, x is the number of non-vaccinators per unit, $\bar{x}$ is the mean non-vaccinators per unit; $\boldsymbol{w_{ij}}$ is a matrix of spatial weights, and W is the sum of all weights $\boldsymbol{w_{ij}}$**.** Values of Moran's I range from -1 to 1, with -1 corresponding to perfect clustering of dissimilar values (e.g. high-low clustering), 0 indicating no clustering, and 1 indicating perfect clustering of similar values (e.g. high-high clustering)[117]. Despite its common use as a measure of clustering, the epidemiological interpretation of Moran's I for non-vaccination is ambiguous. This is because it measures the overall balance of clustering regardless of whether that clustering indicates increased (high-high) vs. diminished (low-low) risk. Because Moran's I is also normalized between -1 and 1, direct interpretation in terms of outbreak thresholds is difficult.

The Isolation Index (or Aggregation Index)[139] measures how much exposure members of a minority group have to one another[118]. In this context, it is computed as the average proportion of non-vaccinators in each areal unit weighted by the proportion of non-vaccinators in the overall population:

Equation 3.2 The Isolation (Aggregation) Index

$$Eq.\,3.2 \qquad \sum_{i=1}^{n}\left[\left(\frac{x_i}{X}\right)\left(\frac{x_i}{t_i}\right)\right]$$

Where x_i is the number of non-vaccinators per geographic unit, X is the total number of non-vaccinators in the environment, and t_i is the total population per geographic unit. If non-vaccinators are randomly distributed across spatial areas, the value of the index will approach the global percent of non-vaccination, and will equal 1 when non-vaccinators are concentrated in a single location with no vaccinators.[118] When applied to kindergarten-level non-vaccination rates, the Isolation Index measures the probability that a kindergartener with a waiver would come into contact with another unvaccinated student at a randomly selected school. Higher values indicate that exempted students are clustered in a few schools, while low values would indicate that such students are distributed across many schools.

The Modified Aggregation Index, proposed by Pingali et al.[108], adjusts the Isolation Index to describe clustering of non-vaccination in only those locations in which transmission between non-vaccinators is possible[139] by modifying the Isolation Index formula so that schools with only one unvaccinated student do not contribute to the value of the index:

Equation 3.3 The Modified Aggregation Index

$$Eq.3.3 \qquad \sum_{i=1}^{n}\left[\left(\frac{x_i}{X}\right)\left(\frac{x_i-1}{t_i-1}\right)\right]$$

The Modified Aggregation Index reflects the probability that an exempted kindergarten student would come into contact with another *exempted* student in some geographic unit in which there are at least two non-vaccinated individuals.

Finally, the Theil Index[140] has been used to characterize scales of racial residential segregation,[134] because it is additively decomposable, meaning that the specific contributions of each level to overall clustering can be isolated. The Theil Index, H, can be calculated as shown below:

Equation 3.4 The Theil Index (H)

$$Eq.3.4 \qquad H_{B\subset M} = \frac{1}{N_M E_M}\sum_{b=1}^{B} N_b(E_M - E_b)$$

Where N_M is the total population, N_b is the total population of a subunit (which will vary in different sizes in this example, schools, block groups, tracts, etc.). E_M is the total Shannon entropy of non-vaccination in the system, and E_b is the Shannon entropy of non-vaccination in a subunit. Entropy (Equation 3.5) measures the amount of uncertainty in an outcome, where p_i is the proportion of non-vaccinators, and reaches a maximum at p_i= 0.5, and equals zero when p_i = 0 or 1:

Equation 3.5 Entropy (E)

$$Eq.3.5 \qquad E = p_i \ln\left(\frac{1}{p_i}\right) + (1 - p_i) \ln\left(\frac{1}{1 - p_i}\right)$$

Because H is a weighted sum of the entropies at different levels, it can be decomposed into its macro and micro components to reveal the importance of within- and between-location heterogeneity for the intensity of clustering.[140] This decomposition is useful for understanding the bias that would be incurred using different scales of analysis as surveillance units. However, the Theil index measures variation in local and global population composition rather than concentration of susceptible individuals, potentially limiting its applicability to outbreak risk.

All statistics were calculated for each year (2008-2018) for each level of aggregation (school, block group, tract, school district, and county). The calculation of these statistics required a definition of spatial neighbors. We conducted the analysis using the K nearest neighbors (KNN) method with K = 5 to represent a local phenomenon (i.e. using a smaller geographic catchment area). We also used K = 10 and 20 as sensitivity tests for the neighborhood definition, finding inconsequential variation in the results (Table 3.2). Analyses were performed in R (Vienna, Austria) version 3.6.0.

3.5 Results

3.5.1 Vaccine exemption rates at different geographic levels

Over the period 2008-2018, statewide vaccine exemption rates for students entering kindergarten in Michigan ranged from a minimum of 3.6% in 2015 to a maximum of 5.9% in

2012 (Table 3.1). The waiver rate increased from 2008-2013, fell in 2015 with institution of Michigan's administrative rules change requiring an in-person education session prior to obtaining an NME, and subsequently increased from 2015 to 2018. The unweighted mean of school-level exemption rates is likely more useful for characterizing local risk than the population-weighted statewide average, with a high of 9.8% in 2014. The standard deviation of school-level waiver rates reached 26.1% in 2014, indicating large school-level variation while also illustrating how state-level aggregate statistics can obscure epidemiologically relevant information. From the block-group level and above, waiver rates converged towards the state average, and variability decreased, suggesting that the majority of spatial information loss occurs locally.

3.5.2 Assessing aggregation bias in identifying high-risk schools

Figure 3.1 shows the percent of students at-risk based on three waiver rate thresholds (5%, 10%, and 20%). For a relatively small threshold (5%), when waiver rates are measured at the block group, tract and school district level, the estimated number of students at-risk is consistent with estimates from the school level. However, aggregation to the county-level resulted in notable over-estimation of the student body at-risk from 2010-2014, and significant under-estimation from both 2008-2009 and 2015-2016 (Table 3.3). For waiver thresholds of 10% and 20%, county-level aggregation always underestimated the number of at-risk students: by an average of 82.2%, and 99.8%, respectively. Most public reporting of vaccination rates occurs at the county or state level, and these results suggest that rates derived from such data are likely to be significant underestimates of the size of at-risk student population.[123] However, it is important to note that even smaller-scale aggregation biased the estimated population at-risk,

with more granular block group-level aggregation resulting in a 5.6%, 23.0%, and 52.9% reduction in the estimated number of students at-risk for 5%, 10%, and 20% waiver thresholds, respectively. The raw number of students estimated to be at-risk at each waiver threshold and aggregation level is available in Appendix B, Figure B.1.

3.5.3 Clustering metrics

Values of the Moran's I, Isolation Index, Modified Aggregation Index, and Theil Index over the study period are illustrated in Figure 2, and show very different trajectories both between levels of aggregation within and across metrics. Moran's I showed substantial variability over time and increased with the level of aggregation, as the statistic measures clustering of like values, regardless of whether they are low or high. Thus, as levels of aggregation increase and fine-scale noise is reduced (NME rates move toward the center), Moran's I increased. The Isolation Index and Modified Aggregation Indices had the largest values at the finest resolution of data and decreased as aggregation increased. Because these indices measure exposure of an unvaccinated student to another unvaccinated student, such values decrease with increasing spatial unit size as aggregation effectively smooths over schools with a large proportion of unvaccinated students. Finally, the decomposed Theil Index showed that the between block-group contribution to heterogeneity in vaccination averaged at 92.4%, between tract-level contribution was 80.5%, and between school district was 44.5%. Thus about 55.5% of the heterogeneity in vaccination waivers occurred *within* school districts, 19.5% of this variability occurred *within* tracts, and only 7.6% occurred *within* block groups. (Figure 3.2, Table 3.4). This within-unit component of variability can be conceptualized as approximating the

heterogeneity, or spatial uncertainty, in vaccination coverage that would be smoothed over by using aggregate estimates at each level.

3.6 Discussion

In this study, we characterized the changing landscape of non-vaccination in Michigan from 2008-2018 and assessed how one's view of this landscape may change based on the measure of clustering and level of data employed. We found that estimates of clustering varied significantly across commonly-employed spatial metrics and four scales of aggregation often found in administrative data and public reports. Perhaps the most commonly used statistic to assess clustering of non-vaccination is Moran's I,[29,30,38,131,133] yet our analysis found that Moran's I values were highly dependent on the spatial scale employed – with higher levels of aggregation resulting in higher values, and no consistent pattern across spatial scales. Because Moran's I does not distinguish between clustering of vaccinators vs. non-vaccinators, a state with many clusters of high vaccination rates would report the same statistic if these were replaced with identical clusters of low vaccination rates. Therefore, interpreting Moran's I as an indicator of outbreak risk is challenging. Additionally, because Moran's I increases with the scale of aggregation, the utility of this metric for assessing outbreak risk ambiguous.

The Isolation and Modified Aggregation Indices, which are measurements of within-group exposure, have been used by Buttenheim et al.[108] and Pingali et al.[134] to evaluate clustering of non-vaccination over space and time. We found that values of these indices decreased with increasing aggregation and reflected the same qualitative patterns at all spatial scales. Because these metrics measure the probability that an unvaccinated student would come

into contact with another unvaccinated student at a given spatial scale, they have a direct and intuitive epidemiologic interpretation, with higher values suggesting increased outbreak risk.

The Theil Index[134] provides a metric for the macro and micro decomposition of contributions to heterogeneity in non-vaccination, with decomposition into between- and within-group components helping to guide how biased aggregate estimates would be to different geographic units, as aggregation implicitly assumes homogeneity at and below that scale. We found that there was more variability in non-vaccination within than between school districts, indicating that epidemiologically relevant heterogeneity may be ignored if even a level as granular as school districts is used as the scale of analysis for vaccination data. At the tract and block group level, ~80 and >90% of variability in vaccination occurred *between* spatial units, indicating that these units are more homogeneous regions of non-vaccination, and perhaps better suited to being used for vaccine surveillance. Like Moran's I, the Theil Index does not yield an intuitive metric of outbreak risk, but is a very useful tool for understanding the appropriate level of vaccination and disease surveillance in different contexts.

Finally, we found that these clustering metrics had varying sensitivity to changes in exemption rates following Michigan's 2015 administrative rules change. Moran's I did not exhibit any discontinuous change before and after the policy change in 2015, and the Theil Index did not show large changes in heterogeneity of non-vaccination or its spatial decomposition. By contrast, the Isolation and Modified Aggregation Indices clearly reflected an impact of the policy change at all scales that is consistent with population-level changes. The differential values and ability of these four metrics to capture changes in the data showcase the importance of choosing a clustering metric to capture *epidemiologic risk*, and evaluate policy changes based on their potential impacts on susceptibility to disease outbreaks. Based on evidence from our findings in

this paper, and in a simulation-based study (Chapter 2) that showed strong correlation of the Isolation Index to outbreak probability and size, we believe that the Isolation Index should be used more readily as a measure of informative clustering of non-vaccinators for assessing outbreak risk and community susceptibility.

3.6.1 Strengths and limitations

Despite its use of highly granular data and thorough review of different clustering measurements, our study has some limitations. Our use of kindergarten exemption data necessarily results in an incomplete picture of the vaccination status of the full student population. It is also possible that the data are incomplete or entries were inconsistent over time. We do not break out exemptions by type in this analysis, however future studies could evaluate differential clustering patterns specific to philosophical, religious, and medical waivers, and could employ medical exemptions as a type of control as they are theoretically less likely to cluster geographically. This study has other notable strengths: this data source represents *all schools*: private, day-care, pre-kindergarten, charter, and public, with at least 5 students in the state of Michigan, providing a more complete assessment of vaccination status and clustering patterns than analyses using only public school data. Additionally, this study uses school-level data, which are appropriate to use as a 'gold standard' for VPD risk, the level at which much transmission occurs.[110]

3.7 Conclusions

In conclusion, we found that aggregating school-level vaccination data to levels commonly used for public reporting can lead to large downward biases in identifying the number

and location of at-risk students. We also found that four commonly-employed clustering metrics provided different interpretations of the landscape of non-vaccination in Michigan, both over time and at different spatial scales. Overall, values of the Isolation and Modified Aggregation Indices appeared to be the most consistent across spatial scale and most sensitive to detecting the 2015 reduction in vaccination waivers. These findings have direct consequences for surveillance and monitoring of vaccination rates in the U.S., as vaccination and exemption rates are typically monitored at the state or county-level. This paper shows the importance of choosing clustering metrics with their mechanistic interpretations in mind: be it large- or fine-scale heterogeneity, or between-and-within group contributions to spatial variation. Additionally, because metrics vary due to the chosen scale of analysis, it is important to present metrics at *multiple spatial scales* whenever possible. If multiple spatial scales and metrics are not possible, we encourage investing in using finer spatial scales to assess spatial clustering, such as the block group or tract level, where all metrics were more able to capture fine-scale heterogeneity that is important for assessing outbreak risk. We also suggest employing the Isolation Index because of its sensitivity to changing vaccination rates and simulation-based evidence of its utility in assessing outbreak potential. Future studies should explore the linkages between different characterizations of spatial clustering of non-vaccination and subsequent outbreak potential to provide additional best practices on the utility of different metrics.

Figure 3.1 Proportion of kindergarten students deemed to be 'at-risk' based on three thresholds of vaccination waivers (5%, 10%, and 20%), at four levels of aggregation: block group, tract, school district, and county, Michigan 2008-2018

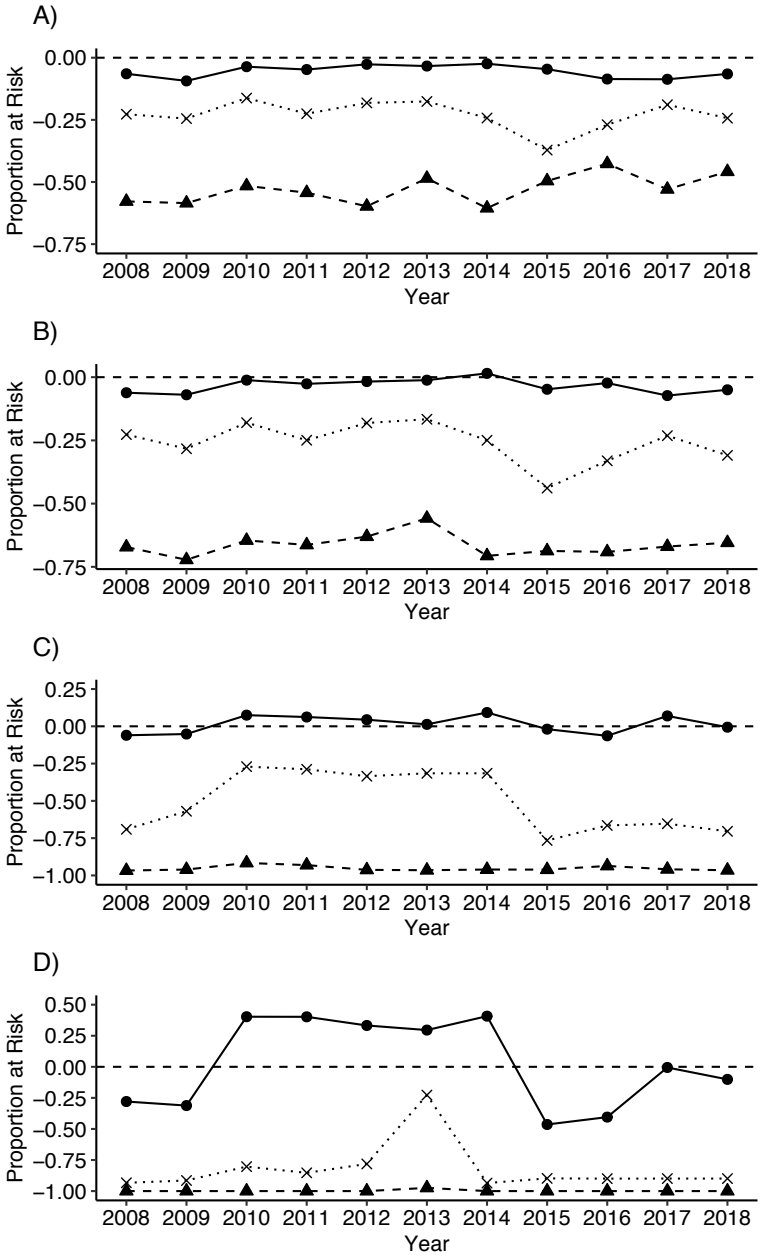

Proportion of detected students deemed to be 'at-risk' based on three thresholds of vaccination waivers: 5% (indicated by circles and solid line), 10% (indicated by x's and dotted line), and 20% (indicated by triangle and dashed line), with aggregation to the A) block group, B) tract, C) school district, and D) county level over the study period from 2008-2018. For the 5% waiver threshold, low-level aggregation (panels A-C) does not lead to much bias, though county-level aggregation results in positive and negative bias in the proportion of at-risk students. For the 10% and 20% waiver thresholds, higher levels of aggregation systematically result in greater *underestimation* of the at-risk population.

Figure 3.2 Assessing four metrics of global clustering at four spatial scales: schools, block groups, tracts, and school districts, to describe vaccination clustering in MI from 2008-2018

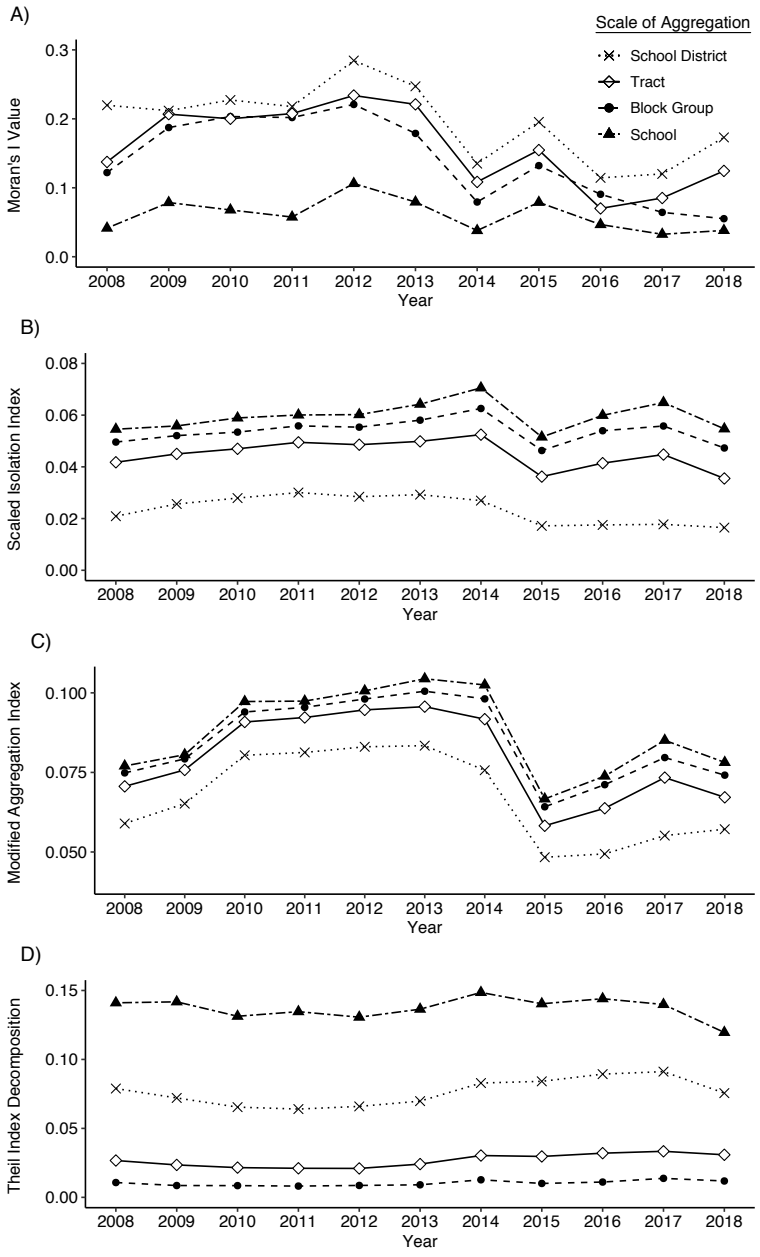

Assessing four metrics of global clustering at four spatial scales to describe vaccination clustering in Michigan from 2008-2018: A) Moran's I, B) the Scaled Isolation Index (the Isolation Index normalized by subtracting the mean overall waiver rate each year, so that the minimum value is 0), C) the Modified Aggregation Index, and D) the decomposed Theil Index – reflecting the within-group segregation or heterogeneity at each spatial scale. Each metric is presented over time and broken out by level of aggregation: baseline values at the school-level, and aggregate values at the block group, tract, and school district-levels. Note – for the Theil Index, the 'school-level' line indicates the total (non-decomposed) value of the Theil Index as schools are the baseline unit of aggregation, thus all of the variability would be within schools.

Table 3.1 Unweighted mean and standard deviation of kindergarten waiver rates (%) in Michigan from 2008-2018 at the school, block group, tract, school district, county, and state-level

	Unweighted Mean Waiver Rate at each Geographic Level (%)[a]					
Year	**Schools**	**Block Groups**	**Tracts**	**School Districts**	**Counties**	**State**
2008	6.1 (14.7)	4.7 (6.5)	4.5 (5.9)	4.3 (4.0)	4.0 (2.4)	4.2
2009	6.5 (15.4)	5.0 (6.7)	4.9 (6.1)	4.7 (4.8)	4.3 (2.7)	4.4
2010	8.8 (18.0)	6.5 (7.6)	6.3 (7.2)	6.3 (5.6)	5.7 (3.4)	5.7
2011	8.5 (20.0)	6.4 (7.9)	6.3 (7.4)	6.2 (5.8)	5.6 (3.2)	5.5
2012	9.3 (15.9)	6.9 (8.1)	6.6 (7.3)	6.0 (4.7)	6.0 (3.0)	5.9
2013	9.2 (19.1)	6.8 (8.5)	6.5 (7.5)	6.3 (6.3)	5.6 (3.8)	5.8
2014	9.8 (26.1)	6.7 (10.8)	6.5 (10.0)	5.8 (8.1)	4.9 (3.0)	5.3
2015	6.0 (13.6)	4.4 (6.4)	4.1 (5.3)	4.0 (3.9)	3.8 (2.3)	3.6
2016	7.3 (23.7)	5.0 (8.8)	4.5 (7.3)	4.2 (5.2)	3.9 (2.3)	3.7
2017	7.7 (20.5)	5.4 (8.6)	5.0 (7.3)	4.8 (5.8)	4.5 (2.5)	4.2
2018	7.3 (14.6)	5.8 (9.0)	5.2 (6.7)	5.0 (5.0)	4.7 (2.3)	4.5

[a] *This table shows the unweighted mean and standard deviation of overall vaccine waiver rates at individual schools, block groups, tracts, school districts, and counties, to express variability in the landscape of vaccination across the state of Michigan depending on which scale is used. The standard deviation indicates the range of waiver rates present at many of these smaller spatial scales, revealing heterogeneity in vaccination levels obscured by state-level averages.*

Table 3.2 Summary of Moran's I values of spatial autocorrelation at three different neighbor definitions: KNN5, KNN10, and KNN20 across vaccine waiver types using kindergarten vaccination data in Michigan, 2008-2018

		KNN5	KNN10	KNN20
YEAR	**Number of Schools**	**Moran's I**	**Moran's I**	**Moran's I**
Total Waivers				
2008	2346	0.0415	0.0433	0.0386
2009	2258	0.0786	0.0661	0.0634
2010	2150	0.0678	0.0644	0.0632
2011	2125	0.0575	0.0552	0.0508
2012	2072	0.1062	0.0947	0.0893
2013	2077	0.0794	0.0725	0.0602
2014	2200	0.038	0.0369	0.0269
2015	2045	0.0789	0.0679	0.0643
2016	2164	0.0467	0.0394	0.0311
2017	2140	0.0326	0.0323	0.0314
2018	2116	0.0382	0.0436	0.0322
Philosophical Waivers				
2008	2346	0.0503	0.0519	0.0457
2009	2258	0.0449	0.0446	0.0478
2010	2150	0.0913	0.0797	0.0787
2011	2125	0.0834	0.0777	0.0718
2012	2072	0.1264	0.1171	0.1024
2013	2077	0.1101	0.1036	0.0835
2014	2200	0.0413	0.0408	0.0317
2015	2045	0.0891	0.0736	0.0699
2016	2164	0.0432	0.0468	0.0343
2017	2140	0.058	0.0557	0.0517
2018	2116	0.046	0.048	0.0368
Religious Waivers				
2008	2346	0.0026	0.0058	0.0024
2009	2258	0.0838	0.0455	0.0265
2010	2150	0.0029	0.0036	0.0024
2011	2125	0.0158	0.0191	0.0135
2012	2072	0.0122	0.0075	0.0057
2013	2077	0.0081	0.0083	0.0066
2014	2200	0.0124	0.0097	0.0075
2015	2045	0.0565	0.0564	0.0507
2016	2164	0.0347	0.0229	0.0244
2017	2140	0.0255	0.0243	0.019
2018	2116	0.0141	0.0122	0.0106
Medical Waivers				
2008	2346	0.023	0.0267	0.0233

2009	2258	0.0221	0.0163	0.0131
2010	2150	0.0208	0.0292	0.0239
2011	2125	0.0318	0.0309	0.0344
2012	2072	0.0219	0.0217	0.0202
2013	2077	0.0698	0.0608	0.0477
2014	2200	0.0213	0.0229	0.0136
2015	2045	0.0152	0.0111	0.0077
2016	2164	0.0316	0.0159	0.0148
2017	2140	-0.0027	-0.0029	-0.0016
2018	2116	0.0222	0.0105	0.0036

Table 3.3 Bias results from aggregation analyses at 5%, 10%, and 20% thresholds of vaccination waivers to show raw bias and bias percent in estimating number of students 'at-risk' (above these thresholds) at different spatial scales using kindergarten vaccination data from Michigan 2008-2018

5% Waiver Threshold										
Year	Total schools at-risk	Total students at-risk	Bias by block group	Bias by tract	Bias by school district	Bias by county	Bias % by block group	Bias % by tract	Bias % by school district	Bias % by county
2008	855	43480	-2806	-2674	-2615	-12148	-6.5%	-6.1%	-6.0%	-27.9%
2009	864	44956	-4196	-3128	-2330	-14021	-9.3%	-7.0%	-5.2%	-31.2%
2010	1002	54121	-1956	-635	4046	21814	-3.6%	-1.2%	7.5%	40.3%
2011	978	53206	-2531	-1399	3315	21410	-4.8%	-2.6%	6.2%	40.2%
2012	1016	56156	-1491	-977	2490	18682	-2.7%	-1.7%	4.4%	33.3%
2013	1006	54577	-1832	-648	715	16138	-3.4%	-1.2%	1.3%	29.6%
2014	965	47542	-1155	715	4394	19375	-2.4%	1.5%	9.2%	40.8%
2015	650	30805	-1420	-1473	-589	-14295	-4.6%	-4.8%	-1.9%	-46.4%
2016	697	31331	-2687	-724	-1998	-12679	-8.6%	-2.3%	-6.4%	-40.5%
2017	760	36778	-3191	-2676	2558	-196	-8.7%	-7.3%	7.0%	-0.5%
2018	860	42021	-2742	-2097	-249	-4251	-6.5%	-5.0%	-0.6%	-10.1%
Avg	**878**	**44998**	**-2364**	**-1429**	**885**	**3621**	**-5.6%**	**-3.4%**	**1.4%**	**2.5%**
10% Waiver Threshold										
Year	Total schools at-risk	Total students at-risk	Bias by block group	Bias by tract	Bias by school district	Bias by county	Bias % by block group	Bias % by tract	Bias % by school district	Bias % by county
2008	370	13514	-3072	-3066	-9335	-12611	-22.7%	-22.7%	-69.1%	-93.3%
2009	418	16808	-4116	-4758	-9574	-15375	-24.5%	-28.3%	-57.0%	-91.5%
2010	580	26370	-4281	-4742	-7130	-21177	-16.2%	-18.0%	-27.0%	-80.3%
2011	553	25274	-5695	-6302	-7284	-21561	-22.5%	-24.9%	-28.8%	-85.3%
2012	593	26858	-4881	-4864	-8986	-20991	-18.2%	-18.1%	-33.5%	-78.2%
2013	575	25709	-4525	-4276	-8107	-5848	-17.6%	-16.6%	-31.5%	-22.7%
2014	573	22748	-5519	-5677	-7168	-21277	-24.3%	-25.0%	-31.5%	-93.5%
2015	303	9407	-3496	-4127	-7202	-8446	-37.2%	-43.9%	-76.6%	-89.8%
2016	310	7941	-2141	-2626	-5280	-7145	-27.0%	-33.1%	-66.5%	-90.0%
2017	367	11262	-2131	-2605	-7356	-10127	-18.9%	-23.1%	-65.3%	-89.9%
2018	394	12933	-3145	-3999	-9107	-11632	-24.3%	-30.9%	-70.4%	-89.9%
Avg	**458**	**18075**	**-3909**	**-4277**	**-7866**	**-14199**	**-23.0%**	**-25.9%**	**-50.7%**	**-82.2%**

20% Waiver Threshold										
Year	Total schools at-risk	Total students at-risk	Bias by block group	Bias by tract	Bias by school district	Bias by county	Bias % by block group	Bias % by tract	Bias % by school district	Bias % by county
2008	121	2776	-1605	-1865	-2685	-2776	-57.8%	-67.2%	-96.7%	-100%
2009	139	3670	-2147	-2650	-3525	-3670	-58.5%	-72.2%	-96.0%	-100%
2010	185	5229	-2697	-3376	-4792	-5229	-51.6%	-64.6%	-91.6%	-100%
2011	192	5975	-3244	-3963	-5561	-5975	-54.3%	-66.3%	-93.1%	-100%
2012	217	6390	-3820	-4029	-6151	-6390	-59.8%	-63.1%	-96.3%	-100%
2013	209	6671	-3238	-3723	-6438	-6499	-48.5%	-55.8%	-96.5%	-97.4%
2014	225	5072	-3070	-3584	-4871	-5072	-60.5%	-70.7%	-96.0%	-100%
2015	105	1876	-930	-1289	-1803	-1876	-49.6%	-68.7%	-96.1%	-100%
2016	145	2281	-973	-1576	-2136	-2281	-42.7%	-69.1%	-93.6%	-100%
2017	164	2771	-1467	-1856	-2657	-2771	-52.9%	-67.0%	-95.9%	-100%
2018	160	2674	-1226	-1750	-2581	-2674	-45.8%	-65.4%	-96.5%	-100%
Avg	**169**	**4126**	**-2220**	**-2696**	**-3927**	**-4110**	**-52.9%**	**-66.4%**	**-95.3%**	**-99.8%**

Table 3.4 Decomposition of Theil Index values using kindergarten vaccination data from Michigan, 2008-2018

Theil Index Decomposition: Values and % Segregation Attributable to Between-Group at Each Spatial Scale							
Year	**Total Segregation (School-Level)**	**Between Block Group Segregation**	**% Between Block Group**	**Between Tract Segregation**	**% Between Tract**	**Between School District Segregation**	**% Between School District**
2008	0.141	0.130	92.4%	0.114	81.1%	0.062	44.1%
2009	0.142	0.133	94.0%	0.118	83.4%	0.070	49.2%
2010	0.131	0.123	93.5%	0.110	83.6%	0.066	50.2%
2011	0.135	0.126	93.9%	0.114	84.4%	0.071	52.5%
2012	0.131	0.122	93.4%	0.110	83.9%	0.065	49.5%
2013	0.136	0.127	93.3%	0.112	82.3%	0.067	48.9%
2014	0.149	0.136	91.4%	0.118	79.6%	0.066	44.2%
2015	0.140	0.130	92.8%	0.111	78.9%	0.056	40.1%
2016	0.144	0.133	92.3%	0.112	77.8%	0.055	38.0%
2017	0.140	0.126	90.2%	0.106	76.1%	0.049	34.8%
2018	0.120	0.108	90.1%	0.089	74.2%	0.044	36.8%
Average	**0.137**	**0.127**	**92.4%**	**0.110**	**80.5%**	**0.061**	**44.5%**

Chapter 4 Does Requiring Parental Vaccine Education Reduce Non-Medical Exemptions? Evaluating the Long-Term Impact of Michigan's 2015 Administrative Rules Change [4]

4.1 Significance statement

In the United States, vaccines are regulated at the state level via school entry requirements. Currently, 45 out of 50 states permit non-medical vaccine exemptions (NMEs) for religious or philosophical reasons. Michigan allows both philosophical and religious exemptions, and facing the fourth highest exemption rate in the U.S. in 2014, changed its state Administrative Rules, effective January 1st, 2015, to curb NME rates. This rule mandated parents to attend an in-person vaccine education session at their local health department before obtaining an NME. There has not been a long-term evaluation of the success of this policy, and Michigan was the first state to try an administrative change regarding parental education as a strategy for reducing NME rates. As a result, in this chapter we explore the impact of this rule change on the landscape of exemptions in Michigan from 2011-2018, how exemptions are geographically clustered throughout the state, and whether the rule change affected the distribution of those exemptions.

---

[4] This manuscript is under review at *Pediatrics* as: Masters NB, Zelner J, Delamater PL, Hutton D, Kay M, Eisenberg MC, Boulton ML. Does Requiring Parental Education Reduce Vaccine Exemptions? Evaluating Michigan's 2015 Administrative Rules Change.

4.2 Abstract

Vaccine hesitancy is a growing threat to health in the United States. Michigan's Administrative Rules were changed in 2015, requiring parents to attend an in-person education session at their local health department prior to obtaining a non-medical vaccine exemption (NME). We evaluated sociodemographic predictors of NMEs before and after this change using binomial regression and measured geographic clustering using the Local Indicators of Spatial Association. Immediately following Michigan's rule change, NMEs fell dramatically. However, NME rates rebounded in subsequent years, returning to near-2014 levels by 2018, although income disparities in NME rates decreased. Additionally, philosophical, religious, and medical vaccine waivers exhibited distinct geographic patterns, which largely persisted after 2015. While the rule change caused a short-term decline in NME rates, the dramatic rise in NMEs in the following four years indicates that requiring parental education prior to receiving a waiver did not cause a sustained reduction on Michigan's NME rates.

4.3 Introduction

Vaccine hesitancy is an alarming global phenomenon, with the World Health Organization (WHO) declaring it one of the top 10 leading threats to health.[141] The WHO defines vaccine hesitancy as: "delay in acceptance or refusal of vaccines despite availability of vaccination services."[45] In higher income countries, vaccine hesitancy is more common among affluent and highly educated groups, though this hesitancy may not directly reflect vaccine uptake, as children living below the federal poverty level have been found to have lower vaccination coverage than those above it.[15,53]

In North America and Europe, parental concerns around vaccine safety and religious and civil liberties are leading to increasing rates of non-medical (philosophical or religious) vaccine exemptions (NMEs).[87] The rising rates of non-vaccination indicated by these NMEs is leading to increasingly frequent and severe outbreaks of vaccine preventable diseases (VPDs), such as measles. In 2019, the U.S. experienced its highest number of measles cases in 27 years[14] and nearly lost its measles elimination status,[10] which is conditional on having no circulation of measles in the community for 12 continuous months.[1,132]

In 2019, U.S. measles outbreaks primarily occurred in areas with high rates of religious exemptions, including Orthodox Jewish communities. The four states most affected were New York (914 cases), Washington (86 cases), California (68 cases), and Michigan (46 cases).[132] In New York, statewide measles vaccination coverage for children in Pre-K through 12th grade was 98%,[1] well above the threshold thought to be sufficient to confer herd immunity (~95%), however, the outbreak occurred in schools with a measles vaccination rate of 77%, illustrating how heterogeneity can lead to outbreaks even when overall coverage reaches herd immunity thresholds.[19] In March 2019, an infectious person traveled from New York to Michigan, initiating an outbreak in the Orthodox Jewish community in Oakland County, which would become the largest measles outbreak in Michigan since 1991.[142]

In response to accelerating VPD outbreaks, some states have sought to reduce the rate of NMEs. In the U.S., school entry vaccination requirements are regulated at the state level and are highly variable in terms of the parental burden imposed to obtain an NME.[91,92] Some state-specific exemption policies recently changed due to measles concerns: in 2019, New York, Maine, and Washington tightened their exemption policies to reduce the number of NMEs.[98] Despite this, as of December 2020, 45 states allow NMEs for religious or philosophical reasons,

all but California, Maine, Mississippi, New York and West Virginia.. More restrictive NME policies have been shown to decrease the number of NMEs,[95,24] reducing outbreak risk because exempted children have a higher risk of acquiring and transmitting VPDs.[87,100] However, as seen in New York, schools with high NME rates, even in well-vaccinated communities, can create local regions of susceptibility to disease, and there is increasing evidence that such geographic clustering of NMEs is a significant driver of outbreaks.[101,93]

In 2014, Michigan had the fourth highest vaccination exemption rate in the U.S. In response to this, Administrative Rule 325.176(12) was changed, effective January 1st, 2015, [143] to require parents to attend an in-person vaccine education session at the local health department before obtaining an NME.[93,129] One study found that philosophical exemptions decreased the year following the rule change, but did not examine longer-term trends, and thus was unable to evaluate whether NME rates remained lower or rebounded to pre-rule change levels.[144] While Michigan was the first state to require in-person waiver education at a local health department, Washington (SB 5005 in 2011[145]) and California (AB 2109 in 2014[24]) both previously passed legislation requiring parents to receive counseling from a health care provider before obtaining an NME. These policies had different results – SB 5005 decreased rates of exemptions and reduced geographic clustering of exemptions,[145] effectively lowering outbreak risk, while AB 2109 reduced NME rates for incoming kindergarteners, but had no apparent effect on geographic clustering, which is just as important a driver of outbreaks, and should be prioritized as an outcome of these policies.[93] California passed SB 277 in 2016, removing NMEs entirely, and making it impossible to evaluate the longer-term impact of AB 2109.[26]

Michigan's 2015 Administrative Rule change thus provides a unique opportunity to evaluate the lasting impact of in-person vaccine education sessions at a local health department

on NME rates, implemented via administrative action. In this study, we: (1) examine the four-year impact of the Administrative Rules change on NME rates in Michigan, and (2) describe the geography and persistence of waiver clustering using a Local Indicators of Spatial Association (LISA) approach, and finally (3) explore predictors of NMEs before and after the policy accounting for spatial variation.

4.4 Methods

4.4.1 Data source

School-level vaccine exemption data from 2008-2018 were obtained from the Michigan Department of Health and Human Services (MDHHS). These data were aggregated and were previously publicly available on the MDHHS website, thus no IRB approval was required. Data included school name, calendar year, grade, number of children enrolled, number of students up-to-date, and number of exemption waivers issued by type. Michigan kindergarteners were required to receive a second dose of the Varicella vaccine in 2010,[146] thus we selected an analytic period of 2011 – 2018 to maintain constant vaccine requirements. Data cleaning and geocoding, described in Masters et al.[147], resulted in a sample of 2,769 schools from 2011-2018, which were spatially joined to 2010 school districts to link per-capita income, percent white population, and percent population over age 25 with a college degree from the American Community Survey (ACS) 5-year estimate 2018 (data from 2013-2017).

4.4.2 Temporal trends of non-vaccination

For each year, the percent of kindergarteners in each school with vaccine exemptions was calculated by dividing the number of students with a vaccine exemption by the number of enrolled students. Data were aggregated to the school district level by summing NME counts in schools based upon their school district. Geographic trends in exemption rates were broken down by religious, philosophical, and medical exemptions and evaluated from 2011-2014 and 2015-2018. Analysis was done using R version 3.6.0 and maps were generated using ESRI ArcMap version 10.7.1.

4.4.3 Impact of the 2015 policy change

We used a hierarchical binomial regression model (using the R package *lme4*[148]) to understand variation in school-level NME rates. This model included random intercepts at the school district-level and a binary variable indicating whether the time period was before or after the rule change. Geographic clustering of waivers (by type) before and after the change was assessed using the Local Indicator of Spatial Association (LISA),[149] which identifies spatial clusters of high and low values of the waiver rate (Appendix Equation 1).[24] The LISA statistic was calculated for school districts, a meaningful administrative unit for policy action and parental decision-making, for each year, and the results were aggregated to determine whether and how long clusters persisted over time in the pre-and post-implementation periods.

4.4.4 Sociodemographic predictors of NMEs

We used a hierarchical, mixed effects Bayesian binomial model with school district-level random intercepts (using the R package *rstanarm*[150]) to evaluate predictors of NMEs over the study period accounting for variation at the school district-level inherent in the data. We used zero-mean Gaussian priors for the intercept (sd = 10), and coefficients (sd = 2.5). We regressed school-level NME rates on school district-level demographics, including percent adults with college education, per-capita income, and percent white, all categorized into tertiles, school type, and a continuous variable calculated as the travel time in hours to the nearest local health department from a given school, using ArcGIS's origin destination cost matrix calculation service. Based on model fitting, health department travel time and per-capita income were interacted with year (centered at 2014), to evaluate whether associations changed after the policy's implementation. We ran a counterfactual exercise using the model output to generate the posterior mean of the marginal probability of obtaining an NME in each year, fixing the distribution of school types, travel times, and demographics. This presents the predicted probability of an NME if every kindergartener in Michigan were in each type of school, or in each category of per-capita income, percent college-education, percent white, or percentile distance to the health department and allows us to make counterfactual comparisons of predicted NME probabilities in these groups.

4.5 Results

4.5.1 Temporal trends of non-vaccination

From 2011–2014, overall waiver rates remained fairly stable, for an average of 5.6% per year. However, the proportion of total waivers due to NMEs increased during this period while

medical exemptions decreased (Figure 4.1). After Michigan's rule change was implemented on January 1st, 2015 (after the 2014-2015 school year began, thus first impacting waiver rates for the 2015 year), a marked reduction in waiver rates to 3.6% is evident. The unadjusted binomial model (Appendix Table C.1) showed that the odds of obtaining an NME were significantly lower in the four years after the policy was put into effect compared to the four years prior. However, after 2015, waiver rates increased each year, rising to 3.7% in 2016, 4.2% in 2017, and 4.5% in 2018 (a 26% fold increase since 2015). Since 2015, medical exemption rates stayed stable while philosophical and religious waiver rates increased by 18% and 70%, respectively.

Public and charter schools had the lowest waiver rates, around 5% for the duration of the study period, though charter schools had notably increasing rates of waivers after 2015 (Figure 4.2, Appendix Table C.2). On average, 91.3% of kindergarteners included in this dataset attended public school, 7.8% attended private school, 0.6% attended charter school, and 0.2% attended virtual school. Private schools had higher rates of waivers from 2011-2018, around 10% prior to the 2015 policy, dropping to 7.3% in 2015, and increasing steadily each year, reaching 8.6% by 2018. Virtual schools had the highest waiver rates – above 27% in 2012, 2013, and 2018.

4.5.2 Impacts of the policy on geographic clustering of NMEs

While NME rates fell in the immediate aftermath of the 2015 rule change, rates have increased steadily since and maintained relatively stable patterns of geographic clustering. Figure 4.3 shows local clusters of high vaccine waiver rates which have persisted across Michigan for the period from 2011-2014 and from 2015-2018. Different types of NMEs followed distinct patterns of clustering within the state, with each type characterized by its own 'at-risk' region.

Figure 4.3A shows that philosophical waiver clusters persisted in rural, remote regions of the Upper Peninsula, that a cluster in the Northwestern lower peninsula disappeared after 2015, and that a new cluster in Mid-Michigan emerged after 2015. There were 56 school districts in a high philosophical exemption cluster from 2011-2014, decreasing to 26 for the period from 2015-2018, though the number of persistent clusters (3+ years) was unchanged, with 8 in each time period (Appendix Table C.3). The distribution of religious exemption clusters showed little change after 2015 (Figure 4.3B): there were 32 religious exemption school district clusters in both time periods, though fewer persistent clusters afterwards. Finally, for medical exemptions (Figure 4.3C), some persistent clusters in the Northeastern lower peninsula disappeared, yet a large, more persistent cluster appeared in Southeast Michigan, overlapping with a philosophical exemption cluster. The number of medical exemption clusters dropped from 43 to 25, though both time periods had one persistent cluster. Overall, the 2015 rule change appeared to reduce the number of philosophical exemption clusters, diminished the spatial distribution of some medical exemption clusters, but religious exemption clusters were largely unchanged – with some additional clusters appearing after implementation of this administrative change.

4.5.3 Identifying predictors of NME rates

Our counterfactual analysis of the predicted probability of an NME if every kindergartener in Michigan were in each category of select demographic variables revealed that the average marginal probability of obtaining an NME was similar for kindergarteners whose school district was in the two lowest tertiles of per-capita income (with the probability of an NME ranging from 2.6% to 4.7% over the study period), but was higher for those in the highest tertile of per-capita income (as high as 7.2% in 2012, Figure 4.4, Appendix Table C.4). After the

rule change in 2015, the discrepancy in the posterior mean average probability of an NME diminished between those in the wealthiest tertile and the poorer two tertiles. School district level percent whiteness was monotonically associated with NME rates: kindergarteners in the lowest (1st) tertile had the lowest NME probability and those in the highest (3rd) tertile had the highest (Appendix Table C.4). For percent college education, a different association was observed; kindergarteners in the middle tertile had the highest probability of an NME vs. the other tertiles (Appendix Table C.4). Increased travel time to the health center did not have a predictive effect on average probability of an NME (Appendix Figure C.2, Appendix Table C.6).

4.6 Discussion

High rates of NMEs, the result of widespread vaccine hesitancy, are a critical public health challenge that have begun to reverse decades of public health success in the control of VPDs. Rising NME rates across the U.S. over the last two decades have led to the passage of legislation that attempts to make them more difficult to obtain.[95] While New York, Maine, and Washington tightened restrictions on NMEs in the wake of the 2019 measles outbreaks, Michigan did not pass comparable legislation. In fact, even minor policy remedies presented in the state have been stymied: Michigan introduced HB 4610 in May 2019 to make schools with >5% waiver rates publicly post such information, but there has been no movement on this bill.[151] As such, it is clear that Michigan's 2015 Administrative Rule change, which did not require legislative action, was a strategic avenue for MDHHS to attempt to reduce NMEs while avoiding political conflict with an unsympathetic state legislature.[93] Although the rule change induced a sharp decline in the number of NMEs in the year after it went into effect, NME rates in Michigan have since rebounded nearly to pre-2015 levels, suggesting that this change has not had an

enduring impact. Interestingly, medical exemption rates decreased after the rule change, and have remained at these reduced levels since 2015. The rate of religious exemptions has rebounded faster than philosophical exemptions, which is concerning given that the 2019 outbreaks were primarily driven by religious clusters. This rebound also suggests that increasing restrictions alone – particularly if other avenues remain to obtain NMEs – is unlikely to reduce vaccine hesitancy and stem the tide of vaccine refusal.

Michigan's increasing waiver rates mirror national trends: from 1991 to 2004, the mean state-level NME rate increased from 0.98% to 1.48%,[87,94] and from 2011-2016, the national rate of NMEs increased from 1.75% to 2.25%.[95] Michigan's high rate of NMEs has put the state at risk: Olive et al. identified Michigan's Oakland, Macomb, and Wayne counties to be among the 10 counties in the U.S. with the highest numbers of NMEs. The risk associated with this falling vaccination coverage became more apparent during 2019, when Oakland County was the epicenter of the measles outbreak in Michigan.[23] Our analysis confirmed that NME rates are persistently high in these counties. Importantly, our study also identified fine-scale school district-level clustering of philosophical exemptions present in Oakland county and clusters of religious exemptions in Macomb county, indicating that VPD risk may also be high within particular schools and localities. Overall, the fact that in four years, waiver rates have already rebounded to nearly pre-rule change levels, indicates that stronger legislative and public health action, combined with multi-faceted approaches that do not rely exclusively on legislative and administrative changes, is needed to curb the increasing VPD outbreak risk in Michigan.[152]

Our findings that private schools had about twice the rate of exemptions as public and charter school aligns with research from California.[93] Though the vast majority of kindergarteners in this dataset attended public school, ~8% of the students attended private

schools, and thus the increase in private school exemption rates is concerning. Virtual schools provide a glimpse at the non-vaccination rates among homeschooled children over this time period, and had extremely high exemption rates. Additionally, the number of kindergarten students enrolled in virtual schools increased nearly ten-fold over the study period, from 57 students in 2011 to 487 students in 2018, thus the high rates of exemptions in the virtual school children is particularly worrying if these numbers continue to rise, which may occur especially in the aftermath of the COVID-19 pandemic.

We also identified persistent spatial clusters with consistently high waiver rates both before and after the rule change.[29,131,133,134] This is important because spatial clustering of non-vaccination may dramatically increase the risk of outbreaks at the local and population level.[153] Given that students who obtain kindergarten vaccine exemptions will age through the educational system, a region with persistently high kindergarten waiver rates is likely to have markedly reduced vaccination levels in its student body, accumulating susceptible children to outbreaks of VPDs.[26] Our analysis showed that many exemption clusters remained persistent after the rule change, which more strongly aligns with the aftermath of AB 2109 in California, which decreased exemption rates but not clustering,[24,126,154] than Washington's SB 5005.

Additionally, the geography of philosophical and religious NMEs were distinct, with philosophical clusters persisting in a stretch of school districts in Southeast and Western Michigan, with some clusters in the Upper Peninsula, while religious waivers clustered in Southeast Michigan. These findings generally concur with Mashinini et al.[154] However, our analysis used school districts as the clustering unit and differentiated clusters based on their persistence, providing results at an actionable geographic unit. The distinct patterns of spatial clustering observed for different waiver types indicate that the downstream impacts of policy

changes to further restrict access to NMEs would likely play out heterogeneously across a state characterized by a diverse socioeconomic, racial, and religious landscape.

Results from our counterfactual exercise using Bayesian regression output underscored that school type was a strong predictor of NME rates, with virtual schools and private schoolers having higher probabilities of waivers than their public school counterparts. Distance to the health center was not a strong predictor of school-level waiver rates, highlighting that this policy likely only reduced exemptions due to convenience, rather than conviction, and potentially indicating that those who pursed an NME after 2015 were sufficiently motivated that the opportunity cost associated with traveling to the health department was not a high barrier. We found non-linear patterns across school-district level percent whiteness, percent college-educated adults, and per-capita income. This generally concurs with prior research where under-vaccinated children are often minorities of lower socioeconomic status and educational attainment, while completely non-vaccinated children are often white, wealthy, educated, and privately insured.[92]

4.6.1 Strengths and limitations

A notable strength of this study is the use of school-level data to identify potential geographic clustering and regions where herd immunity might be broken due to high exemption rates. This data source represents all schools: private, day-care, charter, virtual, and public, with at least five students in Michigan, providing a near-complete assessment of kindergarten vaccination status. Additionally, school-level data is appropriate here given that it is the unit of aggregation at which much of transmission occurs. Geocoding these schools allowed for linkage

of sociodemographic variables from the ACS, permitting measures of community-level demographics while employing transmission-level vaccination data.

This study also has some limitations, most importantly that we only analyzed exemption data for kindergarteners, thus creating an incomplete picture of the vaccination status of the full student population in these schools. Additionally, it is possible that there is missing data, if not all students were present when schools were surveyed for vaccination and enrollment records. Finally, using school district-level demographics may not be a perfect match to the student body from each school, as school catchment areas may extend beyond the boundaries of the units chosen or be very specific sub-segments of a geographic unit, introducing the possibility of ecologic bias.

4.7 Conclusions and policy implications

Our results illustrate that although Michigan's Administrative Rules change reduced the number of NMEs immediately after its implementation, NMEs have since rebounded. Many school district-level clusters with high NME rates have persisted. These findings indicate that this change did not have a strong, lasting impact on the pattern or rate of NMEs in Michigan. Navin et al. found that Michigan's vaccine waiver educators rarely convinced parents to vaccinate their children after attending an education session, underscoring that such a policy is effectively imposing a cost to reduce convenience exemptions, yet unlikely to change perception.[155] They also found that while such burdens may decrease NME rates, there may be a threshold of burden beyond which increasing inconvenience does not further reduce exemptions.[156] As a result, it is important to balance the implementation of stronger policies to

curb NME rates to reduce the frequency of outbreaks with the possibility of backlash against restrictions of individual liberty.[157,158]

Michigan's administrative policy should be viewed within the larger context of the interventions available to reduce incentives to obtain exemptions. Such policies carry risk, because suboptimal vaccine policy design can backfire and fuel anti-vaccine sentiment.[159] In addition to state regulation of vaccine exemptions, interventions should seek to counter growing levels of vaccine hesitancy through education, building confidence in vaccines and government, curbing misinformation, educating doctors about the importance of vaccination and minimizing missed opportunities, and increasing the affordability of vaccines.[160] These recommendations are particularly important against a backdrop of the COVID-19 pandemic, which has led to reduced ambulatory care visits, causing a precipitous drop in pediatric vaccination rates.[80,81] This could create a dangerous environment as underimmunized children return to school. At this critical juncture, we must increase vaccine uptake, reduce the burden of preventable disease, minimize the risk of additional outbreaks, and maintain health care capacity.

Figure 4.1 Percent of children with vaccine exemptions in the state of Michigan broken out by waiver type (philosophical, medical, religious) from 2011-2018 with Administrative Rules change going into effect on January 1st, 2015

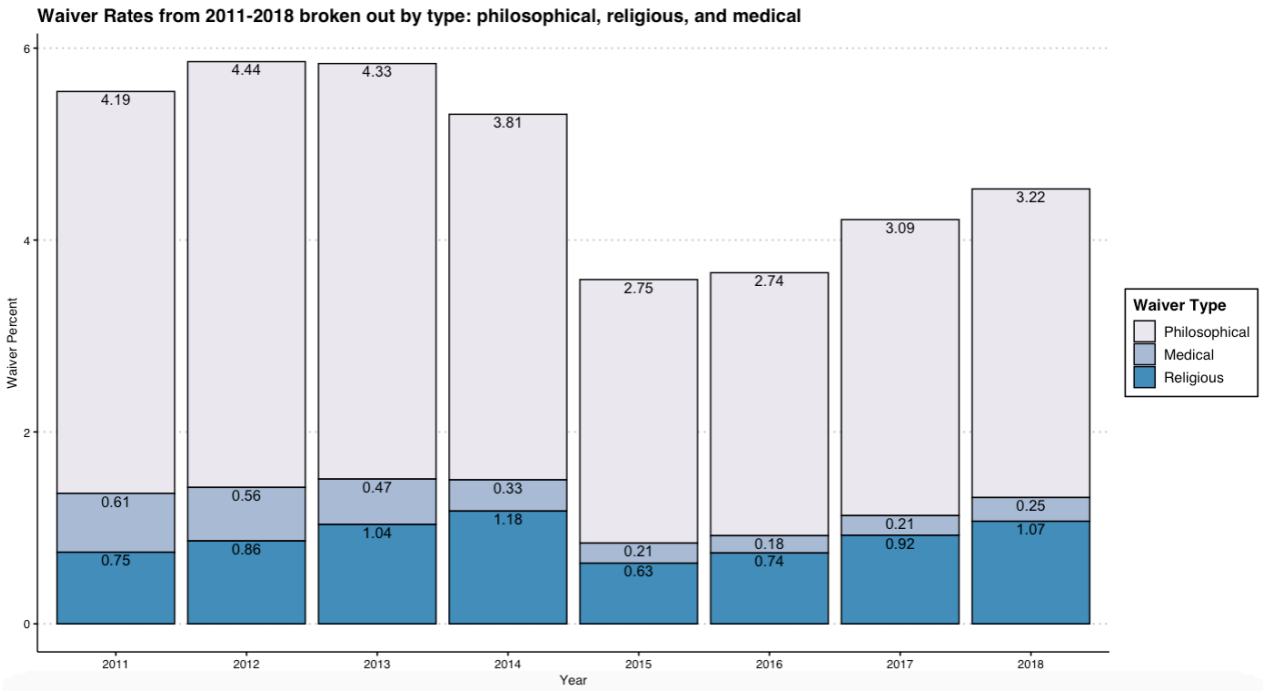

Figure 4.2 Percent of children with vaccine exemptions in the state of Michigan broken out by school type (charter, private, public, and virtual schools) from 2011-2018

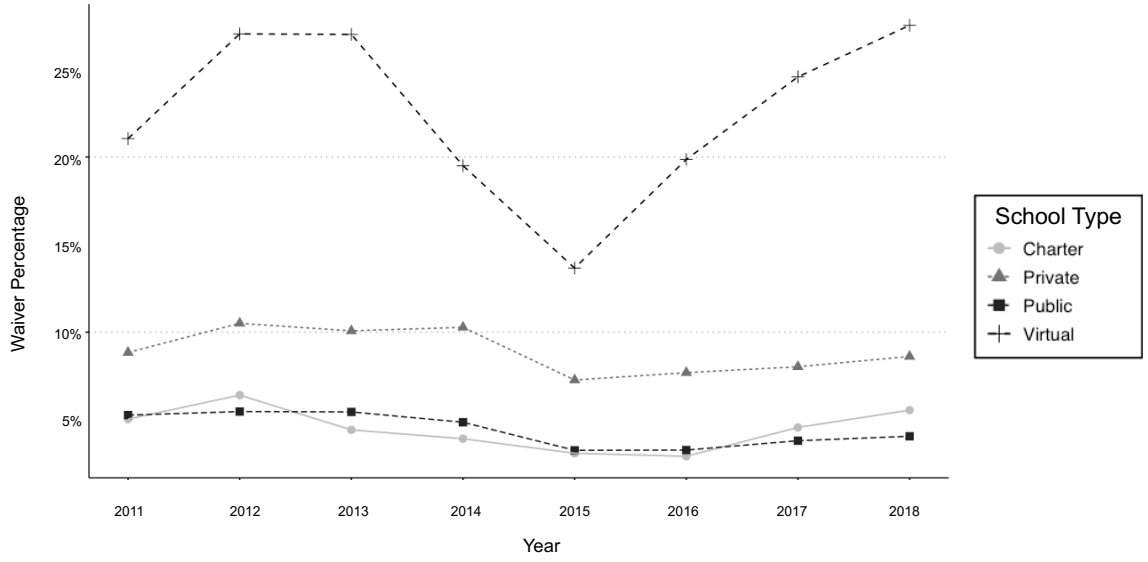

The percent of children with vaccine exemptions in the state of Michigan broken out by school type (charter, private, public, and virtual schools) from 2011-2018 highlights a large rebound in vaccination waiver rates among virtual schools, a notable rebound among charter schools, and less of a rebound among private and public schools since the 2015 policy change.

Figure 4.3 Persistence of LISA clusters of philosophical, religious, and medical exemptions at the school district level, represented as the number of years in which each school district was in a high-high LISA waiver cluster, before and after the January 1st, 2015 policy change

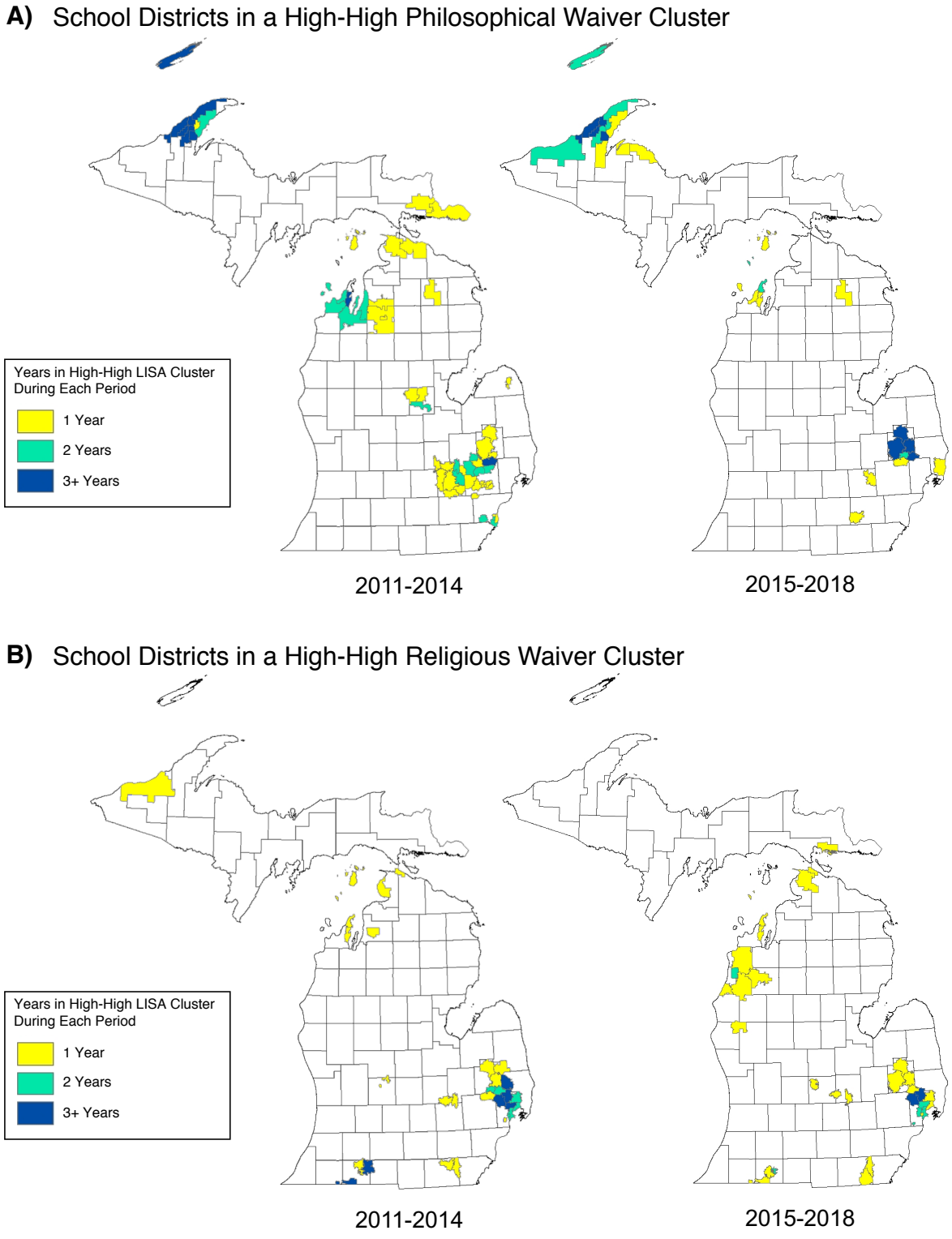

C) School Districts in a High-High Medical Waiver Cluster

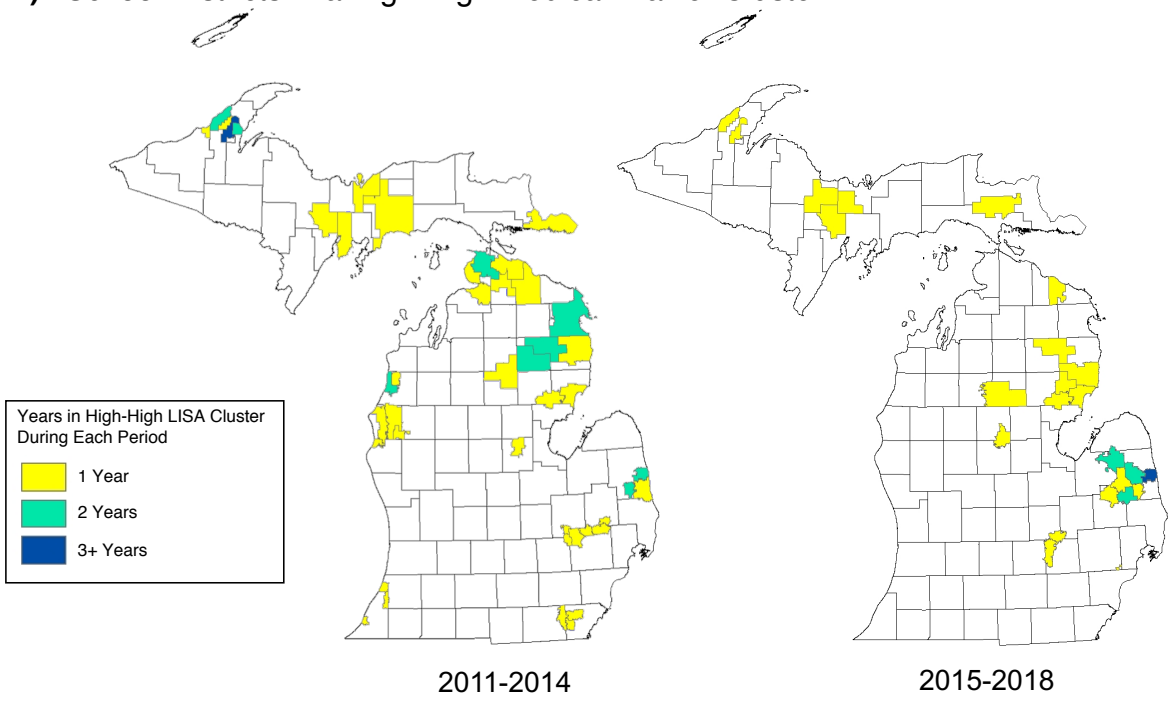

High-high waiver clusters indicate that the highlighted school districts were identified by the LISA statistic as significant clusters of high waiver rates (indicating that both a given school district and the average of its neighboring school districts had significantly high waiver rates). A) Philosophical waiver persistence from 2011-2014 and 2015-2018, B) Religious waiver persistence from 2011-2014 and 2015-2018, and C) Medical waiver persistence from 2011-2014 and 2015-2018. LISA: Local Indicators of Spatial Association

Figure 4.4 Bayesian binomial logistic hierarchical model output showing posterior mean average marginal effects of probability of getting a non-medical exemption (NME) waiver for selected demographic predictors at the school district level: tertiles of percent whiteness, tertiles of percent of adults over 25 with a college education, and per-capita income

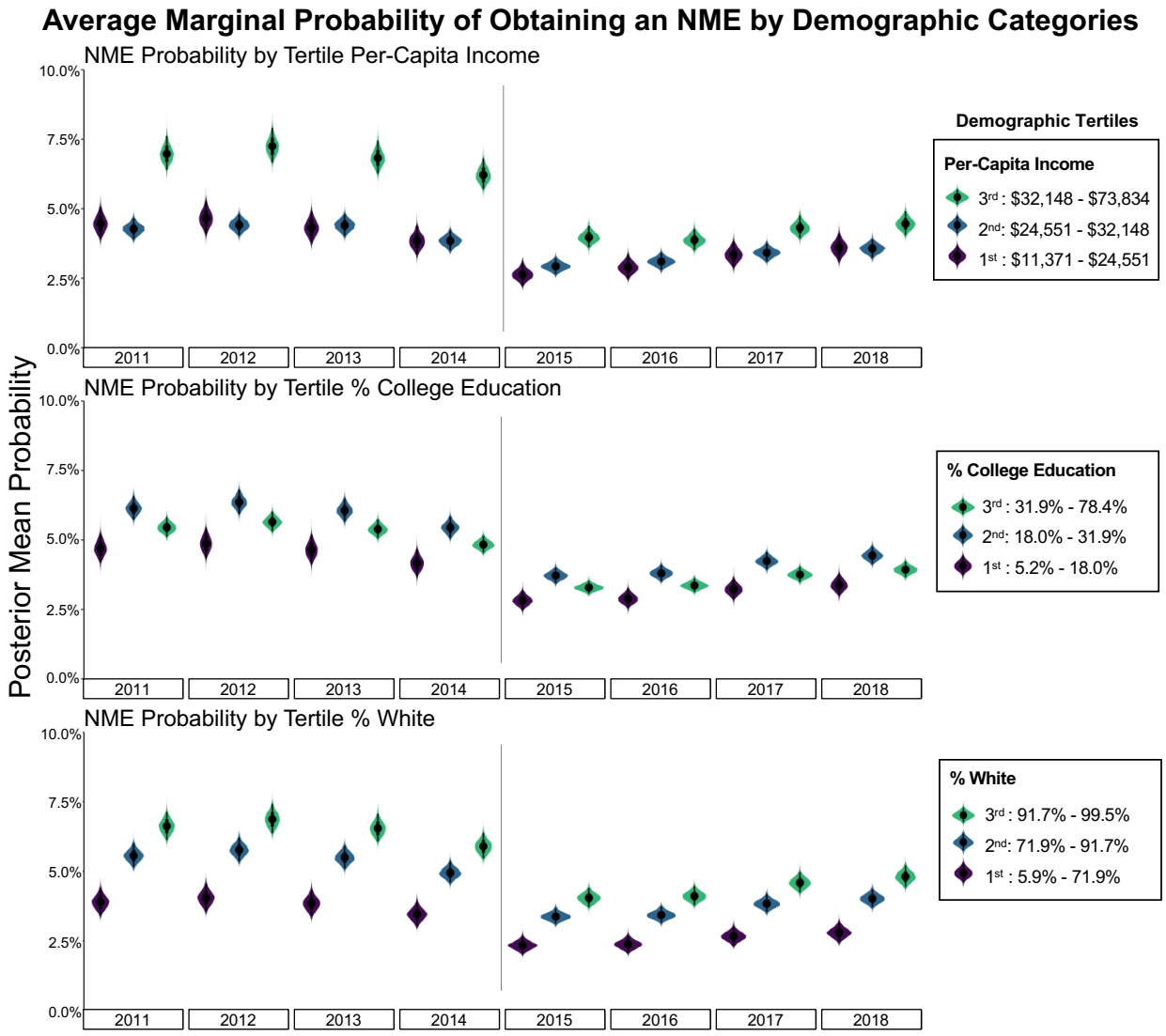

Chapter 5 Summary and Conclusions

5.1 Summary of dissertation findings

This dissertation explored the implications of how spatial clustering of vaccine hesitancy and non-medical vaccine exemptions (NMEs) (which are permitted by 45/50 states' regulations) affects herd immunity, impacts population-level disease dynamics, and has contributed to the resurgence of measles. Aim 1 assessed the impacts of spatially clustered non-vaccination on outbreak probability and size using a theoretical simulation model, and showed how aggregating fine-scale data to the scales often reported (i.e. the county or state level) can obscure important information necessary to accurately determine high-risk areas. While spatial clustering is important for assessing outbreak risk, there is no standard metric recommended to evaluate such clustered landscapes of non-vaccination. Thus, Aim 2 used kindergarten vaccination data from Michigan from 2008-2018 to explore four different metrics at four geographic scales to make recommendations about how best to measure clustering of vaccination data in practice. Finally, Aim 3 addressed the issue of vaccine hesitancy and regulation, analyzing the long-term results of a 2015 Michigan Administrative Rules change that made parents attend a waiver education session at their local health department prior to receiving an NME waiver. The new rule led to an initial drop in NME rates, but there has since been a significant rebound, and waivers across the state remained geographically clustered after the change. More detailed summaries of these

three studies are described below, highlighting the public health implications of such research as well as notable strengths and limitations.

5.1.1 Aim 1

Even though overall measles vaccination rates in the United States averaged over 95% in 2019, meeting the WHO vaccination coverage target and threshold for maintaining measles herd immunity, there were still over 1,200 cases of measles across 31 states that year, and the United States was just a week away from losing elimination status granted 19 years prior.[16] Measles is one of the most contagious infectious diseases known, with a basic reproduction number (R_o) estimated at 12-18. This high R_o necessitates the high proportion of the population that needs to be vaccinated or have natural immunity from prior disease in order to prevent outbreaks, a measure referred to as the critical vaccination fraction (V_c).[111,112] However, the standard calculation of V_c assumes that the population is evenly mixed and that all individuals contact one another with equal likelihood. When non-vaccinated individuals are geographically clustered, the formula can underestimate the V_c, allowing outbreaks to occur despite vaccination coverage targets being met or exceeded at the state or national level, as seen in 2019.[22]

This research used a theoretical environment: a 256-cell grid with 1,000 people per cell and four nested levels approximating scales of real vaccination data: “blocks” of 1,000 people (individual cells, approximating the size of a Census block group), “tracts” of 4,000 people (4 cells, approximating Census tracts), “neighborhoods” of 16,000 people (16 cells, approximating neighborhoods), and “quadrants” of 64,000 people (64 cells, approximating a town). This model incorporated a spatial transmission process, with each block capable of transmitting measles within its cell and to neighboring cells via a spatial force of infection term. The overall number

of non-vaccinated individuals in the environment was fixed at 5%. The only parameter that varied in the analysis was the degree of clustering of non-vaccinated individuals, to evaluate the impact of such clustering on outbreak probability and size.

This analysis found that *without clustering*, overall vaccination coverage levels of 94% and higher upheld herd immunity. However, once clustering was introduced, all vaccination levels tested (up to 99%) allowed breakthrough outbreaks to occur. As the degree of clustering increased, outbreaks occurred with both higher probability and larger size. Additionally, aggregation of the fine-scale data to larger units (analogous to using county, state, or national-level vaccination coverage statistics), severely underestimated expected outbreak probability and size of simulated scenarios. With 95% overall vaccination, the expected outbreak size was 45.4% lower when data were aggregated to the tract level, 76.5% lower at the neighborhood level, and 94.2% lower at the quadrant level. Finally, the clustering and aggregation effects magnified each other: aggregating vaccination data consistently underestimated outbreak potential, and the bias grew as the clustering of the motif increased, measured by the Isolation Index.

These results, while evaluated in a theoretical framework, have real-world implications for vaccine surveillance and outbreak risk assessment. First, they highlight how misleading the assumptions of homogeneous mixing which underlie herd immunity calculations can be. Even at 99% overall vaccination coverage, clustering of non-vaccinators permitted outbreaks. This compels a rethinking of whether calculations of herd immunity are meaningful when applied at large spatial scales. Additionally, aggregating data introduces strong bias into predictions of outbreak potential because it *obscures fine-scale clustering,* illustrating that finer-scale data are needed to fully understand the risk of outbreaks of measles and other vaccine-preventable diseases (VPDs). Such data *are* collected at the school-level for school entry vaccination

requirements, but publicly released data are usually presented at the county- or state-level. The fact that all states have immunization information systems makes the release of such fine-scale data possible, and opens the door to cross-state cooperation to assess regional risk as well – as infectious diseases do not observe administrative boundaries.[161,162] Continuing to release only aggregated vaccination data when much more fine-scaled data exist represents a significant lost opportunity for surveillance.

As with all studies, this research has both strengths and limitations. A major strength is that this simple model helps to explain how clustering impacts outbreak potential. While the simplicity is a strength in communicating the implications of this research, it also carries limitations; this model does not represent the social dynamics of true cities and interpersonal networks. The dynamic SIR model did not have an incubation period, which does not change the total number of cases expected, but also imperfectly represents how measles is transmitted.

Overall, this dissertation chapter effectively presented a proof-of-concept using a simple, easy-to-visualize model that showcases what happens when aggregate vaccination coverage is theoretically high enough to maintain herd immunity, yet non-vaccinators are spatially clustered. As such, this study provides insight into the implications of reported vaccination data in the United States, which aggregates vaccination data to large geographic scales. The findings from this paper will help to successfully implement control strategies for emergent measles outbreaks, and potentially other VPDs, and help make the overall U.S. vaccine reporting system and data dissemination more robust and informative for assessing outbreak risk.

5.1.2 Aim 2

In the United States, the non-medical vaccine exemption (NME) rate for children entering kindergarten has been increasing alongside rising parental concerns about vaccine safety and religious and civil liberties.[126,127] In this context of growing non-vaccination,[163] it is important to explore community-level patterns of vaccination and target pockets of susceptibility to reduce outbreak potential. While vaccination and exemption rates are typically reported at coarse geographic scales,[123,127] vaccination behavior has been shown to vary locally, resulting in clusters of unvaccinated individuals.[101,123,124] Additionally, despite a need to better understand the landscape of non-vaccination, there is no best practice to characterize spatial clustering in terms of outbreak and public health risk.

This dissertation chapter explored the utility of four different clustering metrics to assess the spatiotemporal landscape of vaccine exemptions in Michigan: Moran's I[24] , the Modified Aggregation Index[108], Isolation Index[134], and Theil Index[134] at four spatial scales. These metrics were applied to school-level vaccination exemption data from the Michigan Department of Health and Human Services on 2,896 schools from 2008-2018. These data represent nearly all kindergarteners in Michigan who attended a school with at least 5 enrolled students during this time period.

This research found that estimates of the clustering of vaccine exemptions varied significantly depending on which of the four spatial metrics and scales of aggregation (block group, Census tract, school district, and county) were used. Though Moran's I is perhaps the most commonly used statistic to assess spatial autocorrelation, it was heavily dependent upon the scale of the data. Additionally, Moran's I does not distinguish between clustering of vaccinators vs. non-vaccinators, challenging its interpretation for outbreak risk. The Isolation and Modified

Aggregation Indices can be interpreted as the probability that an unvaccinated student would come into contact with another unvaccinated student at a given spatial scale. These measures thus carry an intuitive epidemiologic interpretation, with higher values suggesting increased outbreak potential. Finally, the Theil Index does not have a direct outbreak risk interpretation, but can be useful in determining the appropriate level of vaccination and disease surveillance in different contexts. Using the Theil Index to characterize heterogeneity, more variability occurred *within* than *between* school districts, suggesting that units larger than Census tracts or block groups contain too much heterogeneity to be assumed to be homogeneous (the baseline assumptions made when choosing an aggregate scale for reporting vaccination data).

This research project culminated in a recommendation to use the Isolation and Modified Aggregation Indices as preferred clustering metrics for future research evaluating non-vaccination. These measures were the most consistent across spatial scale, the most sensitive to detecting the 2015 reduction in vaccination waivers, and have the most sensible interpretation in terms of transmission-dynamics. Because all metrics varied with the scale of analysis, metrics should be presented at multiple scales when possible. If using multiple scales is not possible, we encourage using finer-resolution data to assess clustering (such as the block group or tract) where all metrics were more able to capture outbreak risk-relevant fine-scale heterogeneity.

This study has some limitations, including the restriction to kindergarten exemption data, resulting in an incomplete picture of the vaccination status of all students; and the data may be incomplete entries or contain errors. The strengths of this research include the use of highly granular data and an in-depth methodological comparison of different clustering metrics. This data source represents all schools – private, pre-kindergarten, charter, virtual, and public – with at least five students, nearly providing the complete population of Michigan kindergarteners.

This study also uses school-level data, which captures the level at which much transmission occurs. Finally, this analysis is a natural complement to Aim 1: using real data to contextualize fine-scale clustering and how outbreak prediction is degraded as data are aggregated. Together, these two analyses present important evidence about why clustering of non-vaccination must be measured with the appropriate metrics and fine-scale data.

5.1.3 Aim 3

In response to increasing VPD outbreaks and rising NME rates across the United States, some states have sought to reduce NMEs through legislative and administrative changes. Policies that restrict access or create cumbersome hurdles to obtaining NMEs can be effective in reducing exemption rates.[95,24] In 2014, Michigan had the fourth highest vaccine exemption rate in the U.S. This prompted the state to modify Administrative Rule 325.176 (12)[143], effective January 1st, 2015, to mandate parents to attend an in-person vaccine education session at their local health department prior to obtaining an NME waiver.[93,129] While NME rates for incoming kindergarteners dropped in the following year, no studies have evaluated the longer term impacts of this change.[129] Michigan was the first state to require a waiver education program at the local health department, and to do so through an administrative, not legislative, pathway, thus the impacts of this administrative change can hold important lessons for future policy.

Using MDHHS kindergarten vaccination data from 2011-2018 (the same data utilized in Aim 2, restricted to 2011-2018 such that all vaccination requirements were consistent throughout the study period), this research evaluated the impact of the 2015 policy change on NME rates in Michigan, identified local and persistent clusters of vaccination waivers, and explored sociodemographic predictors of NMEs before and after the policy change. This research showed

that Michigan's 2015 policy achieved mixed results: the state experienced an initial, sharp decline in the number of NMEs followed by a significant rebound. The fact that NME rates have returned nearly to pre-2015 levels in just four years indicates that stronger legislative action may be needed to curb vaccine exemptions in Michigan. This analysis revealed that compared to public and charter schools, private schools had nearly double and virtual schools about five times the rates of vaccine exemptions. This analysis also showed numerous persistent clusters of school districts with consistently high waiver rates, with the geographic distribution of philosophical, religious, and medical waiver clusters each following a separate geographic pattern. Most clusters persisted despite the policy change.

A Bayesian regression analysis found that school type was a strong predictor for NMEs, highlighting the increased probability of waivers among kindergarteners in virtual and private schools. Contrary to our initial hypothesis, distance to the local health department was not a strong predictor of school-level waiver rates, suggesting that those who sought an NME were willing to do so regardless of distance. We also found non-linear patterns of NME probability across school-district level percent whiteness, percent college-educated adults, and per-capita income. These findings generally align with prior research: percent college-educated did not have large impacts on the probability of receiving an NME, but those in the highest per-capita income tertile had significantly increased likelihood of receiving an NME, though this effect decreased in size after the policy change.

Overall, this research found that Michigan's Administrative Rules change did not sustain its reduction of NMEs. Additionally, the fact that distance to the health department was not shown to be predictive of NMEs supports Navin et al., who found that Michigan's vaccine waiver educators rarely convinced parents to vaccinate their children.[155] These findings highlight

that this policy is effectively just a hurdle for parents who seek an exemption – a hurdle that motivated parents can clearly overcome.[155] Navin et al. also found that there may be a threshold of burden beyond which increasing inconvenience does not further reduce exemption rates,[156] which may explain why further driving distance to the health department was not a deterrent beyond the education session itself. The clustering analysis revealed that should future policy changes occur in Michigan to restrict or change access to certain types of NMEs, either religious or philosophical, such policies would impact regions of the state differentially.

This study used school-level data to identify potential geographic clustering and regions where local herd immunity might be broken due to high exemption rates. School-level data is the appropriate scale of analysis, as it is the unit at which much transmission occurs. Geocoding allowed for linkage of socio-demographics using the American Community Survey, joining measures of community-level demographics while employing transmission-level vaccination data and permitting cluster identification. This study also has some limitations, most importantly its restriction to kindergarteners, representing an incomplete picture of the true vaccination status of the full student population in these schools. Additionally, using Census-level demographics also may not be a perfect match to the student body from each school.

5.2 Future work

This dissertation provides insight using both theoretical dynamic modeling of a measles system (Aim 1, Chapter 2) and data-driven, statistical and spatial approaches using Michigan kindergarten vaccination data (Aim 2, Chapter 3 and Aim 3, Chapter 4). While Aim 1 used simulation to illustrate how increased clustering impacts outbreak probability, a real-world test case using fine-scale vaccination data alongside these dynamic simulation methods would be an

interesting project for future work. For example, a useful contribution would be to use school-level vaccination data in Michigan, New York, Washington, or California, the four hardest-hit states by the 2019 measles outbreak, aggregated to different administrative levels (school district, county, state, etc.) to characterize outbreak risk before the 2019 measles outbreak. One could then use these data to measure the impact of differently-scaled predictions of outbreak risk to assess the relative findings of aggregation bias in a real disease system, paired with surveillance data to identify how measles cases actually spread through those communities. Aim 2 explored numerous clustering metrics and spatial scales for their differential ability to distinguish important patterns in vaccination data for outbreak assessment. Using these clustering statistics in combination with compartmental dynamic models can help capture how each metric is able to relate to outbreak potential in a more direct way, better identifying the utility of these metrics for different research scenarios. Finally, Aim 3 evaluated Michigan's 2015 Administrative Rules change to assess clustering of individual waiver types and socio-demographic predictors of obtaining an NME over time. This analysis allowed us to explore ecologic predictors of waiver rates when applied to school-level data. However, individual-level analysis of socio-demographic predictors of non-vaccination is much needed to avoid ecologic bias and better ascertain the reasons for vaccine hesitancy and subsequently obtaining non-medical exemptions in Michigan.

5.3 Conclusions and policy implications

In conclusion, this dissertation provides an explanation for why, despite high national vaccination rates, an extremely immunogenic vaccine, and nearly universal vaccine access, measles has been resurging both across the globe and within the United States. This dissertation

is rooted in understanding the consequences of vaccine hesitancy, which was declared one of the top 10 threats to health by the WHO in 2019. This dissertation also evaluates the impact of policy that permits vaccine hesitant parents to obtain NMEs for their children. This research found that the heterogeneous distribution of NMEs throughout the population, often clustered in small communities that share the same beliefs and sociodemographic characteristics, can cause significant consequences for community disease dynamics, even beyond those groups with high exemption rates.

While this dissertation does not present a solution for the problem of rising vaccine hesitancy itself, the three analyses have strong policy implications. First of all, a greater investment in database management and data sharing is warranted – to use the data collected from the state Immunization Information Systems (IIS), which cover approximately 95% of children under the age of five in the United States,[162] and to permit such data to be used at finer scales to inform surveillance, outbreak control, and immunization programming interventions. Overall, this involves a re-thinking of vaccination data from how it is currently maintained – as registry data – to more of an active surveillance approach, finding clusters of unvaccinated individuals using similar systems to those currently used to detect cases and clusters of infectious diseases. It is important that such finer-scale data are broadly disseminated to researchers and policymakers, rather than the aggregate reported estimates at the county and state-level which are currently available. Second, and contingent upon the availability of such finer-scale data, it is important to measure spatial clustering of non-vaccination with indices that have a direct epidemiologic interpretation, rather than the typical standard of Moran's I, such that the relationship between more highly clustered non-vaccination is actionable and its consequences for outbreak risk are interpretable. Finally, there is a need to construct vaccination policies that

more effectively reduce the rates of NMEs. As seen in Michigan, relying on the local health department for waiver education sessions did not change the minds of parents with anti-vaccine sentiments, and only temporarily reduced the rate of convenience exemptions. In the future, multi-dimensional interventions could improve the root causes of vaccine hesitancy if effective programs are rolled out at the patient, provider, community, school, state, and national levels.

More broadly, halting the resurgence of VPDs such as measles in high-income regions like the United States requires earlier intervention – not just to address the consequences of vaccine hesitancy – but also to curb vaccine hesitancy itself. Interventions should thus go beyond administrative and legislative restrictions, and make an effort to reduce anti-vaccine sentiment through education campaigns, building confidence in vaccines and government, curbing misinformation, educating doctors about the importance of vaccination, minimizing missed opportunities, and increasing affordability of vaccines.[160] Against the backdrop of the COVID-19 pandemic, which has led to reduced ambulatory care and non-emergent health-care visits in the United States, causing plummeting pediatric vaccination rates, along with the suspension of global vaccination programs in developing countries, such measures could be especially impactful.[81,164] The repercussions of COVID-19, with many under-immunized children returning to school, could threaten to spur resurgence of additional VPDs, further endangering population health and leading to increased, preventable morbidity and mortality. As a result, this is a critical moment to address vaccine hesitancy and increase vaccine uptake through effective policies.

Appendix A Chapter 2 Appendix

Data Availability

Code used to generate all simulations and datasets can be found in the Github repository: https://github.com/epibayes/Measles-Spatial-Clustering-and-Aggregation-Effects/

Figure A.1 Relationship between Moran's I of initial conditions and predicted cumulative incidence across 336 motifs that do not exceed cell-level population of 1,000 for 95% overall vaccination coverage

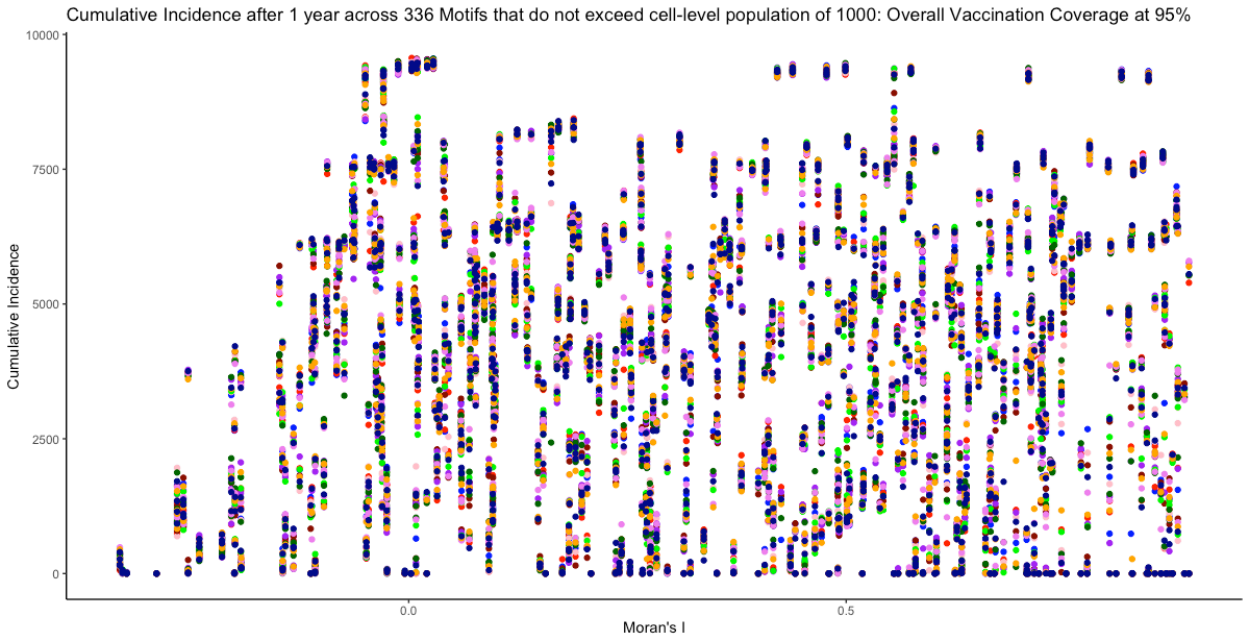

Moran's I of initial conditions (n = 336 possible motifs) representing the distribution of the 5% (n = 12,800) non-vaccinators in the environment vs. cumulative incidence after running measles SIR model for 365 days (with overall vaccination coverage at 95%) shows no clear relationship between Moran's I of the starting motif and cumulative incidence of simulated dynamic model.

Figure A.2 Relationship between Isolation Index of initial conditions and predicted cumulative incidence across 336 motifs that do not exceed cell-level population of 1,000 for 95% overall vaccination coverage

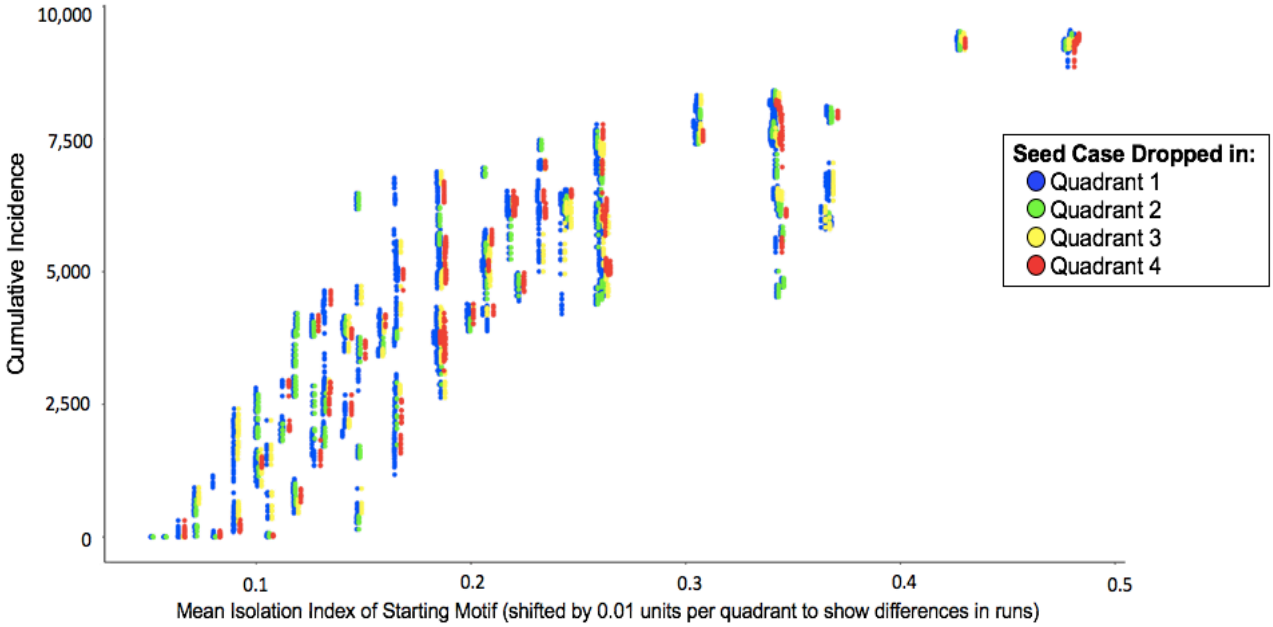

Isolation Index of initial conditions representing the distribution of the 5% (n = 12,800) non-vaccinators in the environment vs. cumulative incidence after running measles SIR model for 365 days (with overall vaccination coverage fixed at 95%) shows a monotonic, positive relationship between initial Isolation Index of starting motif and cumulative incidence of simulated dynamic model.

Figure A.3 Relationship between Isolation Index of initial conditions and predicted cumulative incidence across 296 motifs that do not exceed cell-level population of 1,000 for 94% overall vaccination coverage

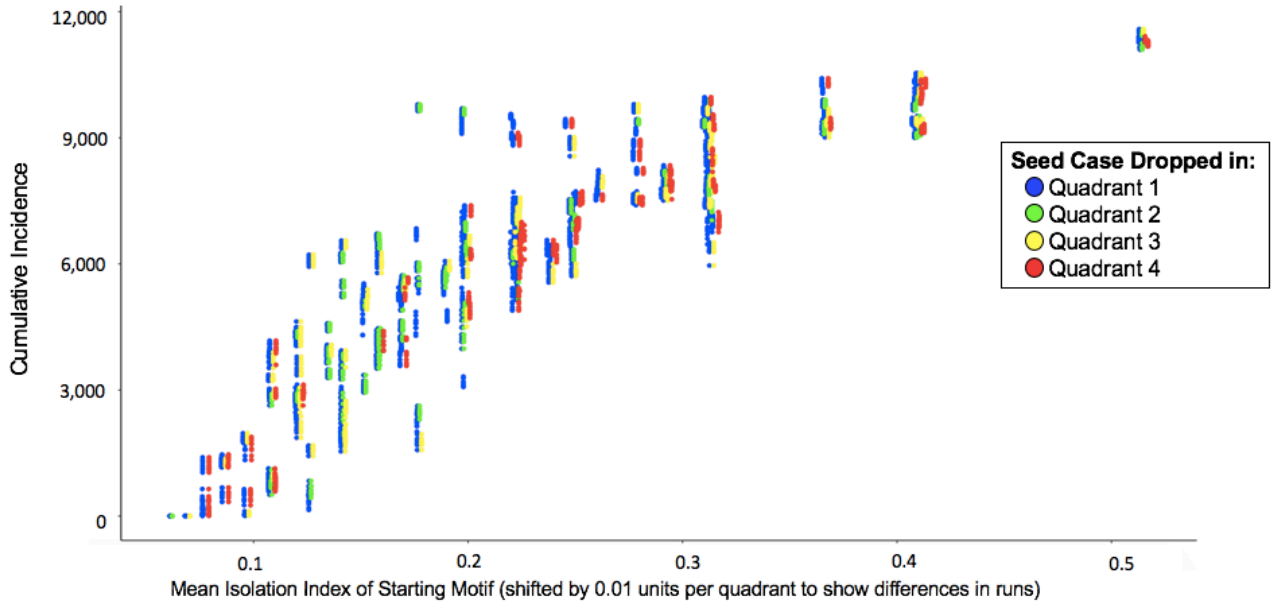

Isolation Index of initial conditions (n = 296 possible motifs) representing the distribution of the 6% (n = 15,360) non-vaccinators in the environment vs. cumulative incidence after running measles SIR model for 365 days (with overall vaccination coverage at 94%) shows a monotonic, positive relationship between initial Isolation Index of starting motif and cumulative incidence of simulated dynamic model at 94% overall vaccination coverage.

Figure A.4 Relationship between Isolation Index of initial conditions and predicted cumulative incidence across 620 motifs that do not exceed cell-level population of 1,000 for 99% overall vaccination coverage

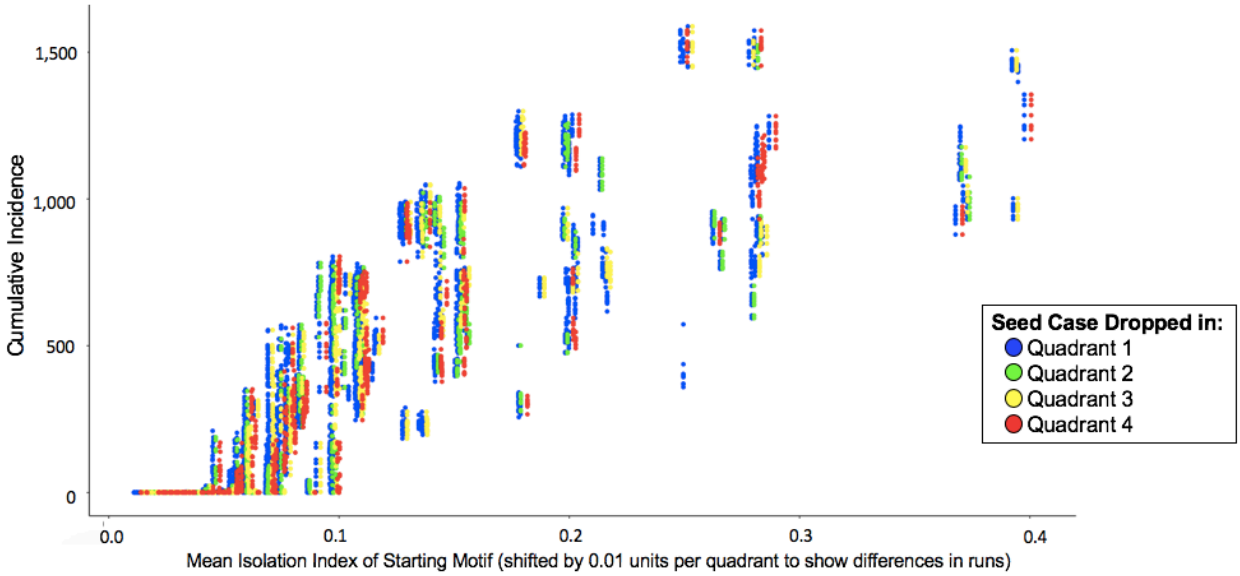

Isolation Index of initial conditions (n = 620 possible motifs) representing the distribution of the 1% (n = 2,560) non-vaccinators in the environment vs. cumulative incidence after running measles SIR model for 365 days (with overall vaccination coverage at 99%), shows a monotonic, positive relationship between initial Isolation Index of starting motif and cumulative incidence of simulated dynamic model at 99% overall vaccination coverage.

Figure A.5 Examining the effect of clustering at each level of aggregation (blocks, tracts, neighborhood, and quadrants) among the 336 possible motifs that do not exceed 1,000 individuals per cell for 95% overall vaccination coverage

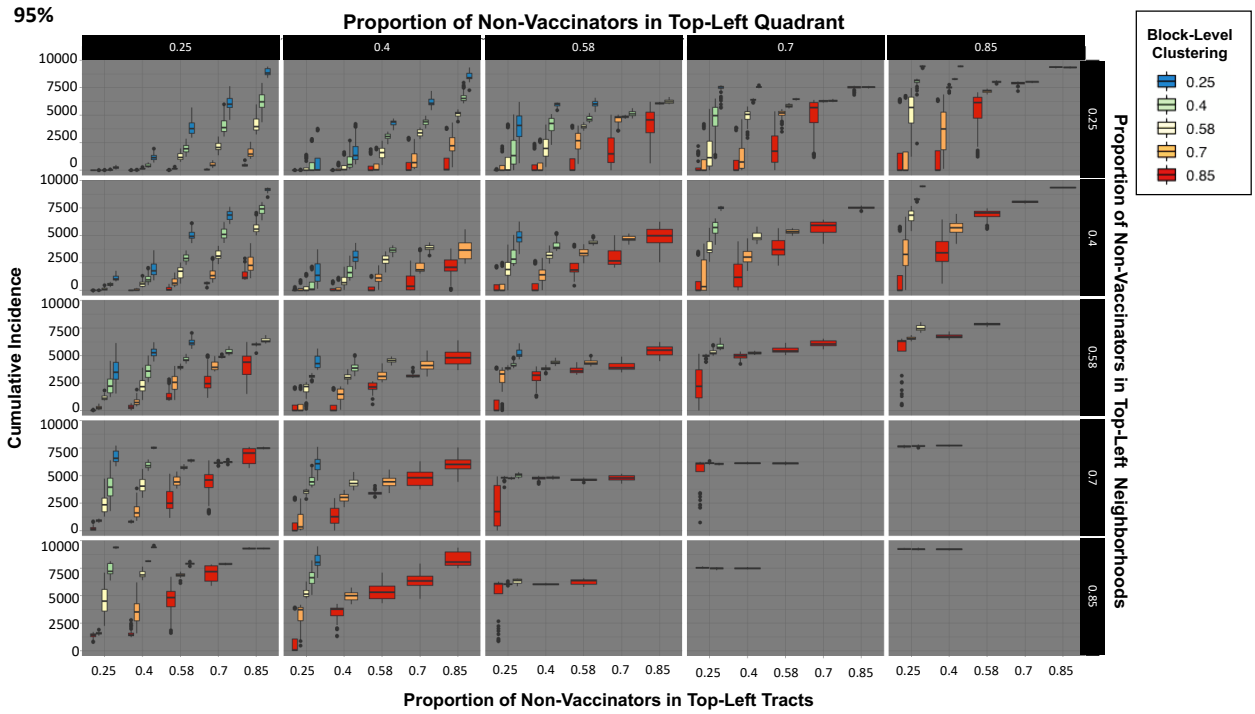

Examining the effect of clustering at each level of aggregation (blocks, tracts, neighborhoods, quadrants) among the 336 possible clustering motifs that do not exceed 1,000 individuals per cell on cumulative incidence for an overall vaccination percentage of 95%. We see a clear pattern illustrating higher cumulative incidence as clustering increases at each level: the block, tract, neighborhood, and quadrant levels, with the most highly clustered motifs (at each level) corresponding to the highest cumulative incidence values.

Figure A.6 Examining the effect of clustering at each level of aggregation (blocks, tracts, neighborhood, and quadrants) among the 296 possible motifs that do not exceed 1,000 individuals per cell for 94% overall vaccination coverage

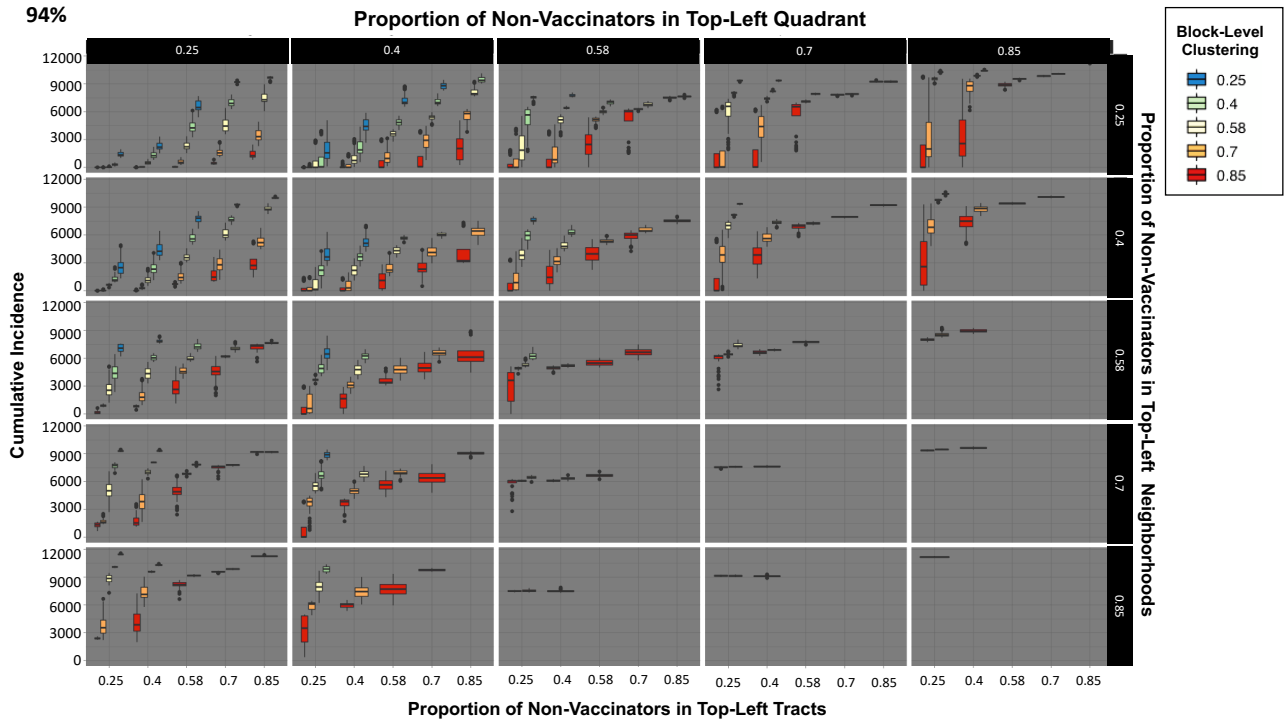

Examining the effect of clustering at each level of aggregation (blocks, tracks, neighborhoods, quadrants) among the 296 possible clustering motifs that do not exceed 1,000 individuals per cell on cumulative incidence for an overall vaccination percentage of 94%. We see a clear pattern illustrating higher cumulative incidence as clustering increases at each level: the block, tract, neighborhood, and quadrant levels, with the most highly clustered motifs (at each level) corresponding to the highest cumulative incidence values.

Figure A.7 Examining the effect of clustering at each level of aggregation (blocks, tracts, neighborhood, and quadrants) among the 543 possible motifs that do not exceed 1,000 individuals per cell for 98% overall vaccination coverage

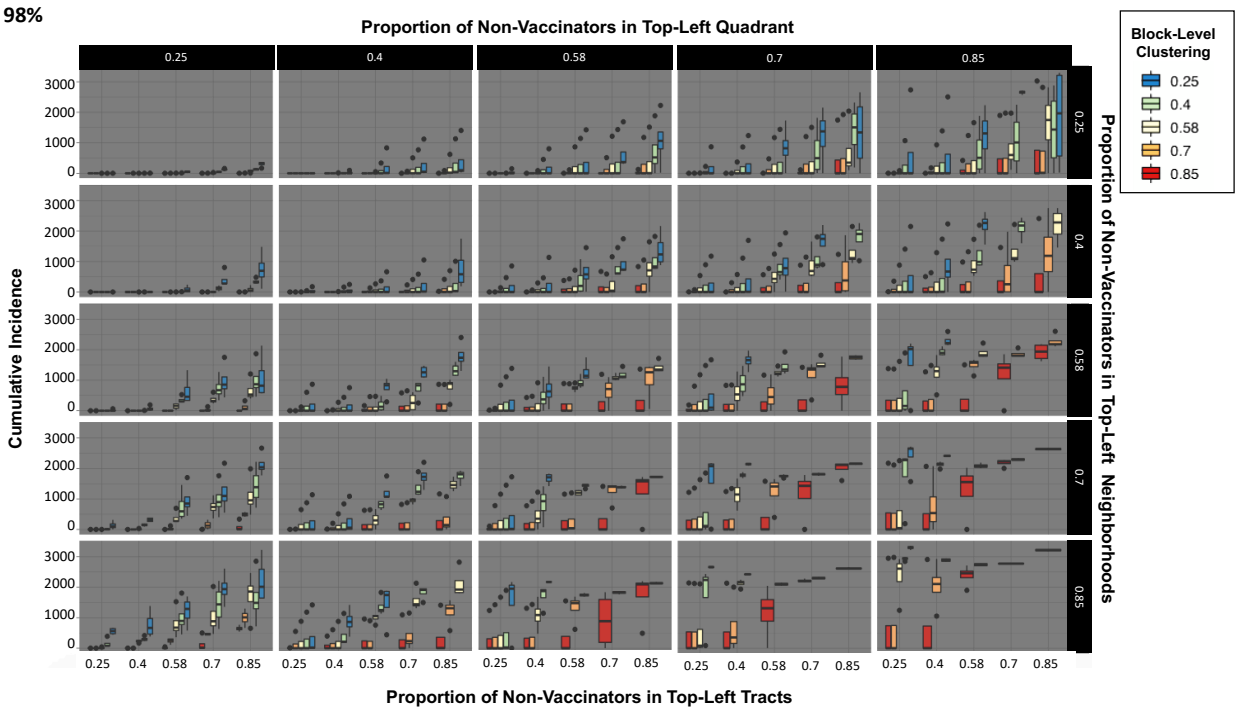

Examining the effect of clustering at each level of aggregation (blocks, tracks, neighborhoods, quadrants) among the 543 possible clustering motifs that do not exceed 1,000 individuals per cell on cumulative incidence for an overall vaccination percentage of 98%. We see a clear pattern illustrating higher cumulative incidence as clustering increases at each level: the block, tract, neighborhood, and quadrant levels, with the most highly clustered motifs (at each level) corresponding to the highest cumulative incidence values.

Figure A.8 Examining the effect of clustering at each level of aggregation (blocks, tracts, neighborhood, and quadrants) among the 620 possible motifs that do not exceed 1,000 individuals per cell for 99% overall vaccination coverage

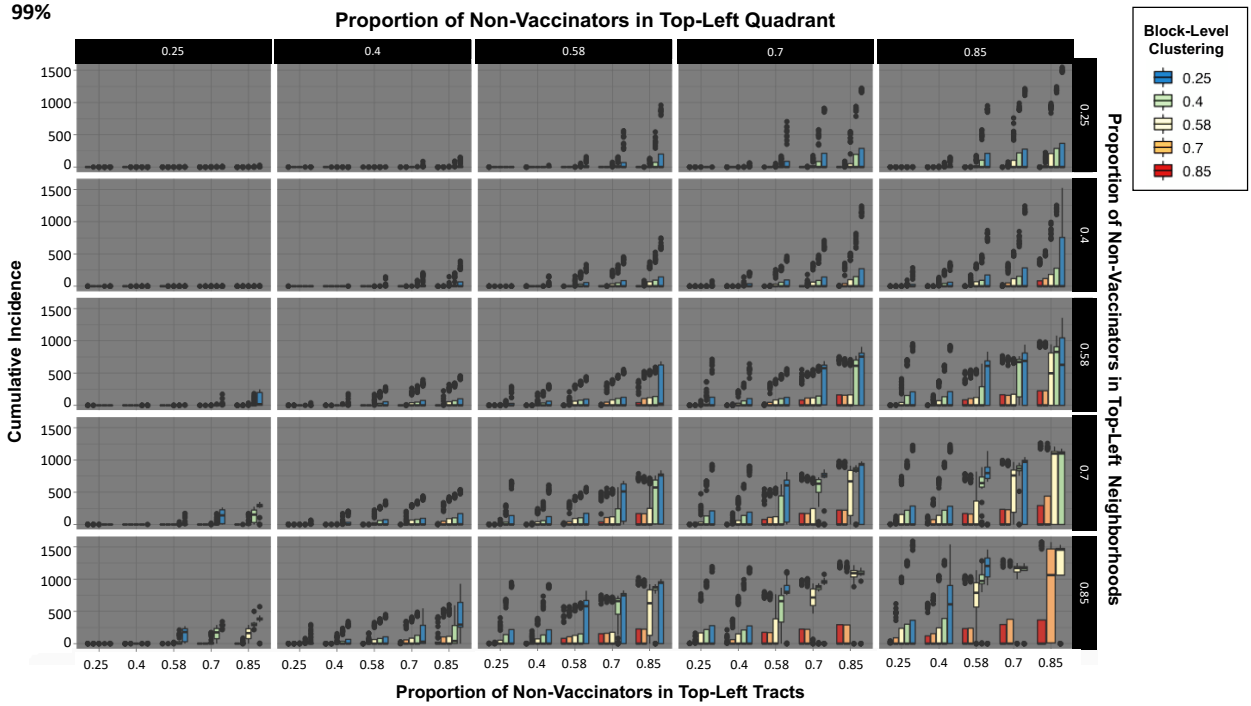

Examining the effect of clustering at each level of aggregation (blocks, tracks, neighborhoods, quadrants) among the 620 possible clustering motifs that do not exceed 1,000 individuals per cell on cumulative incidence for an overall vaccination percentage of 99%. We see a clear pattern illustrating higher cumulative incidence as clustering increases at each level: the block, tract, neighborhood, and quadrant levels, with the most highly clustered motifs (at each level) corresponding to the highest cumulative incidence values.

Figure A.9 Examining the effect of aggregation on Isolation Index of initial motifs

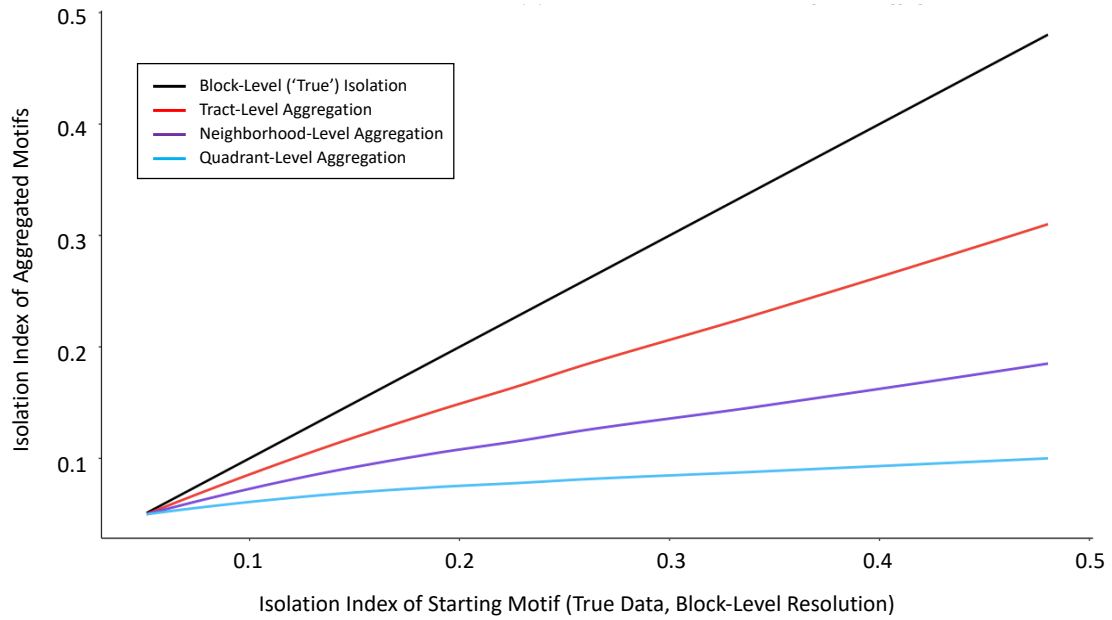

The effect of aggregation on Isolation Index of initial motifs, with black line representing 'truth', or a slope of 1, or the value of the initial motif, and the subsequent aggregated isolation values plotted for the tract, neighborhood, and quadrant-level aggregation levels.

Figure A.10 Underestimation of outbreak risk grows with intensity of isolation of non-vaccinators across 296 motifs that do not exceed cell-level populations of 1,000 at an overall vaccination coverage rate of 94%

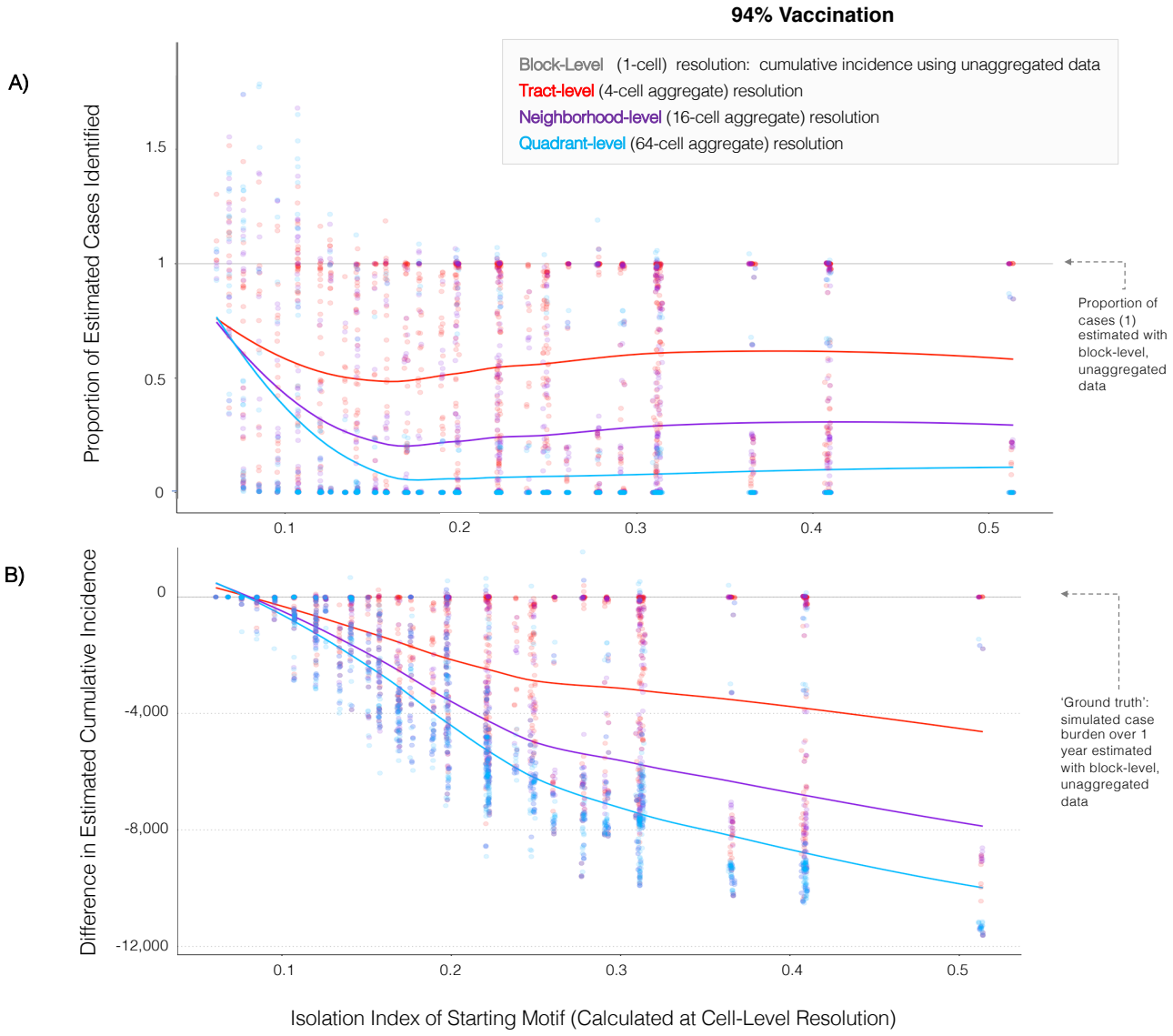

A) Proportion of estimated cases identified, treating the block-level, or individual-cell level simulation results as 'truth', in grey, when motifs are aggregated to the tract, neighborhood, and quadrant levels, sorted by Isolation Index of starting motif. B) Difference in number of estimated cases, or cumulative incidence, by aggregation level and Isolation Index of initial motif, illustrating greater loss in predicted number of cases as both aggregation level and Isolation Index increase.

Figure A.11 Underestimation of outbreak risk grows with intensity of isolation of non-vaccinators across 543 motifs that do not exceed cell-level populations of 1,000 at an overall vaccination coverage rate of 98%

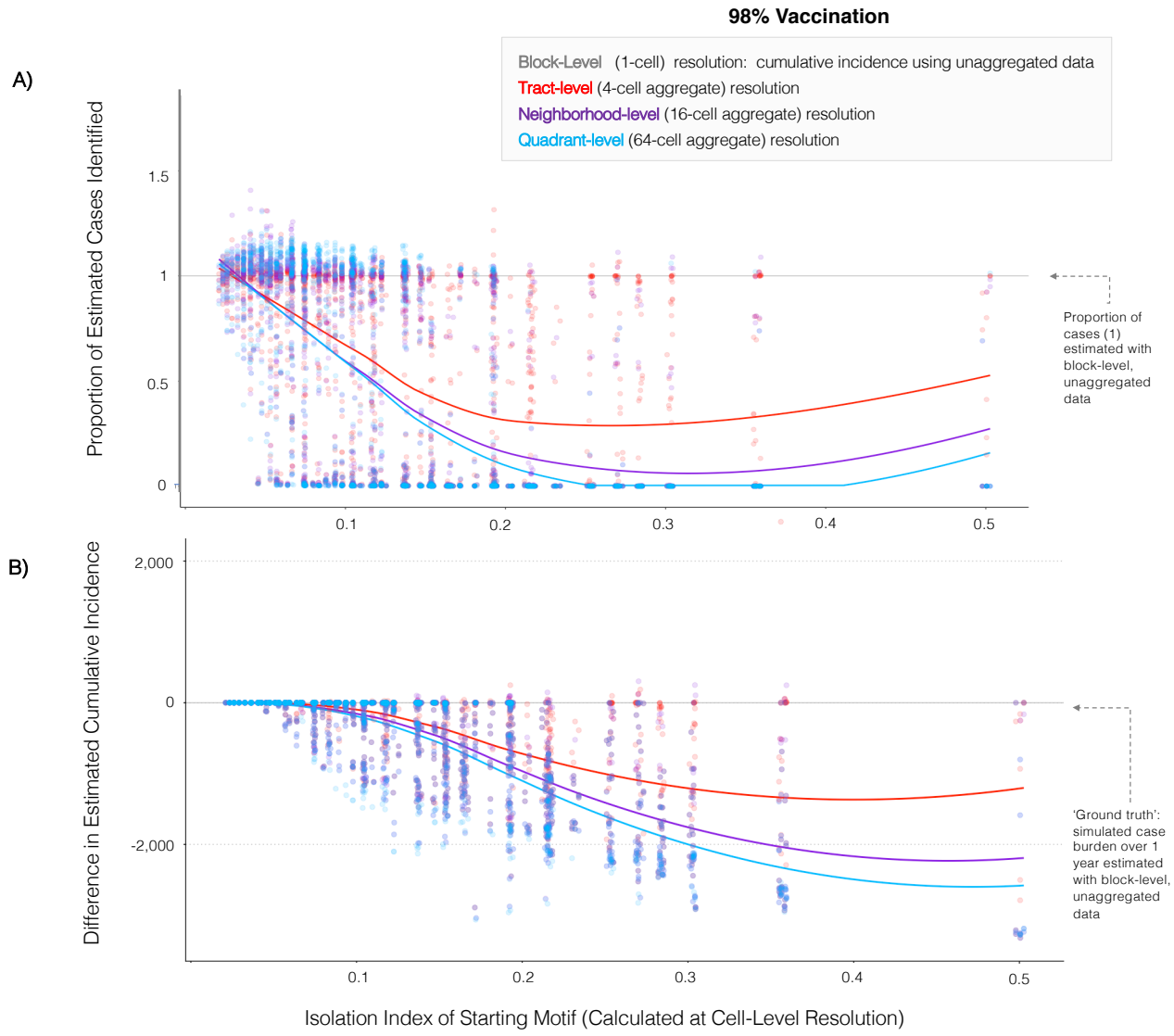

A) Proportion of estimated cases identified, treating the block-level, or individual-cell level simulation results as 'truth', in grey, when motifs are aggregated to the tract, neighborhood, and quadrant levels, sorted by Isolation Index of starting motif. B) Difference in number of estimated cases, or cumulative incidence, by aggregation level and Isolation Index of initial motif, illustrating greater loss in predicted number of cases as both aggregation level and Isolation Index increase.

Figure A.12 Underestimation of outbreak risk grows with intensity of isolation of non-vaccinators across 620 motifs that do not exceed cell-level populations of 1,000 at an overall vaccination coverage rate of 99%

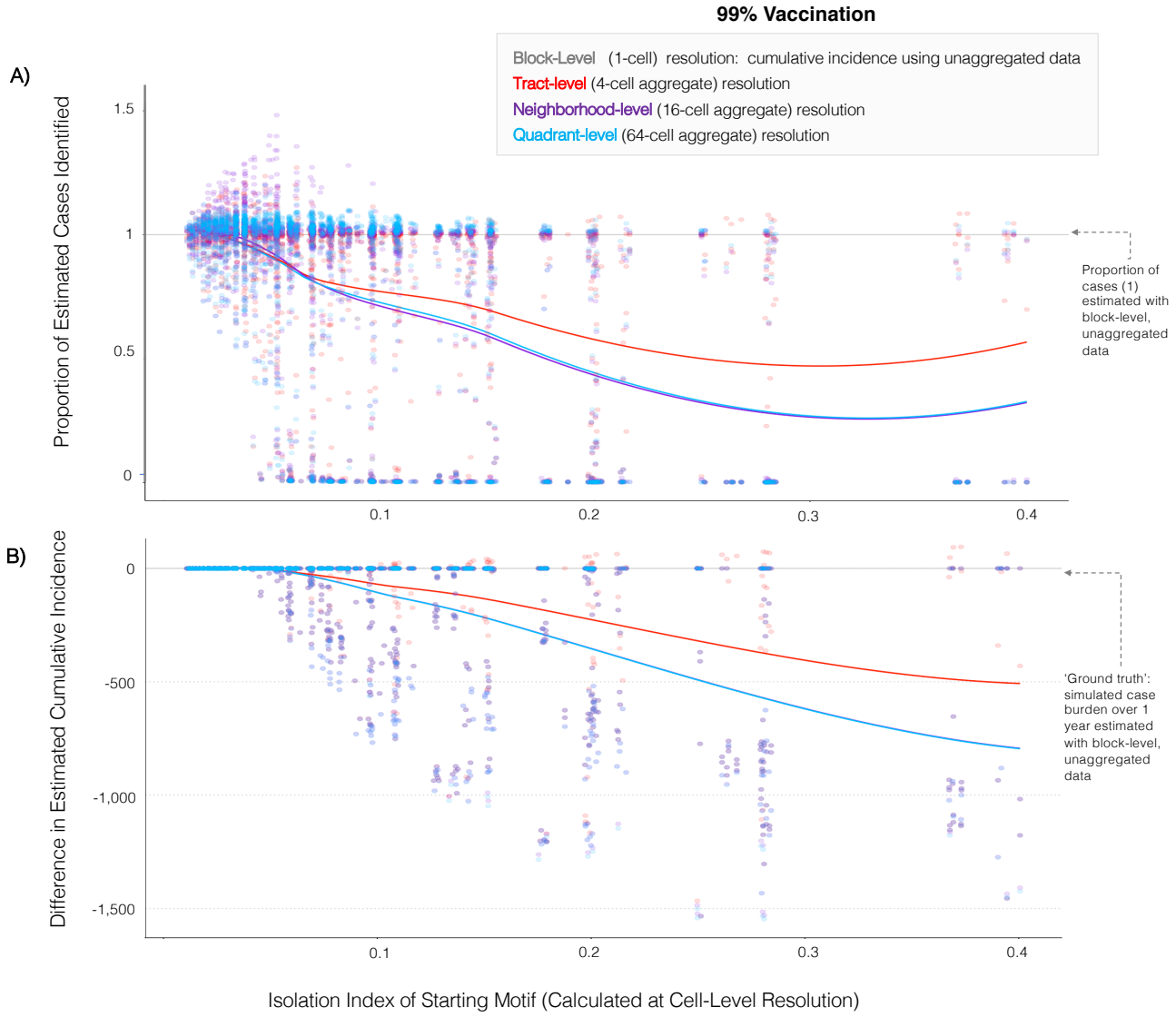

A) Proportion of estimated cases identified, treating the block-level, or individual-cell level simulation results as 'truth', in grey, when motifs are aggregated to the tract, neighborhood, and quadrant levels, sorted by Isolation Index of starting motif. B) Difference in number of estimated cases, or cumulative incidence, by aggregation level and Isolation Index of initial motif, illustrating greater loss in predicted number of cases as both aggregation level and Isolation Index increase.

Figure A.13 95% Overall vaccination coverage: outbreak probability increases with Isolation Index of starting motif, regardless of which quadrant the seed case is placed in

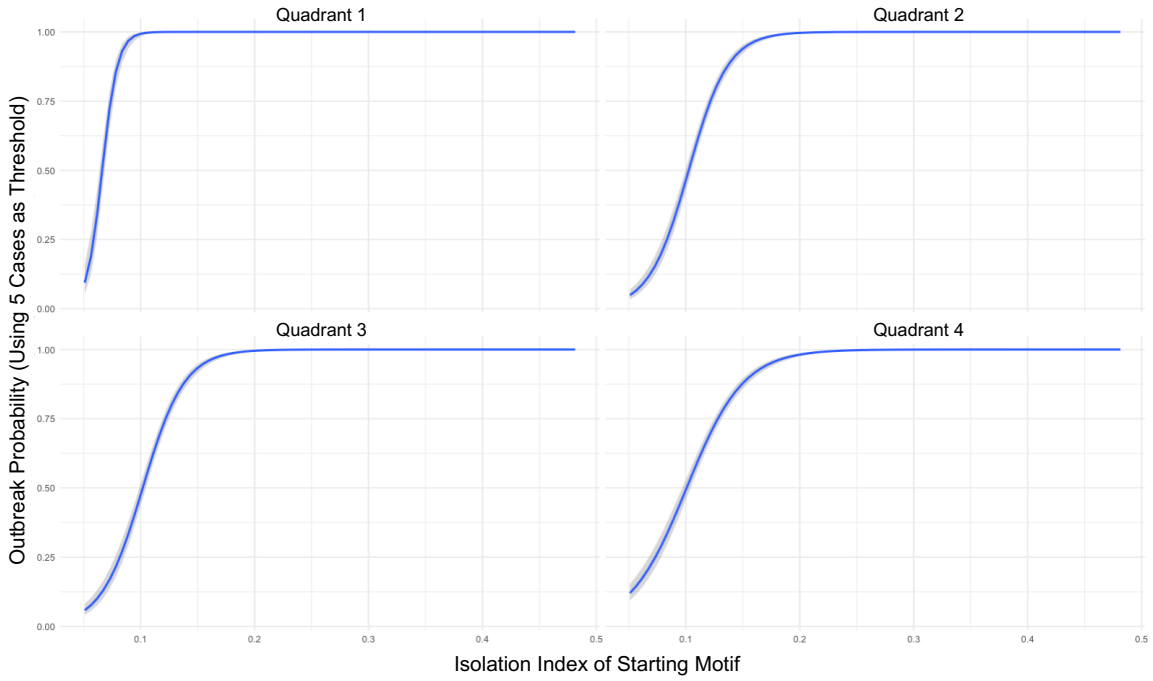

Binomial loess plots comparing 95% vaccination coverage with seed introductions into the center of quadrant 1 (top left), quadrant 2 (top right), quadrant 3 (bottom left), and quadrant 4 (bottom right) illustrate that as the Isolation Index increases of the starting motif (indicating a higher degree of clustering in the vaccination landscape), the outbreak probability increases to nearly 100%. The outbreak probability certainly is reduced in quadrant 4, furthest from the high-level clustering of non-vaccinators, requiring higher values of the Isolation Index to correspond to increased outbreak probability. However even introductions to the bottom right quadrant can yield fairly high outbreak probability at high values of the Isolation Index of the starting motif for 95% overall vaccination.

Figure A.14 99% Overall vaccination coverage: outbreak probability increases with Isolation Index of starting motif, regardless of which quadrant the seed case is placed in

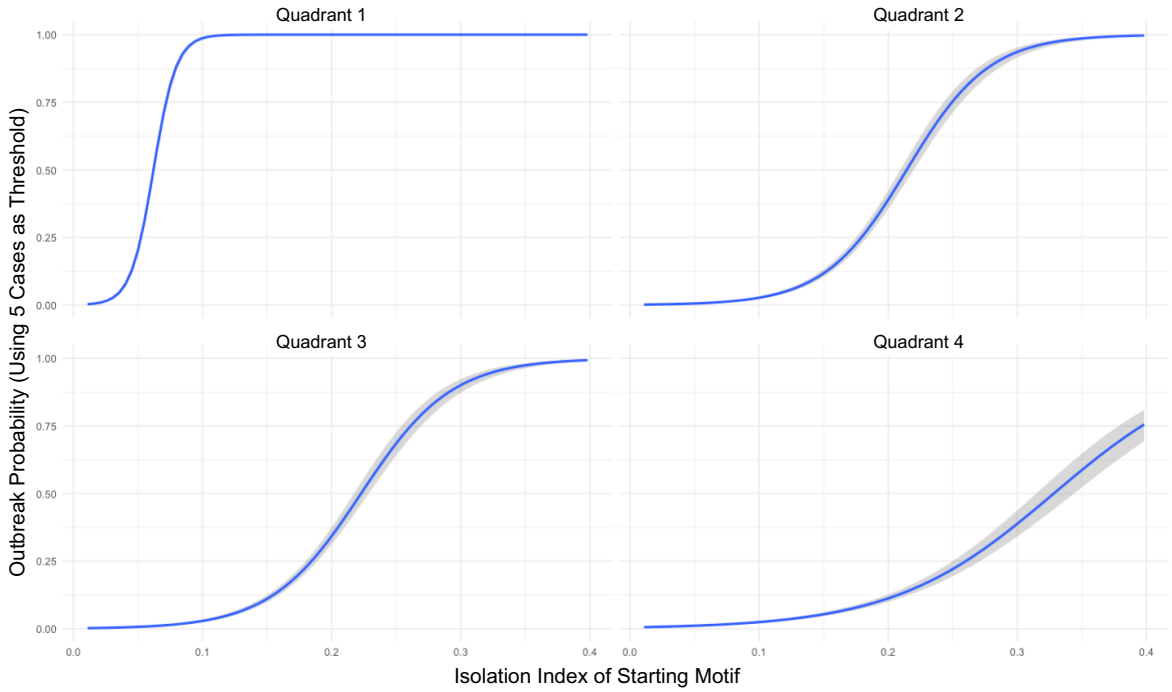

Binomial loess plots comparing 99% vaccination coverage with seed introductions into the center of quadrant 1 (top left), quadrant 2 (top right), quadrant 3 (bottom left), and quadrant 4 (bottom right) illustrate that as the Isolation Index increases of the starting motif (indicating a higher degree of clustering in the vaccination landscape), the outbreak probability increases, nearly to 100% for introductions in quadrant 1-3. However, the outbreak probability is reduced more notably in quadrant 4, reaching a maximum of about 75% for the most clustered motifs. 99% overall vaccination shows more clearly what we would expect – that because our clustering motifs placed unvaccinated individuals into the top left quadrant at each level, introductions into the fourth quadrant are the least likely to start an outbreak, even if they are highly clustered.

Table A.1 94% overall vaccination: linear multivariate model fit to attack rate over 1 year of simulation time, with estimates fit to cumulative incidence models in parentheticals, shows that clustering at each level correspond to higher cumulative incidence

	Univariate Analysis			Multivariate Analysis		
Predictor	**Attack Rate Estimate (CI Estimate)**	**p-value**	**R^2**	**Attack Rate Estimate (CI Estimate)**	**p-value**	**R^2**
Moran's I	0.016 (246.0)	0.0085	0.001	-0.033 (-506.2)	<0.001	
Isolation Index*	0.865 (13,279.9)	<0.001	0.805	0.505 (7,759.3)	<0.001	
Level 1 clustering**	0.056 (854.3)	<0.001	0.122	0.059 (907.2)	<0.001	
Level 2 clustering**	0.046 (703.9)	<0.001	0.083	0.052 (797.2)	<0.001	
Level 3 clustering**	0.039 (601.0)	<0.001	0.060	0.049 (749.5)	<0.001	
Level 4 clustering**	0.037 (561.7)	<0.001	0.053	0.052 (797.9)	<0.001	
						0.844

**Isolation Index was normalized so that a one-unit increase in Isolation Index represented the spread from the minimum value to maximum value of the Isolation Index for a given level of overall vaccination*

***The clustering levels were operationalized as ordinal variables with steps increasing from 25% (homogeneous) in one quadrant, 40%, 58%, 70%,and 85%.*

Table A.2 99% overall vaccination: linear multivariate model fit to attack rate over 1 year of simulation time, with estimates fit to cumulative incidence models in parentheticals, shows that clustering at each level correspond to higher cumulative incidence

	Univariate Analysis			Multivariate Analysis		
Predictor	**Attack Rate Estimate (CI Estimate)**	**p-value**	**R^2**	**Attack Rate Estimate (CI Estimate)**	**p-value**	**R^2**
Moran's I	-0.023 (-58)	<0.001	0.003	-0.043 (-110.6)	<0.001	
Isolation Index*	0.355 (909.9)	<0.001	0.379	0.451 (1,154.2)	<0.001	
Level 1 clustering**	0.022 (56.9)	<0.001	0.085	-0.001 (-3.0)	0.124	
Level 2 clustering**	0.020 (51.7)	<0.001	0.070	-0.004 (-10.0)	<0.001	
Level 3 clustering**	0.017 (43.8)	<0.001	0.050	-0.009 (-23.6)	<0.001	
Level 4 clustering**	0.015 (38.5)	<0.001	0.039	0.018 (-46.2)	<0.001	
						0.395

**Isolation Index was normalized so that a one-unit increase in Isolation Index represented the spread from the minimum value to maximum value of the Isolation Index for a given level of overall vaccination*

***The clustering levels were operationalized as ordinal variables with steps increasing from 25% (homogeneous) in one quadrant, 40%, 58%, 70%,and 85%.*

Table A.3 Simulated outbreak probability results by overall vaccination level and three different outbreak thresholds: 5, 10, and 20 cases at three selected overall vaccination coverage rates: 94%, 95%, and 99%

Overall vaccination %	Outbreak threshold (number of cases)	Number of simulation runs exceeding outbreak threshold	Total number of simulation runs	% of simulations exceeding outbreak threshold	% of simulations without an outbreak
94%	5	11074	11840	93.5%	6.5%
	10	10991	11840	92.8%	7.2%
	20	10923	11840	92.3%	7.7%
95%	5	11962	13440	89.0%	11.0%
	10	11864	13440	88.3%	11.7%
	20	11743	13440	87.4%	12.6%
99%	5	4785	24800	19.3%	80.7%
	10	4626	24800	18.7%	81.3%
	20	4479	24800	18.1%	81.9%

Simulated outbreak probability results by overall vaccination level and three different outbreak thresholds: 5, 10, and 20 cases for selected vaccination coverages: 94%, 95%, and 99%. This table highlights that with 94% overall vaccination, the outbreak probability across all motifs ranges from 93.5% (with a threshold of 5 cases to 98.2% with a threshold of 20 cases), the outbreak probability for 95% ranges from 89.0% (for 5 cases) to 87.4% (for 20 cases), and the outbreak probability for 99% vaccination ranges from 19.3% (for 5 cases) to 18.1% (for 20 cases). Outbreak probability here was defined as any of the simulation runs for each set of motifs at each vaccination threshold that generated an outbreak with at least the threshold number of cases.

Table A.4 Simulated cumulative incidence results by overall vaccination level and level of aggregation for selected vaccination coverages: 94%, 95%, 98%, and 99%

Aggregation Level	Median Simulated Cases	Mean Simulated Cases	Inter-Quartile Range (IQR)	% Reduction in Mean Cases Detected after Aggregating
Overall Vaccination Level: 94%				
Block	6059.98	5381.72	5187.60	ref
Tract	2060.60	3157.50	6048.68	-41.3%
Neighborhood	3.67	1521.14	2331.15	-71.7%
Quadrant	1.03	499.48	0.73	-90.7%
Overall Vaccination Level: 95%				
Block	3999.06	3886.31	4931.25	ref
Tract	825.76	2122.29	3897.61	-45.4%
Neighborhood	0.77	911.16	513.04	-76.6%
Quadrant	0.56	227.29	0.48	-94.2%
Overall Vaccination Level: 98%				
Block	8.02	581.42	1090.29	ref
Tract	1.10	227.17	0.69	-60.9%
Neighborhood	1.09	77.28	0.17	-86.7%
Quadrant	1.16	1.26	0.14	-99.8%
Overall Vaccination Level: 99%				
Block	1.05	106.36	0.45	ref
Tract	1.03	37.40	0.11	-64.8%
Neighborhood	1.03	1.40	0.08	-98.7%
Quadrant	1.07	1.10	0.06	-99.0%

Simulated cumulative incidence results by overall vaccination level and level of aggregation for selected vaccination coverages: 94%, 95%, 98%, and 99%: highlighting the percent of mean cases detected after aggregating data to the three levels of aggregation, showing a 90.7% reduction in mean detected cases after aggregating at 94% overall vaccination, 94.2% reduction after aggregating at 95% coverage, and over 99% reduction in estimated cases for both 98% and 99% vaccination.

Appendix B Chapter 3 Appendix

Data Availability

Code used to generate all analyses can be found in the Github repository:
https://github.com/epibayes/MDHHS-Vaccination-Data

Figure B.1 Difference in raw number of detected students deemed to be 'at-risk' based upon three thresholds of vaccination waivers: 5%, 10%, and 20%

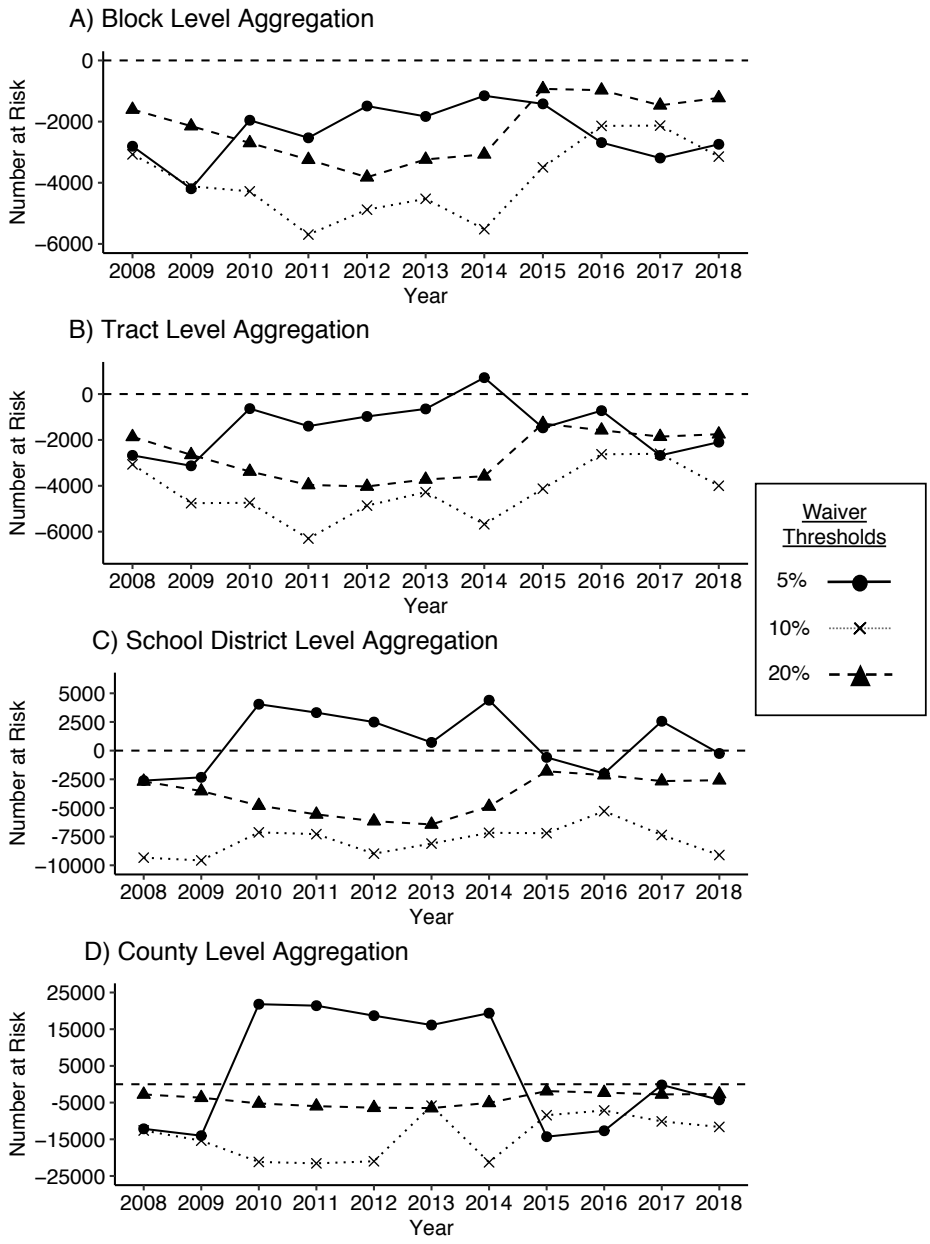

Difference in raw number of detected students deemed to be 'at risk' based upon three thresholds of vaccination waivers: 5%, 10%, and 20%, with aggregation to the A) block group, B) tract, C) school district, and D) county levels over the study period from 2008-2018. For the 5% waiver threshold, low-level aggregation (panels A-C) does not lead to much bias, though county-level aggregation results in positive and negative bias in the percent of at-risk students. For the 10% and 20% waiver thresholds, higher levels of aggregation result in greater *underestimation* of the at-risk population.

Table B.1 Kindergarten enrollment over the study period for 32 missing school records from kindergarten vaccination data in Michigan, 2008-2018

School Name	County	'08	'09	'10	'11	'12	'13	'14	'15	'16	'17	'18	Total
Country Meadows	Missaukee	-	-	-	-	-	-	-	-	-	-	-	0
Misty Mornings	Clare	-	-	-	-	-	-	-	-	-	-	-	0
Chappel Dam	Gladwin	-	-	-	-	-	-	-	-	-	-	-	0
Mapleview Amish	Gladwin	-	-	-	-	-	-	-	-	-	-	-	0
Parker Amish	Gladwin	-	-	-	-	-	-	-	-	-	-	-	0
Whispering Pines Amish	Isabella	-	-	-	-	-	-	-	-	-	-	-	0
St Peters Developmental Kindergartner	Kent	-	-	-	-	-	-	1	-	-	-	-	1
Community Christian Academy KD	Macomb	-	-	-	-	-	-	0	-	-	-	-	0
Applegrove Amish	Mecosta	-	-	-	-	-	-	-	-	-	-	-	0
Deerfield Acres Amish	Mecosta	-	-	-	-	-	-	-	-	-	-	-	0
Jersey Acres Amish	Mecosta	-	-	-	-	-	-	0	-	-	-	-	0
Maple Lane Amish	Mecosta	-	-	-	-	-	-	-	-	-	-	-	0
Meadow Lane Amish	Mecosta	-	-	-	-	-	-	-	-	-	-	-	0
Miller Amish	Mecosta	-	-	-	-	-	-	-	-	-	-	-	0
North Hinton Amish	Mecosta	-	-	-	-	-	-	-	-	-	-	-	0
Quigly Creek Amish	Mecosta	-	-	-	-	-	-	-	-	-	-	-	0
Ribble Amish	Mecosta	-	-	-	-	-	-	-	-	-	-	-	0
Rolling Acres Amish	Mecosta	-	-	-	-	-	-	-	-	-	-	-	0
Shady Maple Amish	Mecosta	-	-	-	-	-	-	-	-	-	-	-	0
Morning Star (Amish)	Oscoda	-	-	-	-	-	-	-	-	-	-	-	0
Sunrise View (Amish)	Oscoda	-	-	-	-	-	-	-	-	-	-	-	0

Pilgrim Pathway School Amish	Presque Isle	-	-	-	-	-	-	-	-	-	-	-	0
Small Steps Big Dreams LL	St. Clair	-	-	-	-	-	-	-	-	-	-	-	0
The Paris Academy	Kent	-	-	-	-	-	-	-	-	11	-	-	11
Alternative Education	Barry	-	-	-	-	-	-	-	-	-	-	-	0
Center for Excellence Children Academy	Oakland	-	-	-	-	-	-	3	-	-	-	-	3
Outbreak Site 2	Ingham	-	-	-	-	-	-	-	-	-	-	12	12
Outbreak Site	Ingham	-	-	-	-	-	-	-	-	0	0	0	0
School Test Site	Ingham	-	-	-	-	-	-	-	-	0	0	0	0
Blain Elementary	Kent	-	-	-	-	-	-	-	-	-	-	0	0
JC ISD East Campus	Jackson	-	-	-	-	-	-	-	-	-	-	-	0
Ontonagon ISD	Ontonagon	-	-	-	-	-	-	-	-	-	-	-	0
Total number of students in unmatched, unidentifiable schools from 2008-2018													27

Appendix C Chapter 4 Appendix

Data Availability

Code used to generate all analyses can be found in the Github repository:
https://github.com/epibayes/MDHHS-Vaccination-Data

Equation C.1 The Local Indicators of Spatial Association (LISA statistic)

$$Eq\ C.1 \qquad I_i = \frac{x_i - \bar{X}}{S_i^2} \sum_{j=1, j \neq i}^{n} w_{i,j}(x_i - \bar{X})$$

$$with \qquad S_i^2 = \frac{\sum_{j=1, j \neq i}^{n} w_{i,j}}{n-1} - \bar{X}^2$$

where x_i is the number of non-vaccinators for geographic unit i, $\bar{X}$ is the mean of non-vaccination rates, $w_{i,j}$ is the spatial weight between geographic units i and j, and n represents the number of spatial units.[149] A positive I indicates that a given spatial unit (in this case, school districts) has neighboring features (school districts) that have similarly high or low attribute values, indicating that the school district is part of a high- or low-waiver cluster. A negative I instead indicates that a school district has neighbors with dissimilar values, making a given school district an outlier. Setting the confidence limits to 95% selects only statistically significant clusters of high values (HH clusters, as shown in Figure 4.3), low values (LL), or outliers (HL, LH).

Table C.1 Unadjusted binomial logistic model of NMEs at the school-level with random intercepts for school district and indicator variable for vaccine policy change, 2011-2018

	Estimate (β)	Odds Ratio	Standard Error	p-value
Intercept	-3.102	0.045	0.0327	<0.001
Policy Change Indicator (2015-2018 vs. 2011-2014)	-0.435	0.647	0.0112	<0.001

Table C.2 State-level vaccination exemption data in Michigan with student enrollment figures, broken out by non-medical waiver types and by and school type from 2011-2018

Year	Student Enrollment	% Waivers	% Philosophical Waivers	% Religious Waivers
Charter Schools				
2011	278	5.04	71.43	14.29
2012	359	6.41	47.83	47.83
2013	362	4.42	43.75	50.00
2014	562	3.91	54.55	45.45
2015	713	3.09	59.09	36.36
2016	961	2.91	57.14	35.71
2017	1009	4.56	67.39	30.43
2018	1280	5.55	56.34	40.85
Private Schools				
2011	9459	8.84	70.33	14.83
2012	9072	10.50	75.03	14.27
2013	9113	10.07	74.73	17.86
2014	9128	10.28	72.17	21.86
2015	8901	7.27	73.88	20.56
2016	9263	7.69	73.60	23.03
2017	9134	8.02	72.85	24.01
2018	9184	8.61	68.90	26.93
Public Schools				
2011	111279	5.26	76.21	13.25
2012	111375	5.47	76.01	14.59
2013	107363	5.45	74.24	17.46
2014	105130	4.85	71.92	21.85
2015	103217	3.25	77.26	16.82
2016	105286	3.27	75.44	19.27
2017	105650	3.80	73.41	21.36
2018	104742	4.06	71.89	22.58
Virtual Schools				
2011	57	21.05	91.67	8.33
2012	74	27.03	55.00	45.00
2013	200	27.00	64.81	35.19
2014	241	19.50	53.19	46.81
2015	205	13.66	67.86	28.57
2016	287	19.86	66.67	31.58
2017	411	24.57	71.29	23.76
2018	487	27.52	61.19	26.12

Table C.3 Local Indicators of Spatial Association (LISA) school and school district-level cluster persistence in pre- and post-administrative rules change time periods (2011-2014 and 2015-2018)

Persistence of spatial unit in waiver cluster	Pre-or Post-Policy Change Time Period	Number of total clusters*	Number of philosophical waiver clusters	Number of religious clusters	Number of medical clusters
School District Level					
1+ year	2011-2014	52	56	32	43
1+ year	2015-2018	34	26	32	25
2+ years	2011-2014	20	23	12	10
2+ years	2015-2018	14	14	8	4
3+ years	2011-2014	12	8	6	1
3+ years	2015-2018	8	8	2	1
all 4 years	2011-2014	3	2	3	0
all 4 years	2015-2018	3	4	0	0
Individual Schools					
1+ year	2011-2014	101	131	28	70
1+ year	2015-2018	63	87	56	34
2+ years	2011-2014	18	37	5	7
2+ years	2015-2018	16	20	11	0
3+ years	2011-2014	2	7	1	0
3+ years	2015-2018	4	7	2	0
all 4 years	2011-2014	1	2	0	0
all 4 years	2015-2018	3	1	1	0

**For this table, only showing "high-high" waiver clusters, meaning that these clusters were identified by the LISA statistic as significant clusters of high waiver rates (indicating that both a given school district and the average of its neighboring school districts had significantly high waiver rates).*

Table C.4 Bayesian binomial hierarchical model output showing posterior mean average marginal effects of the probability of getting an NME waiver for selected demographic predictors at the school district level (tertiles of school district percent whiteness, percent college education, and per-capita income)

Year	*Tertile of School-District Level % Whiteness**	*Posterior mean average probability of obtaining an NME[1]*	*Tertile of School-District Level % College Education***	*Posterior mean average probability of obtaining an NME[2]*	*Tertile of School-District Level Per-Capita Income****	*Posterior mean average probability of obtaining an NME[3]*
2011	1st	3.9%	1st	4.7%	1st	4.5%
	2nd	5.6%	2nd	6.1%	2nd	4.3%
	3rd	6.6%	3rd	5.5%	3rd	7.0%
2012	1st	4.0%	1st	4.9%	1st	4.7%
	2nd	5.8%	2nd	6.4%	2nd	4.4%
	3rd	6.9%	3rd	5.6%	3rd	7.2%
2013	1st	3.8%	1st	4.6%	1st	4.3%
	2nd	5.5%	2nd	6.1%	2nd	4.4%
	3rd	6.5%	3rd	5.4%	3rd	6.8%
2014	1st	3.5%	1st	4.2%	1st	3.8%
	2nd	4.9%	2nd	5.4%	2nd	3.8%
	3rd	5.9%	3rd	4.8%	3rd	6.2%
2015	1st	2.3%	1st	2.8%	1st	2.6%
	2nd	3.4%	2nd	3.7%	2nd	2.9%
	3rd	4.0%	3rd	3.3%	3rd	4.0%
2016	1st	2.4%	1st	2.9%	1st	2.9%
	2nd	3.4%	2nd	3.8%	2nd	3.1%
	3rd	4.1%	3rd	3.4%	3rd	3.9%
2017	1st	2.7%	1st	3.2%	1st	3.3%
	2nd	3.8%	2nd	4.2%	2nd	3.4%
	3rd	4.6%	3rd	3.8%	3rd	4.3%
2018	1st	2.8%	1st	3.4%	1st	3.6%
	2nd	4.0%	2nd	4.4%	2nd	3.6%
	3rd	4.8%	3rd	3.9%	3rd	4.5%

[1] Marginalized over the distribution of covariates excluding year and School District Level % Whiteness
[2] Marginalized over the distribution of covariates excluding year and School District Level % College Education
[3] Marginalized over the distribution of covariates excluding year and School District Level Per-Capita Income
** Tertiles of School District-Level Percent White are: 1st Tertile: 5.9% - 73.9%, 2nd Tertile: 73.9% - 91.7%, 3rd Tertile: 91.7% - 99.5%*
*** Tertiles of School District-Level Percent College Education are: 1st Tertile: 5.2% - 18.0%, 2nd Tertile: 18.0% - 31.9%, 3rd Tertile: 31.9% - 78.4%*
**** Tertiles of School District-Level Per-Capita Income are: 1st Tertile: $11,371 - $24,551, 2nd Tertile: $24, 551 - $32,148, 3rd Tertile: $32,148 - $73,834*

Table C.5 Bayesian binomial hierarchical model output showing posterior mean average marginal effects of the probability of getting an NME waiver by school type from 2011-2018

Year	***School Type***	***Posterior mean average probability of obtaining an NME[1]***
2011	Public	4.5%
	Charter	4.9%
	Private	8.4%
	Virtual	22.1%
2012	Public	4.7%
	Charter	5.1%
	Private	8.7%
	Virtual	22.9%
2013	Public	4.5%
	Charter	4.9%
	Private	8.3%
	Virtual	22.0%
2014	Public	3.9%
	Charter	4.2%
	Private	7.2%
	Virtual	19.7%
2015	Public	2.7%
	Charter	2.9%
	Private	5.1%
	Virtual	14.7%
2016	Public	2.7%
	Charter	2.9%
	Private	5.1%
	Virtual	14.7%
2017	Public	3.0%
	Charter	3.3%
	Private	5.7%
	Virtual	16.1%
2018	Public	3.1%
	Charter	3.4%
	Private	5.9%
	Virtual	16.7%

[1] *Marginalized over the distribution of covariates excluding year and School Type*

Table C.6 Bayesian binomial hierarchical model output showing posterior mean average marginal effects of the probability of getting an NME waiver by distance to the health department from 2011-2018

Year	***Percentile of Travel Time (Distance to Local Health Department)****	***Posterior mean average probability of obtaining an NME[1]***
2011	10th Percentile	5.1%
	90th Percentile	5.9%
2012	10th Percentile	5.2%
	90th Percentile	6.2%
2013	10th Percentile	4.9%
	90th Percentile	6.0%
2014	10th Percentile	4.5%
	90th Percentile	5.2%
2015	10th Percentile	3.3%
	90th Percentile	3.3%
2016	10th Percentile	3.2%
	90th Percentile	3.6%
2017	10th Percentile	3.7%
	90th Percentile	3.9%
2018	10th Percentile	3.9%
	90th Percentile	4.0%

** The 10th Percentile of travel time to the local health department was 0.101 hours (~6 minutes). The 90th Percentile of travel time was 0.592 hours (~35 minutes)*

[1] Marginalized over the distribution of covariates excluding year and travel time to the health department

Figure C.1 Bayesian binomial hierarchical model output showing posterior mean average marginal effects of probability of getting an NME comparing charter, private, public, and virtual schools

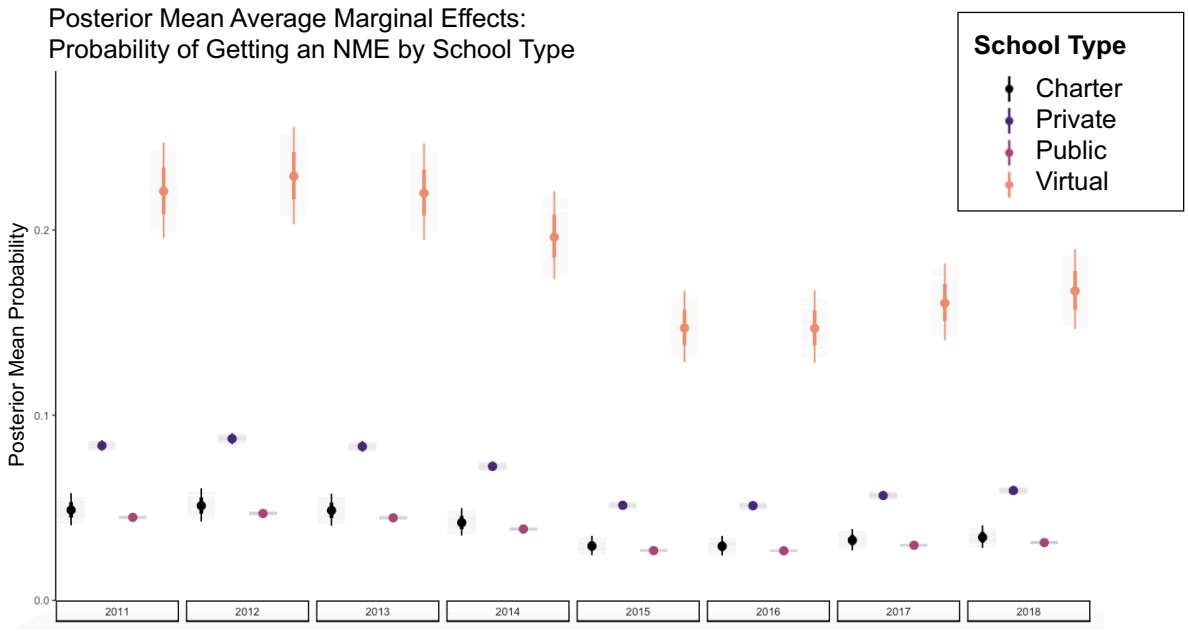

Figure C.2 Bayesian binomial hierarchical model output showing posterior mean average marginal effects of probability of getting an NME comparing the 10th and 90th percentile of travel time to the local health department

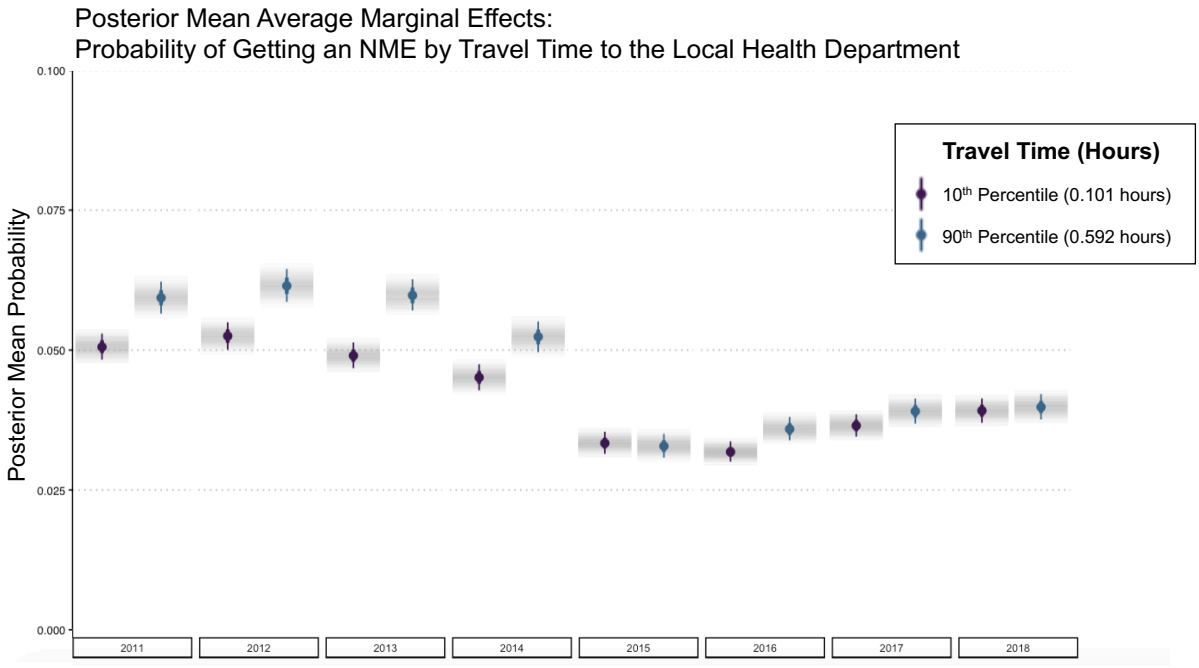

Figure C.3 Bayesian binomial hierarchical model output showing mean differences of posterior mean average marginal effects of probability of getting an NME comparing private, virtual, and charter schools to public schools

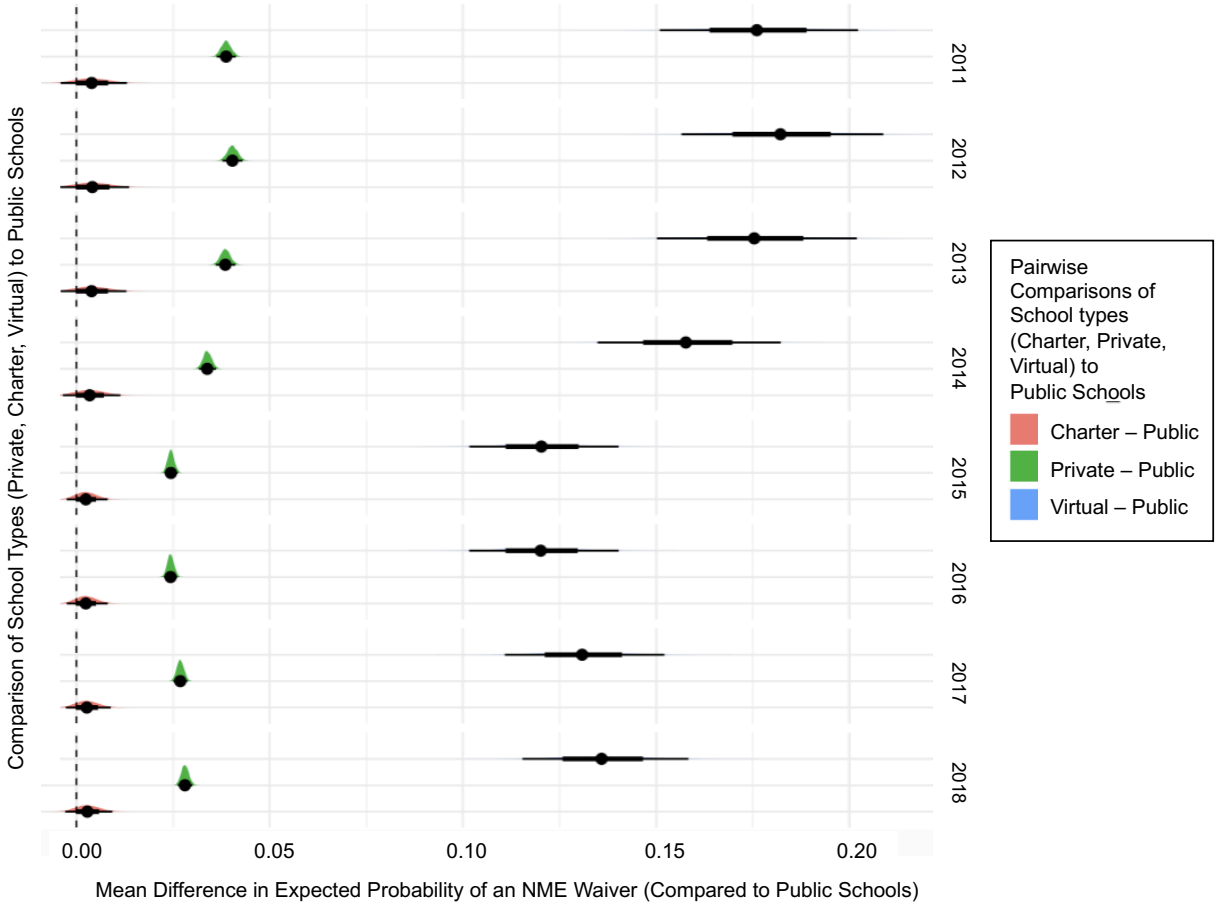

The probability that the mean difference for virtual and private schools is higher than that of public schools was ~1, indicating no overlap in the distributions. The probability that the mean difference for charter schools – public schools was greater than 0 was 0.8248, thus these distributions were not significantly different.

Figure C.4 Bayesian binomial hierarchical model output showing mean differences of posterior mean average marginal effects of probability of getting an NME comparing the third (highest) tertile of school district level percent college education and the second (middle) tertile of school district level percent college education to the 1st tertile

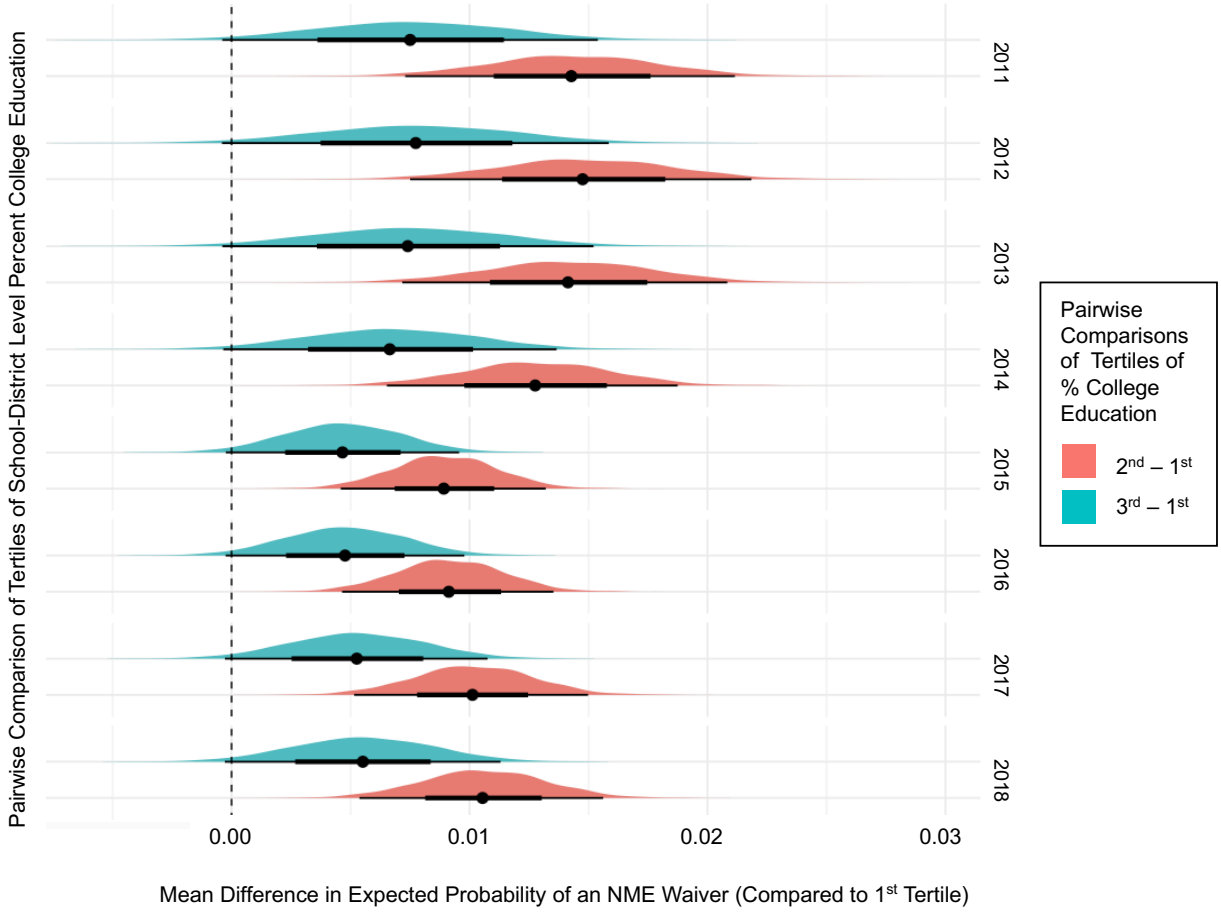

The probability that the mean difference for the third tertile – the first tertile of percent college education was > 0 was 0.971, and the probability that the second tertile was greater than the first tertile was 0.9996.

Figure C.5 Bayesian binomial hierarchical model output showing mean differences of posterior mean average marginal effects of probability of getting an NME comparing the third (highest) tertile of school district level per-capita income and the second (middle) tertile of school district level per-capita income to the 1st tertile

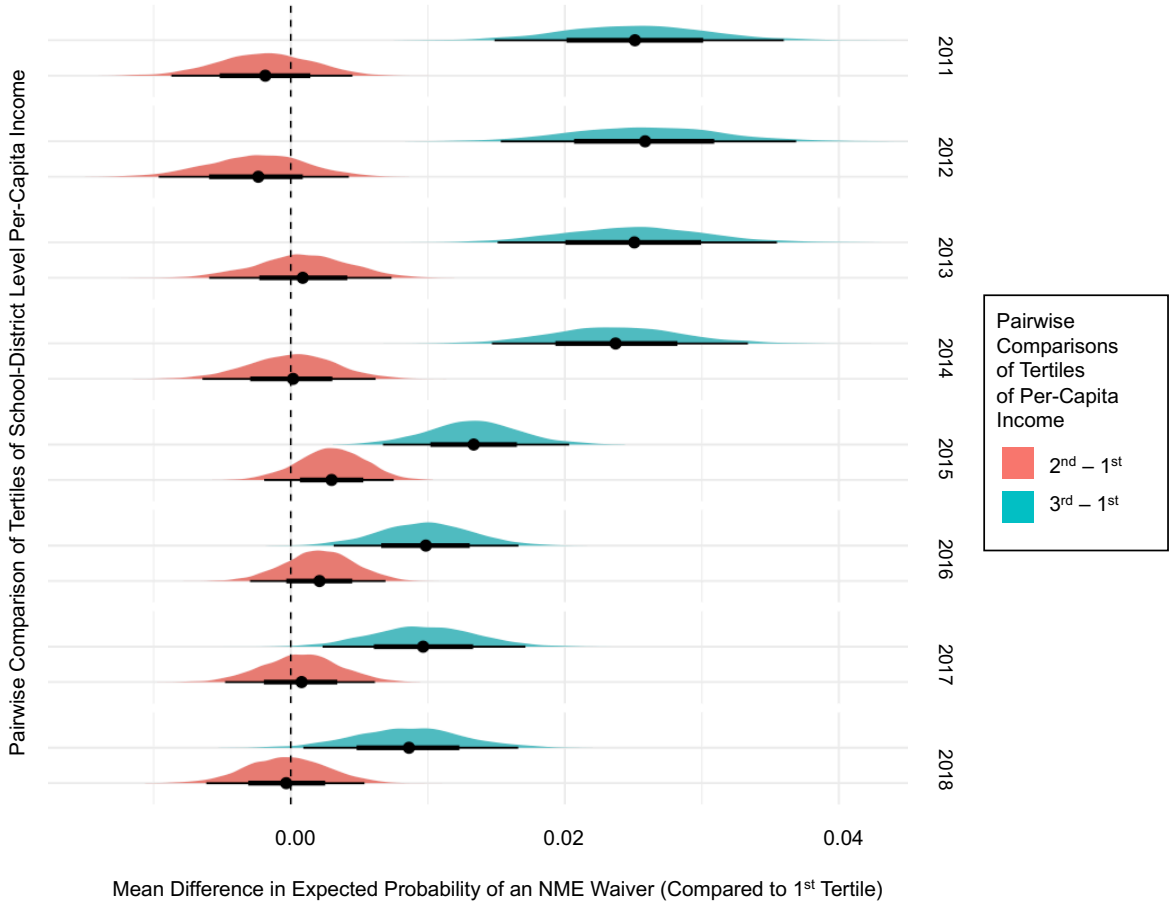

The probability that the mean difference for the second tertile – the first tertile of per-capita income was > 0 was 0.5534, not significant, and the probability that the third tertile was greater than the first tertile was 0.997. This illustrates that overall, the third, and wealthiest tertile of per-capita income had significantly increased probability of an NME waiver compared to the first, though it is clear that this effect does diminish somewhat after the 2015 policy.

Figure C.6 Bayesian binomial hierarchical model output showing mean differences of posterior mean average marginal effects of probability of getting an NME comparing the third (highest) tertile of school district level percent white and the second (middle) tertile of school district level percent white to the 1st tertile

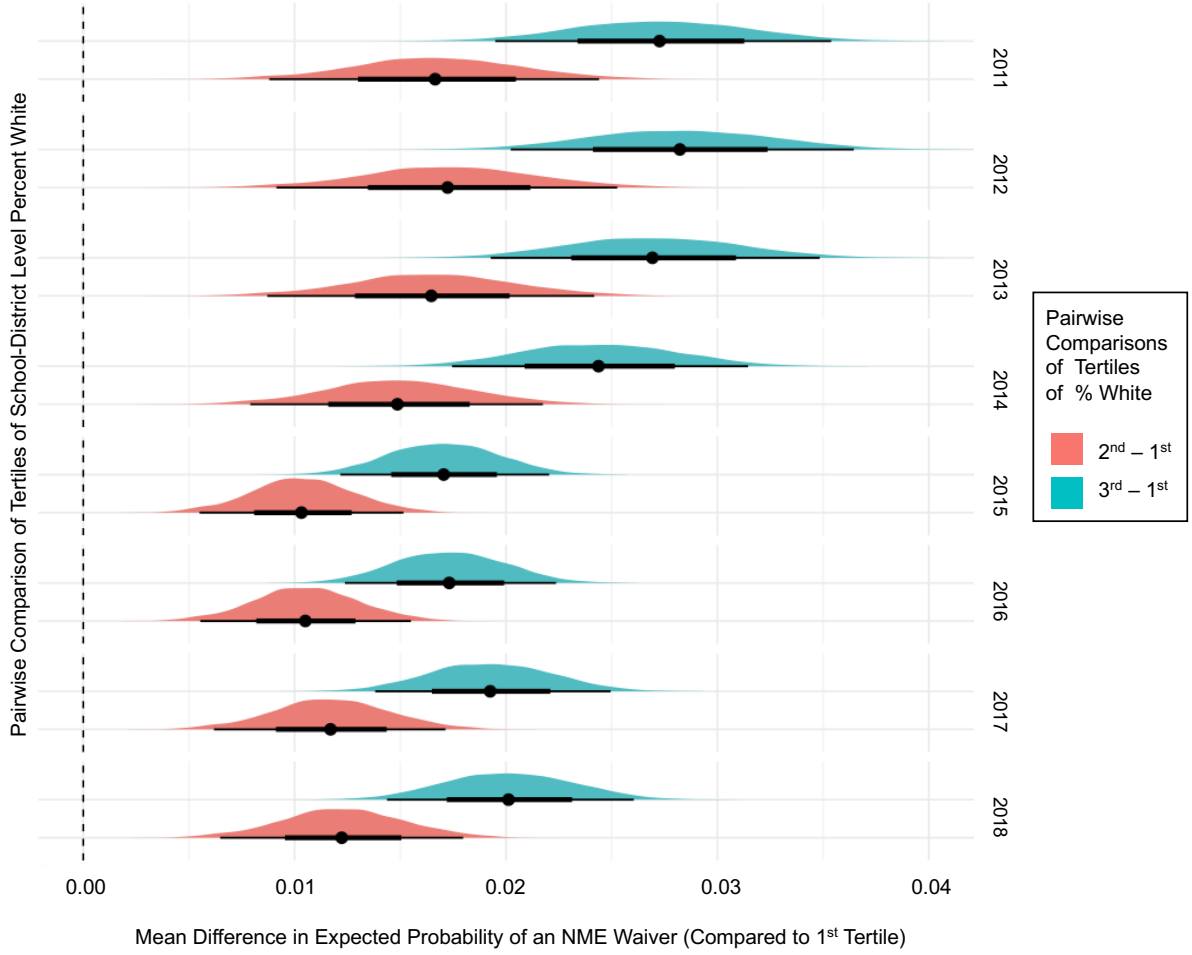

The probability that the mean difference for both the third and second tertiles minus the first tertile was ~1, indicating no overlap between the distributions and illustrating that both the second and third tertile of school district-level percent whiteness had significantly higher expected probability of an NME.

Figure C.7 Bayesian binomial hierarchical model output showing mean differences of posterior mean average marginal effects of probability of getting an NME comparing the 90th percentile to the 10th percentile of distance (in hours) to the local health department

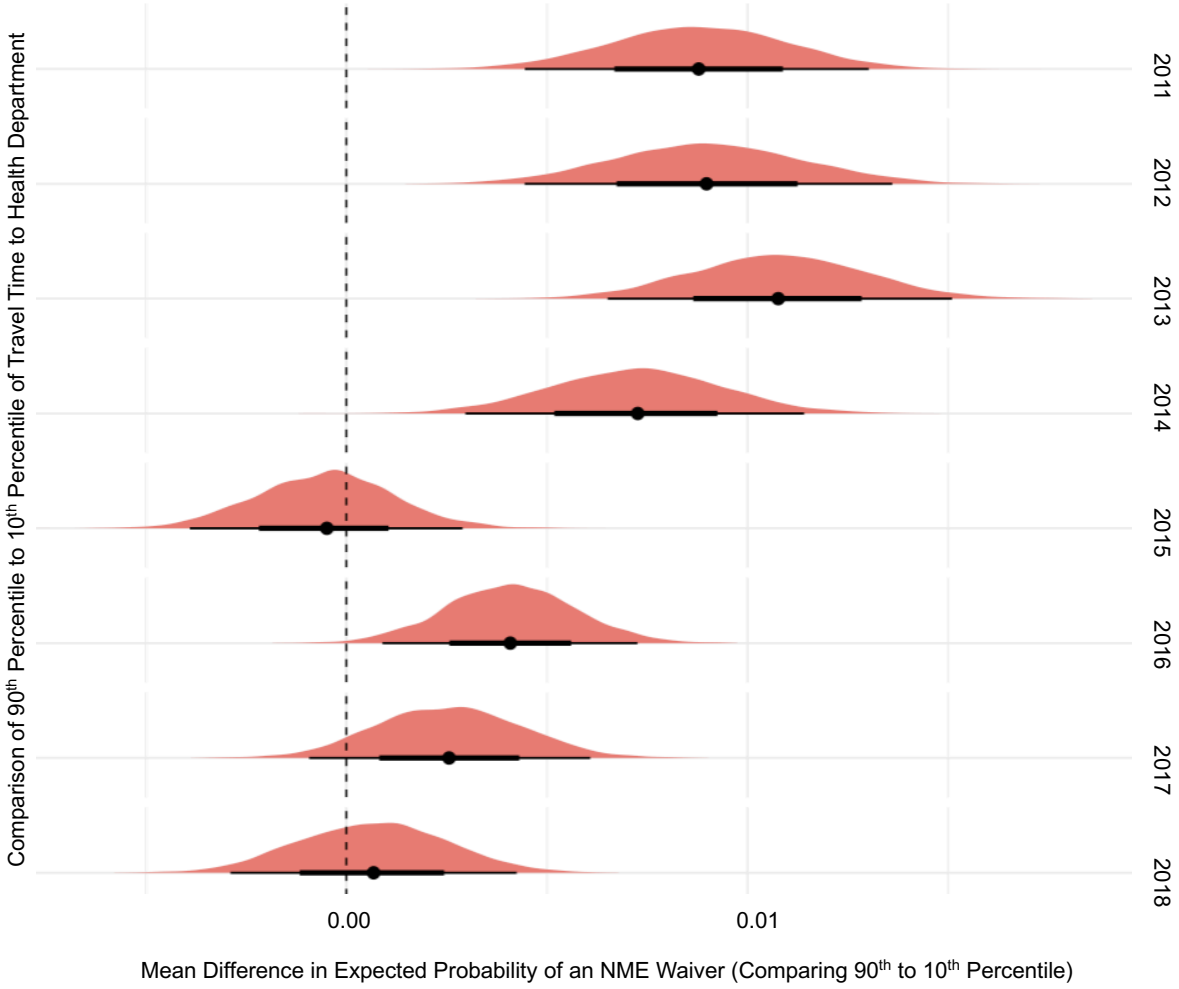

The probability that the mean difference from the 90th to 10th percentile was > 0 over the study period was 0.866,which is not significant. Additionally, it is clear that the effect size of the mean difference is very small, with the maximum mean difference between the 90th and 10th percentile of travel time at 0.01 hours.

Bibliography

1. Centers for Disease Control and Prevention (CDC). Measles. In: Hamborsky J, Kroger A, Wolfe SE, ed. *Epidemiology and Prevention of Vaccine-Preventable Diseases, 13th Edition*. 13th ed. Washington D.C.: Public Health Foundation; 2015:209-229. http://www.cdc.gov/vaccines/pubs/pinkbook/meas.html.

2. CDC. Transmission of Measles. https://www.cdc.gov/measles/transmission.html. Published 2018. Accessed June 27, 2019.

3. Majumder MS, Cohn EL, Mekaru SR, Huston JE, Brownstein JS. Substandard Vaccination Compliance and the 2015 Measles Outbreak. *JAMA Pediatr*. 2015;169(5):494-495. doi:10.1001/jamapediatrics.2015.0384

4. CDC. Recommended Child and Adolescent Immunization Schedule for ages 18 years or younger, United States 2019. Immunization Schedules.

5. Moss WJ, Griffin DE. Global measles elimination. *Nat Rev Microbiol*. 2006;4(12):900-908. doi:10.1038/nrmicro1550

6. World Health Organization (WHO). *Global Measles and Rubella Strategic Plan: 2012 - 2020*.; 2012.

7. Measles & Rubella Initiative. *Measles & Rubella Strategic Framework 2021-2030*.; 2020. https://measlesrubellainitiative.org/measles-rubella-strategic-framework-2021-2030/.

8. Perry RT, Murray JS, Gacic-Dobo M, Dabbagh A, Mulders MN SP et al. Progress toward regional measles elimination - worldwide, 2000-2014. *MMWR Morb Mortal Wkly Rep*. 2015;64(44):1245-1251. doi:10.15585/mmwr.mm6444a2

9. Lo Vecchio A, Montagnani C, Krzysztofiak A, et al. Measles Outbreak in a High-Income Country: Are Pediatricians Ready? *J Pediatric Infect Dis Soc*. 2020;9(4):416-420. doi:10.1093/jpids/piz061

10. Silverberg R, Caceres J, Greene S, Hart M, Hennekens CH. Lack of Measles Vaccination of a Few Portends Future Epidemics and Vaccination of Many. *Am J Med*. May 2019. doi:10.1016/j.amjmed.2019.04.041

11. Hotez PJ, Nuzhath T, Colwell B. Combating vaccine hesitancy and other 21st century social determinants in the global fight against measles. *Curr Opin Virol*. 2020;41:1-7. doi:10.1016/j.coviro.2020.01.001

12. Pananos AD, Bury TM, Wang C, et al. Critical dynamics in population vaccinating behavior. *Proc Natl Acad Sci*. 2017;114(52):13762-13767. doi:10.1073/pnas.1704093114

13. Worden L, Ackley SF, Zipprich J, et al. Measles transmission during a large outbreak in California. *Epidemics*. 2020;30:100375. doi:10.1016/j.epidem.2019.100375

14. CDC. Measles Cases and Outbreaks. https://www.cdc.gov/measles/cases-outbreaks.html. Published 2019. Accessed June 28, 2019.

15. Hill H, Elam-Evans L, Yankey D, Singleton J, Dietz V. Vaccination Coverage Among Children Aged 19–35 Months — United States, 2015. *MMWR Morb Mortal Wkly Rep*. 2016;65:1065-1071. doi:http://dx.doi.org/10.15585/mmwr.mm6539a

16. CDC. US measles cases in first five months of 2019 surpass total cases per year for past 25 years. *Press Release: Thursday May 30, 2019*.

17. Tanne JH. Measles cases and deaths are increasing worldwide, warn health agencies. *BMJ*. 2020;(November):m4450. doi:10.1136/bmj.m4450

18. Zucker JR, Rosen JB, Iwamoto M, et al. Consequences of Undervaccination — Measles Outbreak, New York City, 2018–2019. *N Engl J Med*. 2020;382(11):1009-1017. doi:10.1056/NEJMoa1912514

19. McDonald R, Ruppert P, Souto M, et al. Notes from the Field: Measles Outbreaks from Imported Cases in Orthodox Jewish Communities — New York and New Jersey, 2018–2019. *MMWR Morb Mortal Wkly Rep*. 2019;68(19):444-445.

20. City of New York. Measles: Recent Outbreak in Brooklyn and Queens. NYC Health.

21. Cantor JD. Mandatory Measles Vaccination in New York City — Reflections on a Bold Experiment. *N Engl J Med*. June 2019:NEJMp1905941. doi:10.1056/NEJMp1905941

22. Truelove SA, Graham M, Moss WJ, Metcalf CJE, Ferrari MJ, Lessler J. Characterizing the impact of spatial clustering of susceptibility for measles elimination. *Vaccine*. 2019;37(5):732-741. doi:10.1016/j.vaccine.2018.12.012

23. Olive JK, Hotez PJ, Damania A, Nolan MS. The state of the antivaccine movement in the United States: A focused examination of nonmedical exemptions in states and counties. *PLOS Med*. 2018;15(6):e1002578. doi:10.1371/journal.pmed.1002578

24. Delamater PL, Leslie TF, Yang YT. Examining the spatiotemporal evolution of vaccine refusal: nonmedical exemptions from vaccination in California, 2000–2013. *BMC Public*

Health. 2018;18(1):458. doi:10.1186/s12889-018-5368-y

25. Pingali SC, Delamater PL, Buttenheim AM, Salmon DA, Klein NP, Omer SB. Associations of Statewide Legislative and Administrative Interventions With Vaccination Status Among Kindergartners in California. *JAMA*. 2019;322(1):49. doi:10.1001/jama.2019.7924

26. Delamater PL, Leslie TF, Yang YT. A spatiotemporal analysis of non-medical exemptions from vaccination: California schools before and after SB277. *Soc Sci Med*. 2016;168(13):230-238. doi:10.1016/j.socscimed.2016.08.011

27. Delamater PL, Lesliem TF, Yang YT. California senate bill 277's grandfather clause and nonmedical vaccine exemptions in California, 2015-2022. *JAMA Pediatr*. 2016;170(6):619-620. doi:10.1001/jamapediatrics.2015.4856

28. Cliff AD, Haggett P, Stroup DF. The geographic structures of measles epidemics in the northeastern United States. *Am J Epidemiol*. 1992;136(5):592-602.

29. Brownwright TK, Dodson ZM, Van Panhuis WG. Spatial clustering of measles vaccination coverage among children in sub-Saharan Africa. *BMC Public Health*. 2017;17(1):1-7. doi:10.1186/s12889-017-4961-9

30. Sartorius B, Cohen C, Chirwa T, Ntshoe G, Puren A, Hofman K. Identifying high-risk areas for sporadic measles outbreaks: lessons from South Africa. *Bull World Health Organ*. 2013;91(3):174-183. doi:10.2471/BLT.12.110726

31. Ntirampeba D, Neema I, Kazembe L. Modelling spatio-temporal patterns of disease for spatially misaligned data: An application on measles incidence data in Namibia from 2005-2014. Devleesschauwer B, ed. *PLoS One*. 2018;13(8):e0201700. doi:10.1371/journal.pone.0201700

32. Wesolowski A, Winter A, Tatem AJ, et al. Measles outbreak risk in Pakistan : exploring the potential of combining vaccination coverage and incidence data with novel data-streams to strengthen control. *Epidemiol Infect*. 2018:1-9.

33. Lo NC, Hotez PJ. Public health and economic consequences of vaccine hesitancy for measles in the United States. *JAMA Pediatr*. 2017;171(9):887-892. doi:10.1001/jamapediatrics.2017.1695

34. Kundrick A, Huang Z, Carran S, et al. Sub-national variation in measles vaccine coverage and outbreak risk: a case study from a 2010 outbreak in Malawi. *BMC Public Health*. 2018;18(1):741-751. doi:10.1186/s12889-018-5628-x

35. Bharti N, Tatem AJ, Ferrari MJ, Grais RF, Djibo A, Grenfell BT. Explaining seasonal fluctuations of measles in Niger using nighttime lights imagery. *Science (80-)*. 2011;334(6061):1424-1427. doi:10.1126/science.1210554

36. Utazi CE, Thorley J, Alegana VA, et al. High resolution age-structured mapping of childhood vaccination coverage in low and middle income countries. *Vaccine*. 2018;36(12):1583-1591. doi:10.1016/j.vaccine.2018.02.020

37. Grenfell BT, Bjørnstad ON, Kappey J. Travelling waves and spartial hierarchies in measles epidemics. *Nature*. 2001;414(December):716-723.

38. Lessler J, Salje H, Grabowski MK, Cummings DAT. Measuring Spatial Dependence for Infectious Disease Epidemiology. *PLoS One*. 2016;11(5):e0155249. doi:10.1371/journal.pone.0155249

39. Baker R, Park SW, Yang W, Vecchi G, Metcalf CJE, Grenfell B. The impact of COVID-19 non-pharmaceutical interventions on the future dynamics of endemic infections. 2020. doi:10.1101/2020.06.22.20137588

40. Wang C, Li Z, Clay Mathews M, Praharaj S, Karna B, Solís P. The spatial association of social vulnerability with COVID-19 prevalence in the contiguous United States. *Int J Environ Health Res*. November 2020:1-8. doi:10.1080/09603123.2020.1847258

41. Saint-Victor DS, Omer SB. Vaccine refusal and the endgame : walking the last mile first. *Phil Trans R Soc B*. 2013;368:20120148.

42. Eggertson L. Lancet retracts 12-year-old article linking autism to MMR vaccines. *CMAJ*. 2010;182(4):199-200. doi:10.1503/cmaj.109-3179

43. Smith A, Yarwood J, Salisbury DM. Tracking mothers' attitudes to MMR immunisation 1996-2006. *Vaccine*. 2007;25(20):3996-4002. doi:10.1016/j.vaccine.2007.02.071

44. Liu K, King M, Bearman PS. Social Influence and the Autism Epidemic. *Am J Sociol*. 2010;115(5):1387-1434. doi:10.1086/651448

45. The Strategic Advisory Group of Experts (SAGE). Report of the SAGE working group on vaccine hesitancy. https://www.who.int/immunization/sage/meetings/2014/october/1_Report_WORKING_GROUP_vaccine_hesitancy_final.pdf. Published 2014. Accessed January 12, 2019.

46. Larson HJ, Jarrett C, Schulz WS, et al. Measuring vaccine hesitancy: The development of a survey tool. *Vaccine*. 2015;33(34):4165-4175. doi:10.1016/j.vaccine.2015.04.037

47. Opel DJ, Taylor JA, Mangione-Smith R, et al. Validity and reliability of a survey to identify vaccine-hesitant parents. *Vaccine*. 2011;29(38):6598-6605. doi:10.1016/j.vaccine.2011.06.115

48. Zerbo O, Modaressi S, Goddard K, et al. Vaccination Patterns in Children After Autism Spectrum Disorder Diagnosis and in Their Younger Siblings. *JAMA Pediatr*. 2018;94612(5):469-475. doi:10.1001/jamapediatrics.2018.0082

49. Cooper LZ, Larson HJ, Katz SL. Protecting public trust in immunization. *Pediatrics*. 2008;122(1):149-153. doi:DOI 10.1542/peds.2008-0987

50. Slovic P, Finucane ML, Peters E, MacGregor DG. The affect heuristic. *Eur J Oper Res*. 2007;177(3):1333-1352. doi:10.1016/j.ejor.2005.04.006

51. Seethaler SL. Shades of Grey in Vaccination Decision Making. *Sci Commun*. 2016;38(2):261-271. doi:10.1177/1075547016637083

52. Tomljenovic H, Bubic A, Erceg N. It just doesn't feel right – the relevance of emotions and intuition for parental vaccine conspiracy beliefs and vaccination uptake. *Psychol Health*. 2020;35(5):538-554. doi:10.1080/08870446.2019.1673894

53. Larson HJ, Jarrett C, Eckersberger E, Smith DMD, Paterson P. Understanding vaccine hesitancy around vaccines and vaccination from a global perspective: A systematic review of published literature, 2007-2012. *Vaccine*. 2014;32(19):2150-2159. doi:10.1016/j.vaccine.2014.01.081

54. Victora CG, Joseph G, Silva ICM, et al. The Inverse Equity Hypothesis: Analyses of Institutional Deliveries in 286 National Surveys. *Am J Public Health*. 2018;108(4):464-471. doi:10.2105/AJPH.2017.304277

55. Domek GJ, O'Leary ST, Bull S, et al. Measuring vaccine hesitancy: Field testing the WHO SAGE Working Group on Vaccine Hesitancy survey tool in Guatemala. *Vaccine*. 2018;(35):5273-5281. doi:10.1016/j.vaccine.2018.07.046

56. Ren J, Wagner AL, Zheng A, et al. The demographics of vaccine hesitancy in Shanghai, China. *PLoS One*. 2018;13(12):e0209117. doi:10.1371/journal.pone.0209117

57. Wagner AL, Boulton ML, Sun X, et al. Parents' concerns about vaccine scheduling in Shanghai, China. *Vaccine*. 2017;35(34):4362-4367. doi:10.1016/j.vaccine.2017.06.077

58. Henrikson NB, Anderson ML, Opel DJ, Dunn J, Marcuse EK, Grossman DC. Longitudinal trends in vaccine hesitancy in a cohort of mothers surveyed in Washington State, 2013-2015. *Public Health Rep*. 2017;132(4):451-454. doi:10.1177/0033354917711175

59. Gust DA, Darling N, Kennedy A, Schwartz B. Parents With Doubts About Vaccines: Which Vaccines and Reasons Why. *Pediatrics*. 2008;122(4):718-725. doi:10.1542/peds.2007-0538

60. Freed GL, Clark SJ, Butchart AT, Singer DC, Davis MM. Parental Vaccine Safety Concerns in 2009. *Pediatrics*. 2010;125(4):654-659. doi:10.1542/peds.2009-1962

61. Corben P, Leask J. Vaccination hesitancy in the antenatal period: A cross-sectional survey. *BMC Public Health*. 2018;18(1):1-14. doi:10.1186/s12889-018-5389-6

62. Costa-Pinto JC, Willaby HW, Leask J, et al. Parental immunisation needs and attitudes survey in paediatric hospital clinics and community maternal and child health centres in Melbourne, Australia. *J Paediatr Child Health*. 2018;54(5):522-529. doi:10.1111/jpc.13790

63. Betsch C, Bödeker B, Schmid P, Wichmann O. How baby's first shot determines the development of maternal attitudes towards vaccination. *Vaccine*. 2018;36(21):3018-3026. doi:10.1016/j.vaccine.2018.04.023

64. Weiner JL, Fisher AM, Nowak GJ, Basket MM, Gellin BG. Childhood immunizations: First-time expectant mothers' knowledge, beliefs, intentions, and behaviors. *Vaccine*. 2015;33:D92-D98. doi:10.1016/j.vaccine.2015.09.037

65. Opel DJ, Mangione-Smith R, Robinson JD, et al. The influence of provider communication behaviors on parental vaccine acceptance and visit experience. *Am J Public Health*. 2015;105(10):1998-2004. doi:10.2105/AJPH.2014.302425

66. Sears R. *The Vaccine Book: Making the Right Decision for Your Child*. New York, NY: Little, Brown and Company; 2007.

67. Offit PA, Moser CA. The Problem With Dr Bob's Alternative Vaccine Schedule. *Pediatrics*. 2009;123(1):e164-e169. doi:10.1542/peds.2008-2189

68. Gutierrez M. Dr. Bob Sears' views on vaccines have inspired loyal followers — and a crush of criticism. *Los Angeles Times*. https://www.latimes.com/california/story/2019-09-02/bob-sears-controversial-views-on-vaccines-inspire-critics-and-fans. Published September 3, 2019.

69. Moyer-Gusé E, Robinson MJ, Mcknight J. The Role of Humor in Messaging about the MMR Vaccine. *J Health Commun*. 2018;00(00):1-9. doi:10.1080/10810730.2018.1473533

70. Masters NB, Shih SF, Bukoff A, et al. Social distancing in response to the novel coronavirus (COVID-19) in the United States. *PLoS One*. 2020;15(9 September):1-12. doi:10.1371/journal.pone.0239025

71. Peretti-Watel P, Seror V, Cortaredona S, et al. A future vaccination campaign against COVID-19 at risk of vaccine hesitancy and politicisation. *Lancet Infect Dis*. 2020;20(7):769-770. doi:10.1016/S1473-3099(20)30426-6

72. Verger P, Dubé E. Restoring confidence in vaccines in the COVID-19 era. *Expert Rev Vaccines*. 2020;0(0):14760584.2020.1825945. doi:10.1080/14760584.2020.1825945

73. Fisher KA, Bloomstone SJ, Walder J, Crawford S, Fouayzi H, Mazor KM. Attitudes Toward a Potential SARS-CoV-2 Vaccine: A Survey of U.S. Adults. *Ann Intern Med*. 2020. doi:10.7326/m20-3569

74. Palamenghi L, Barello S, Boccia S, Graffigna G. Mistrust in biomedical research and vaccine hesitancy: the forefront challenge in the battle against COVID-19 in Italy. *Eur J Epidemiol*. 2020;35(8):785-788. doi:10.1007/s10654-020-00675-8

75. Zelner J, Trangucci R, Naraharisetti R, et al. Racial disparities in COVID-19 mortality are driven by unequal infection risks. *Clin Infect Dis*. 2020;(1). doi:10.1093/cid/ciaa1723

76. COVID Collaborative. Coronavirus Vaccine Hesitancy in Black and Latinx Communities. https://www.covidcollaborative.us/content/vaccine-treatments/coronavirus-vaccine-hesitancy-in-black-and-latinx-communities. Published 2020. Accessed November 23, 2020.

77. LaFraniere S, Weiland No. White House Blocks News Coronavirus Vaccine Guidelines. *New York Times*. October 5, 2020.

78. Kreps S, Prasad S, Brownstein JS, et al. Factors Associated With US Adults' Likelihood of Accepting COVID-19 Vaccination. *JAMA Netw Open*. 2020;3(10):e2025594. doi:10.1001/jamanetworkopen.2020.25594

79. Weintraub RL, Subramanian L, Karlage A, Ahmad I, Rosenberg J. COVID-19 Vaccine To Vaccination: Why Leaders Must Invest In Delivery Strategies Now. *Health Aff*. November 2020:10.1377/hlthaff. doi:10.1377/hlthaff.2020.01523

80. Santoli JM, Lindley MC, DeSilva MB, et al. Effects of the COVID-19 Pandemic on Routine Pediatric Vaccine Ordering and Administration — United States, 2020. *MMWR Morb Mortal Wkly Rep*. 2020;69(19):591-593. doi:10.15585/mmwr.mm6919e2

81. Bramer CA, Kimmins LM, Swanson R, Kuo J, Vranesich P. Decline in Child Vaccination Coverage During the COVID-19 Pandemic — Michigan Care Improvement Registry , May 2016 – May 2020. *MMWR Morb Mortal Wkly Rep*. 2020;69(May 2016):2016-2018.

82. The College of Physicians of Philadelphia. The History of Vaccines: Government Regulation.

83. U.S. *Jacobson v. Massachusetts*. 197, 11 (1905).

84. Fadel M. 360 Years of Measles: Limiting Liberty Now for a Healthier Future. *J Leg Med*. 2019;39(1):1-13. doi:10.1080/01947648.2019.1568937

85. Thomas MS. Parens Patriae and the States' Historic Police Power. *SMU Law Rev*. 2016;69(759).

86. United States. *Zucht v. King*. 260, 174 (1922).

87. Omer SB, Salmon DA, Orenstein WA, DeHart MP, Halsey N. Vaccine Refusal, Mandatory Immunization, and the Risks of Vaccine-Preventable Diseases. *N Engl J Med*.

2009;360(19):1981-1988. doi:10.1056/NEJMsa0806477

88. Phadke VK, Bednarczyk RA, Salmon DA, Omer SB. Association Between Vaccine Refusal and Vaccine-Preventable Diseases in the United States. *JAMA*. 2016;315(11):1149. doi:10.1001/jama.2016.1353

89. Gravagna K, Becker A, Valeris-Chacin R, et al. Global assessment of national mandatory vaccination policies and consequences of non-compliance. *Vaccine*. 2020;38(49):7865-7873. doi:10.1016/j.vaccine.2020.09.063

90. Draeger E, Bedford HE, Elliman DAC. Should measles vaccination be compulsory? *BMJ*. 2019;2359(January 2018):l2359. doi:10.1136/bmj.l2359

91. Gastañaduy PA, Paul P, Fiebelkorn AP, et al. Assessment of the status of measles elimination in the United States, 2001-2014. *Am J Epidemiol*. 2017;185(7):562-569. doi:10.1093/aje/kww168

92. Olive JK, Matthews KR. How Too Much Freedom of Choice Endangers Public Health: The Effect of Nonmedical Exemptions from School-Entry Vaccinations in Texas. *Policy Brief, no 101316*. 2016.

93. Bednarczyk RA, King AR, Lahijani A, Omer SB. Current landscape of nonmedical vaccination exemptions in the United States: impact of policy changes. *Expert Rev Vaccines*. 2019;18(2):175-190. doi:10.1080/14760584.2019.1562344

94. Omer SB, Richards JL, Ward M, Bednarczyk RA. Vaccination Policies and Rates of Exemption from Immunization, 2005–2011. *N Engl J Med*. 2012;367(12):1170-1171. doi:10.1056/NEJMc1209037

95. Omer SB, Porter RM, Allen K, Salmon DA, Bednarczyk RA. Trends in kindergarten rates of vaccine exemption and state-level policy, 2011-2016. *Open Forum Infect Dis*. 2018;5(2):2011-2016. doi:10.1093/ofid/ofx244

96. Tony Yang Y, Delamater PL, Leslie TF, Mello MM. Sociodemographic predictors of vaccination exemptions on the basis of personal belief in California. *Am J Public Health*. 2016;106(1):172-177. doi:10.2105/AJPH.2015.302926

97. Caron C. Vaccine Laws Are Changing. Here's What You Need to Know. The New York Times. https://parenting.nytimes.com/health/vaccine-exemptions-measles. Published June 14, 2019. Accessed September 12, 2019.

98. McKinley J. Measles Outbreak: NY Eliminates Religious Exemptions for Vaccinations. The New York Times. https://www.nytimes.com/2019/06/13/nyregion/measles-vaccinations-new-york.html. Published June 13, 2019. Accessed July 30, 2019.

99. Sarkar S, Zlojutro A, Khan K, Gardner L. Measles resurgence in the USA: how

international travel compounds vaccine resistance. *Lancet Infect Dis*. 2019;3099(19):2017-2019. doi:10.1016/S1473-3099(19)30231-2

100. Aloe C, Kulldorff M, Bloom BR. Geospatial analysis of nonmedical vaccine exemptions and pertussis outbreaks in the United States. *Proc Natl Acad Sci*. 2017;114(27):7101-7105. doi:10.1073/pnas.1700240114

101. Omer SB, Enger KS, Moulton LH, Halsey NA, Stokley S, Salmon DA. Geographic Clustering of Nonmedical Exemptions to School Immunization Requirements and Associations With Geographic Clustering of Pertussis. *Am J Epidemiol*. 2008;168(12):1389-1396. doi:10.1093/aje/kwn263

102. Robison SG, Liko J. The Timing of Pertussis Cases in Unvaccinated Children in an Outbreak Year: Oregon 2012. *J Pediatr*. 2017;183:159-163. doi:10.1016/j.jpeds.2016.12.047

103. Centers for Disease Control and Prevention (CDC). Measles Cases and Outbreaks. Measles (Rubeola). https://www.cdc.gov/measles/cases-outbreaks.html. Published 2019. Accessed July 9, 2019.

104. Immunization Action Coalition. Exemptions Permitted to School and Child Care Immunization Requirements. http://www.immunize.org/laws/exemptions.pdf. Published 2019. Accessed July 8, 2019.

105. World Health Organization (WHO). *Measles and Rubella Surveillance Data*.; 2020. https://www.who.int/immunization/monitoring_surveillance/burden/vpd/surveillance_type/active/measles_monthlydata/en/.

106. World Health Organization (WHO). Immunization, Vaccines, and Biologicals | New measles surveillance data for 2019. https://www.who.int/immunization/newsroom/measles-data-2019/en/. Published 2019. Accessed January 22, 2020.

107. World Health Orgranization. *Global Measles and Rubella Monthly Update: March, 2020*. Geneva, Switzerland; 2020. https://www.who.int/immunization/monitoring_surveillance/burden/vpd/surveillance_type/active/measles_monthlydata/en/.

108. Pingali SC, Delamater PL, Buttenheim AM, Salmon DA, Klein NP, Omer SB. Associations of Statewide Legislative and Administrative Interventions with Vaccination Status among Kindergartners in California. *JAMA - J Am Med Assoc*. 2019;322(1):49-56. doi:10.1001/jama.2019.7924

109. Omer SB, Enger KS, Moulton LH, Halsey NA, Stokley S, Salmon DA. Geographic Clustering of Nonmedical Exemptions to School Immunization Requirements and Associations With Geographic Clustering of Pertussis. *Am J Epidemiol*.

2008;168(12):1389-1396. doi:10.1093/aje/kwn263

110. Matthias J, Dusek C, Scott Pritchard P, Rutledge L, Kinchen P, Lander M. Outbreak of pertussis in a school and religious community averse to health care and vaccinations — Columbia County, Florida, 2013. *Morb Mortal Wkly Rep*. 2014;(30):655.

111. Fine PEM, Clarkson JA. Measles in England and Wales—I: An Analysis of Factors Underlying Seasonal Patterns. *Int J Epidemiol*. 1982;11(1):5-14. doi:10.1093/ije/11.1.5

112. Guerra FM, Bolotin S, Lim G, et al. The basic reproduction number (R0) of measles: a systematic review. *Lancet Infect Dis*. 2017;17(12):e420-e428. doi:10.1016/S1473-3099(17)30307-9

113. Gastañaduy PA, Budd J, Fisher N, et al. A measles outbreak in an underimmunized amish community in Ohio. *N Engl J Med*. 2016;375(14):1343-1354. doi:10.1056/NEJMoa1602295

114. Lloyd-Smith JO, Schreiber SJ, Kopp PE, Getz WM. Superspreading and the effect of individual variation on disease emergence. *Nature*. 2005;438(7066):355-359. doi:10.1038/nature04153

115. Sugerman DE, Barskey AE, Delea MG, et al. Measles Outbreak in a highly vaccinated population, San Diego, 2008: Role of the intentionally undervaccinated. *Pediatrics*. 2010;125(4):747-755. doi:10.1542/peds.2009-1653

116. Salathé M, Bonhoeffer S. The effect of opinion clustering on disease outbreaks. *J R Soc Interface*. 2008;5(29):1505-1508. doi:10.1098/rsif.2008.0271

117. MORAN PAP. Notes on continuous stochastic phenomena. *Biometrika*. 1950;37(1-2):17-23.

118. Iceland J, Weinberg DH, Steinmetz E. *Appendix B. Measures of Residential Segregation*. U.S. Government Printing Washington, DC; 2000.

119. Gelman A, Carlin J. Beyond Power Calculations: Assessing Type S (Sign) and Type M (Magnitude) Errors. *Perspect Psychol Sci*. 2014;9(6):641-651. doi:10.1177/1745691614551642

120. Brownwright TK, Dodson ZM, Van Panhuis WG. Spatial clustering of measles vaccination coverage among children in sub-Saharan Africa. *BMC Public Health*. 2017;17(1):1-7. doi:10.1186/s12889-017-4961-9

121. Tatem AJ. Innovation to impact in spatial epidemiology. *BMC Med*. 2018;16(1):209. doi:10.1186/s12916-018-1205-5

122. Leslie TF, Street EJ, Delamater PL, Tony Yang Y, Jacobsen KH. Variation in vaccination

data available at school entry across the United States. *Am J Public Health*. 2016;106(12):2180-2182. doi:10.2105/AJPH.2016.303455

123. Hill HA, Elam-Evans LD, Yankey D, Singleton JA, Kolasa M. National, State, and Selected Local Area Vaccination Coverage Among Children Aged 19–35 Months — United States, 2014. *MMWR Morb Mortal Wkly Rep*. 2015;64(33):889-896. doi:10.15585/mmwr.mm6433a1

124. Anderson RM, May RM. *Infectious Diseases of Humans: Dynamics and Control*. Oxford, UK: Oxford University Press; 1991.

125. Centers for Disease Control and Prevention (CDC). Ten Great Public Health Achievements - United States, 2001-2010. *Morb Mortal Wkly Rep*. 2011;60(19):605-609. www.cdc.gov/mmwr/preview/mmwrhtml/mm6019a5.htm.

126. Bednarczyk RA, King AR, Lahijani A, Omer SB. Current landscape of nonmedical vaccination exemptions in the United States: impact of policy changes. *Expert Rev Vaccines*. 2019;18(2):175-190. doi:10.1080/14760584.2019.1562344

127. Seither R, Loretan C, Driver K, Mellerson JL, Knighton CL, Black CL. Vaccination Coverage with Selected Vaccines and Exemption Rates Among Children in Kindergarten - United States, 2018-19 School Year. *MMWR Morb Mortal Wkly Rep*. 2019;68(41):905-912. doi:10.15585/mmwr.mm6841e1

128. King AR, Salmon KS, Bednarczyk RA. Understanding the impact of state vaccination laws on exemption rates. *Curr Opin Pediatr*. 2020;32(1):160-166. doi:10.1097/MOP.0000000000000844

129. Navin MC, Kozak AT, Clark EC. The evolution of immunization waiver education in Michigan: A qualitative study of vaccine educators. *Vaccine*. 2018;36(13):1751-1756. doi:10.1016/j.vaccine.2018.02.046

130. Morrison M, Castro LA, Ancel Meyers L. Conscientious vaccination exemptions in kindergarten to eighth-grade children across Texas schools from 2012 to 2018: A regression analysis. *PLOS Med*. 2020;17(3):e1003049. doi:10.1371/journal.pmed.1003049

131. Garnier R, Nedell ER, Omer SB, Bansal S. Getting personal: how childhood vaccination policies shape the landscape of vaccine exemptions. *Open Forum Infect Dis*. 2020:1-9. doi:10.1093/ofid/ofaa088

132. Patel M, Lee AD, Clemmons NS, et al. National Update on Measles Cases and Outbreaks — United States, January 1–October 1, 2019. *MMWR Morb Mortal Wkly Rep*. 2019;68(40):893-896. doi:10.15585/mmwr.mm6840e2

133. Sparks PJ, Sparks CS. An application of spatially autoregressive models to the study of US county mortality rates. *Popul Space Place*. 2010;16(6):465-481. doi:10.1002/psp.564

134. Brown LA, Chung S. Spatial segregation, segregation indices and the geographical perspective. *Popul Space Place*. 2006;12(2):125-143. doi:10.1002/psp.403

135. Michigan Educational Entity Master. https://cepi.state.mi.us/eem/. Published 2019. Accessed July 3, 2019.

136. Delamater PL, Street EJ, Leslie TF, Yang YT, Jacobsen KH. Complexity of the basic reproduction number (R0). *Emerg Infect Dis*. 2019;25(1):1-4. doi:10.3201/eid2501.171901

137. Wallinga J, Teunis P, Kretzschmar M. Using data on social contacts to estimate age-specific transmission parameters for respiratory-spread infectious agents. *Am J Epidemiol*. 2006;164(10):936-944. doi:10.1093/aje/kwj317

138. Kanaan MN, Farrington CP. Matrix models for childhood infections: a Bayesian approach with applications to rubella and mumps. *Epidemiol Infect*. 2005;133(06):1009. doi:10.1017/S0950268805004528

139. Buttenheim A, Jones M, Baras Y. Exposure of California kindergartners to students with personal belief exemptions from mandated school entry vaccinations. *Am J Public Health*. 2012;102(8):59-67. doi:10.2105/AJPH.2012.300821

140. Lichter DT, Parisi D, Taquino MC. Toward a New Macro-Segregation? Decomposing Segregation within and between Metropolitan Cities and Suburbs. *Am Sociol Rev*. 2015;80(4):843-873. doi:10.1177/0003122415588558

141. World Health Organization (WHO). Ten threats to global health in 2019. Newsroom.

142. Michigan Department of Health and Human Services (MDHHS). 2019 Michigan Measles Outbreak Information.

143. Michigan Department of Health and Human Services Department of Community Health Bureau of Epidemiology Communicable and Related Diseases. MDHHS Communicable and Related Diseases Administrative Rules. https://www.michigan.gov/documents/mdhhs/1472_2014-073CH_AdminCode_1_676105_7.pdf. Published 2015. Accessed September 21, 2020.

144. Mashinini DP, Fogarty KJ, Potter RC, Lagerwey MD. The Impact of Michigan's Nonmedical Vaccine Exemption Rule Change on Philosophical Exemption Rates. *J Community Health*. 2020;45(1):148-153. doi:10.1007/s10900-019-00727-5

145. Omer SB, Allen K, Chang DH, et al. Exemptions From Mandatory Immunization After Legally Mandated Parental Counseling. *Pediatrics*. 2018;141(1). doi:10.1542/peds.2017-2364

146. Michigan Department of Health and Human Services (MDHHS). *Immunization Program*.;

2020. https://www.michigan.gov/mdhhs/0,5885,7-339-73971_4911_4914---,00.html.

147. Masters NB, Delamater PL, Boulton ML, Zelner J. Measuring Multiple Dimensions and Indices of Non-Vaccination Clustering in Michigan: 2008-2018. *Am J Epidemiol*. December 2020:2008-2018. doi:10.1093/aje/kwaa264

148. Bates D, Mächler M, Bolker B, Walker S. lme4: Linear mixed-effects models using Eigen and S4. 2015. http://cran.r-project.org/package=lme4.

149. Anselin L. Local Indicators of Spatial Association—LISA. *Geogr Anal*. 1995;27(2):93-115. doi:10.1111/j.1538-4632.1995.tb00338.x

150. Goodrich B, Gabry J, Ali I, Brilleman S. rstanarm: Bayesian applied regression modeling via Stan. 2020.

151. Elder B. *HB4610*. Michigan State House; 2019. http://legislature.mi.gov/doc.aspx?2019-HB-4610.

152. Centers for Disease Control and Prevention (CDC). National Immunization Survey | 2015 Dataset.

153. Masters NB, Eisenberg MC, Delamater PL, Kay M, Boulton ML, Zelner J. Fine-scale spatial clustering of measles nonvaccination that increases outbreak potential is obscured by aggregated reporting data. *Proc Natl Acad Sci*. 2020;117(45):28506-28514. doi:10.1073/pnas.2011529117

154. Mashinini DP, Fogarty KJ, Potter RC, Berles JD. Geographic hot spot analysis of vaccine exemption clustering patterns in Michigan from 2008 to 2017. *Vaccine*. 2020;(xxxx). doi:10.1016/j.vaccine.2020.10.091

155. Navin MC, Kozak AT, Clark EC. The evolution of immunization waiver education in Michigan: A qualitative study of vaccine educators. *Vaccine*. 2018;36(13):1751-1756. doi:j.socscimed.2016.08.011

156. Navin MC, Largent MA, Mccright AM. Efficient burdens decrease nonmedical exemption rates : A cross-county comparison of Michigan ' s vaccination waiver education efforts. *Prev Med Reports*. 2020;17(January):101049. doi:10.1016/j.pmedr.2020.101049

157. Salmon DA, MacIntyre CR, Omer SB. Making mandatory vaccination truly compulsory: well intentioned but ill conceived. *Lancet Infect Dis*. 2015;15(8):872-873. doi:10.1016/S1473-3099(15)00156-5

158. Mello MM, Studdert DM, Parmet WE. Shifting Vaccination Politics — The End of Personal-Belief Exemptions in California. *N Engl J Med*. 2015;373(9):785-787. doi:10.1056/NEJMp1508701

159. Mello MM. Narrowing Vaccination Exemption Laws: Lessons From California and Beyond. *Ann Intern Med*. 2020;172(5):358. doi:10.7326/M19-3111

160. Gostin LO, Hodge JG, Bloom BR, et al. The public health crisis of underimmunisation: a global plan of action. *Lancet Infect Dis*. 2020;20(1):e11-e16. doi:10.1016/S1473-3099(19)30558-4

161. Centers for Disease Control and Prevention (CDC). About immunization information systems. Centers for Disease Control and Prevention Website.

162. Centers for Disease Control and Prevention (CDC). 2017 IISAR data participation rates.

163. Zipfel CM, Garnier R, Kuney MC, Bansal S. The landscape of childhood vaccine exemptions in the United States. *Sci Data 2020 71*. 2020;7(1):1-7. doi:10.1038/s41597-020-00742-5

164. McNally VV, Bernstein HH. The Effect of the COVID-19 Pandemic on Childhood Immunizations: Ways to Strengthen Routine Vaccination. *Pediatr Ann*. 2020;49(12):e516-e522. doi:10.3928/19382359-20201115-01